The role of T cells in mucosal immunity

Inauguraldissertation

zur

Erlangung der Würde eines Doktors der Philosophie

vorgelegt der

Philosophisch-Naturwissenschaftlichen Fakultät

der Universität Basel

von

Jan Devan

Basel, 2024

Genehmigt von der Philosophisch-Naturwissenschaftlichen Fakultät

auf Antrag von

Erstbetreuer: Prof. Gennaro De Libero

Zweitbetreuer: Prof. Dirk Bumann

Externer Experte: Prof. Stephan Brand

Basel 13.12.2022

Prof. Dr. Marcel Mayor

The Dean of Faculty

TABLE OF CONTENTS

Acknowledgments

I would like to thank Prof. Gennaro de Libero and Prof. Petr Hruz for supervising me, and for the good advice, support, and trust they provided me during my studies. Thanks to Vladimir Nosi who significantly contributed to the results published in this thesis through his bioinformatical analysis. Thank you to Lucia Mori for her advice and help. Thanks to Pedro Loureiro, Aisha Beshirova, Andrew Chancellor, Alessandro Vacchini, Mei Yang, Verena Schafer, and Corinne de Gregorio for valuable support and advice, generation of models and preparation of reagents and cells. Thank you also to other members of the lab namely Daniel Constantin, Marco Stringhini, Gennaro Prota, Giulianno Berloffa, Natalie Kehrer, Vanshika Rastogi, and Rodrigo Colombo who together with the aforementioned people created a great working environment.

I would like to acknowledge all members of my PhD committee, Prof. Gennaro de Libero, Prof. Dirk Bumann, and Prof. Stephan Brand for their valuable advice on my projects and their help in solving difficult situations during my PhD. I also want to thank to Flow cytometry facility members at DBM, especially Jelena Markovic-Djuric and Stella Stefanova for their support.

Finally, I want to express my honest thanks to my wife, my family, and my friends for their unconditional love and support without which this would not be possible.

Summary

The mucosal immune system protects the human body on anatomic sites serving to transport and exchange gases and nutrients with the outer environment. This makes them exposed to pathogens more than any other tissue type, and to protect it, many phenotypically and functionally different cell types contribute to the immune response in the mucosal tissues. Maintaining the balance between an excessive and insufficient immune response in such environmental conditions is key to homeostasis in the mucosa. When disrupted, illnesses like Crohn's disease (CD) or Eosinophilic esophagitis (EoE) may develop.

My PhD thesis aimed to describe the changes in the phenotype and function of immune cells associated with CD and EoE. Both of these diseases represent chronic immune-mediated disorders with worldwide increasing incidence. T cells are thought to play a key role in CD and EoE pathogenesis, and my research was therefore primarily focused on their investigation.

I established an anti-CD45 mAbs-based barcoding approach to simultaneously analyse hundreds of surface molecules expressed on cells isolated from intestinal tissue samples. It led to identifying unique T cell populations in inflamed intestinal tissue of CD patients and functional characterization of these T cells. In the EoE part, I established a multicolour flow cytometry panel, which allowed the description of changes in immune cell subsets composition, activation, and functional maturation associated with EoE. In addition, I unraveled the possible existence of a vicious circle in EoE where eosinophils present bacterial ligands to MAIT cells, which than produce soluble factors stimulatory and chemotactic for eosinophils. Such a mechanism can contribute to the perpetuation of chronic inflammation in EoE.

These results increase our understanding of the pathobiology of the studied diseases, paving the design of novel successful targeted therapies in the future.

Abbreviations

5-OE-RU	5-(2-oxoethylideneamino)-6-D-ribitylaminouracil
5-OP-RU	5-(2-oxopropilidenamino)-6-D-ribitylaminouracil
Ag	Antigen
AHR	Aryl hydrocarbon receptor
AIEC	Adherent invasive *E. coli*
APC	Antigen-presenting cell
arcsinh	Hyperbolic arcsine
BCL6	B cell lymphoma 6
BCR	B cell receptor
BSA	Bovine serum albumine
BTNL	Butyrophilin-like
CAPN14	Calpain 14
CCR	C-C chemokine receptor
CD	Crohn's disease
CRP	C-reactive protein
CXCR	C-X-C chemokine receptor
DAPI	4′,6-diamidino-2-phenylindole
DC	Dendritic cell
DMSO	Dimethyl sulfoxide
DNA	Deoxyribonucleic acid
DNAase	Deoxyribonucleotidase
DOP	Delta opioid receptor
DSG1	Desmoglein 1
EC50	Half maximal effective concentration
EDTA	Ethylenediaminetetraacetic acid
EGFP	Enhanced green fluorescent protein
EGFR	Epithelial growth factor receptor
ELISA	Enzyme-linked immunosorbent assay
EoE	Eosinophilic esophagitis
ER	Endoplasmic reticulum
ERK	Extracellular signal-regulated kinase
FACS	Fluorescence -activated cell sorting
Fc	Fragment constant
FCS	Fetal calf serum
FDR	False discovery rate
FLG	Filaggrin
FMO	Fluorescence minus one
FOXP3	Forkhead box P3
GATA3	GATA binding protein 3

GC	Germinal centre
GERD	Gastroesophageal reflux disease
GO	Gene ontology
GPR83	G-protein coupled receptor 83
HEPES	4-(2-hydroxyethyl)-1-piperazineethanesulfonic acid
IBD	Inflammatory bowel disease
IFN	Interferon
Ig	Immunoglobulin
IL	Interleukin
ILC	Innate lymphoid cell
iNKT	Invariant natural killer T cells
IRF	Interferon regulatory factor
KLRG1	Killer Cell Lectin Like Receptor G1
KO	Knock-out
LTBR	Lymphotoxin beta receptor
MAdCAM1	Mucosal addressin cell adhesion molecule-1
MAIT	Mucosal-associated invariant T cells
MBL	Mannan-binding lectin
MEM	Minimal essential medium
MERTK	MER receptor tyrosine kinase
MHC	Major histocompatibility complex
MNR	Macrophage mannose receptor
MR1	Major Histocompatibility Complex Class I-Related
MRGX2	Mass related G-protein coupled receptor member X2
MSR	Macrophage scavenger receptor
MUC	Mucin
NCR	Natural cytotoxicity receptor
Negl2fc	Negative binary logarithm of fold change
Neglfdr	Negative decadic logarithm of false discovery rate
NFAT	Nuclear factor of activated T cells
NKT	Natural killer T
NOD	Nucleotide oligomerization domain
NOTCH	Neurogenic locus notch homolog protein 1
OPD	*o*-Phenylendiamin-dihydrochloride
PBMCs	Peripheral blood mononuclear cells
PBS	Phosphate-buffered saline
PC	Paneth cell
PCR	Polymerase chain reaction
PD1	Programmed cell death protein 1
PDPN	Podoplanin
PMA	Phorbol 12-myristate 13-acetate

PPI	Proton pump inhibitor
PRR	Pattern recognition receptor
RL-6, 7-diMe	6, 7-dimethyl-8-d-ribityllumazine
RORγT	Retinoic acid receptor-related orphan receptor γ
SAP	Serum amyloid protein
SCFA	Short chain fatty acid
SD	Standard deviation
SFB	Segmental filamentous bacteria
Siglec	Sialic acid-binding immunoglobulin-type lectins
SLAMF6	Slam family member 6
SNP	Single nucleotide polymorphism
STAT	Signal transducer and activator of transcription
TCM	T central memory
TCR	T cell receptor
TEM	T effector memory
TEMRA	T effector memory expressing CD45RA
TGF	Transforming growth factor
Th	T helper
TIGIT	T cell immunoreceptor with Ig and ITIM domains
TLR	Toll-like receptor
TMEM8A	Transmembrane protein 8A
TMM	Trimmed mean of M-values
TNF	Tumor necrosis factor
TRAJ	T cell receptor alpha joining
TRAV	T cell receptor alpha variable
TRDJ	T cell receptor delta joining
TRDV	T cell receptor delta variable
TREC	T cell receptor excision circle
Treg	T regulatory cell
UC	Ulcerative colitis
UPR	Unfolded protein response
XCR1	X-C motif chemokine receptor 1
β2m	β2 microglobulin

Introduction

Immune system

The immune system is a complex network consisting of effector cells and molecules that protect our body against pathogens and toxins and against our modified malfunctioning cells. It should be able to recognize and eliminate danger while it should tolerate its own tissues and commensal organisms. Multiple control mechanisms of immune cell development evolved to ensure these goals will be achieved. The immune system is organized into two main parts: innate immunity and adaptive immunity (1). Cooperation between both of these elements is required for the adequate protection of the organism. Notably, some immune cell subsets are functionally located rather between innate and adaptive immunity than strictly belonging to only one part, which further underscores the importance of the connection between these two arms of the immune system.

Mucosal immunity

Mucous membranes represent specific surfaces covering the urogenital tract, gastrointestinal tract, airways, inner ear, conjunctiva of the eye, and all exocrine glands. These tissues enable the exchange between the body and the outer environment, which expose them to toxic elements and high numbers of potentially harmful pathogens. Mechanical, chemical, and biological mechanisms that protect against these harms allow to identify, kill, degrade and repel the pathogens present at mucosal surfaces. While chemical and mechanical mechanisms are highly unspecific, the cellular component of the immune system allows specific recognition of pathogens and specific responses. Many different cell types vastly differing in their phenotype, function, origin, and spatial distribution contribute to immune response occurring in the mucosal tissues (2).

The innate immune system

The innate immune system represents the evolutionary ancient part of the host defense mechanisms and is the first barrier against invading pathogens. Most pathogens trying to enter through mucosal surfaces fail to cross it or are rapidly eliminated thanks to the innate immune system consisting of physical barriers, chemical substances, and innate immune cells.

Cell-to-cell adhesion among mucosal epithelia through tight junctions formed by occluding and claudin family of proteins represents a strong physical barrier against pathogens (3). In addition, the mucosal surface is covered by a layer of large glycoproteins called mucins, which forms further physical and chemical barrier (4). The layer of mucus is difficult to penetrate for pathogens, and they can also be expelled out of the body by the rhythmic beating of cilia of the mucosal epithelium of the respiratory tract or by peristaltic of the intestine (5, 6). Mucus is also essential for antigen-specific IgA antibodies responses at mucosal surfaces (7).

The acidic pH of the stomach, secretion of enzymes such as pepsins in the gut, lysozyme, and phospholipase in the oral cavity, nasal cavity, and tears or the secretion of pulmonary surfactants in the lungs represent additional mechanisms of chemical protection (1). While unspecific anti-microbial peptides produced by mucosal surfaces such as pepsin, lysozyme, or defensins destroy bacteria directly (1, 8), proteins of the complement system can induce both direct lysis, phagocytosis by cells of the innate immune system and activation of the adaptive immune system (1, 9, 10).

Cellular immunity is required once the physical and chemical mechanisms are not sufficient. Cells of the innate immune system, such as macrophages, dendritic cells, neutrophils, eosinophils, basophils, or mast cells, respond to conserved features of pathogenic microorganisms recognized via a limited number of germline-encoded pattern-recognition receptors (PRRs) (11). PRRs are a broad family of conserved intracellular, cell-surface, or secreted proteins recognizing products of microbial metabolism not produced by the host. Intracellular nucleotide oligomerization domain (NOD) receptors and protein kinase R (PKR), surface-expressed Toll-like receptors (TLR), macrophage scavenger receptor (MSR), and macrophage mannose receptor (MNR) or secreted mannan-binding lectin (MBL), serum amyloid protein (SAP) and C-reactive protein (CRP) are examples of important PRRs in human body (12). Binding of microbial antigens such as dsRNA (PKR), muramyl dipeptide (NOD2 receptor),

lipopolysaccharides (NOD receptors and MSR), peptidoglycan (TLR2), LTA (MSR), mannose (MMR, MBL), phosphorylcholine (SAP, CRP) by PRRs activate downstream signaling pathways and induces the expression of pro-inflammatory cytokines and antimicrobial genes (12). This set of evolutionarily conserved danger sensors allows the innate immune system to react and efficiently and rapidly destroy intruding pathogens (13).

The ability to respond quickly makes the innate immune system critical during the first hours and days of exposure to the new pathogen because effective adaptive immune system responses take up to seven days to develop. In response to pathogen recognition, innate immune system cells release small chemical mediators called cytokines and chemokines, which attract other immune cells to the site of infection and facilitate their activation. Soluble factors produced by innate immune cells are essential for the effective activation of the adaptive arm of the immune system.

The adaptive immune system

The adaptive immune system is evolutionarily younger than innate immunity and plays a crucial role when the innate immune system is ineffective in eliminating infectious agents. The advantage of the adaptive immune system lies in its specificity and immunological memory. It consists of B cells and T cells, which action is based on their TCR and BCR receptors. The basis of specificity lies in the potentially unlimited variability of surface receptors achieved through the mechanisms involving the rearrangement of DNA segments and their joining by random N nucleotides (1). Additional variability of BCRs is later introduced based on the somatic hypermutations and class-switching reactions during B cell maturation in germinal centers (14). Similarly, as with all hematopoietic cells, the initial development of B and T cells starts in the bone marrow.

B cells

Naïve (IgM^+, IgD^+) B lymphocytes leave the bone marrow and migrate through the bloodstream to the secondary or tertiary lymphoid organs. These organs are the site of proliferation, affinity maturation, and selection of B cells, which occurs in their specialized compartments called germinal centers (GCs) (15). After early GC is

established in the follicle center next to the follicular dendritic cell zone, it is divided into light and dark zones. The dark zone is the place of proliferation, somatic hypermutations, and, eventually, class switching. In contrast, the light zone is where the selection occurs based on the affinity of BCRs to antigens stored on follicular dendritic cells. B cells bearing low-affinity BCRs are eliminated, and those with higher affinity for antigen either recycle, become effector plasma cells, or memory B cells (14). All of the fate decisions seem to be strictly related to the absolute affinity of BCR of each B cell to antigen and to the affinity of BCR of each B cell to antigen compared to BCRs of other B cells in the germinal center (14). Plasma cells are unique producers of soluble antibodies, contributing to humoral immunity. The heavy chains of antibodies can be of IgM, IgD, IgG, IgE, or IgA isotype, which significantly influences their function. IgA molecules are the most abundant class in the mucosal tissues (16). Secreted antibodies significantly contribute to the activation of the complement system, opsonization of pathogens, their neutralization and phagocytosis by specialized immune cells, and the antibody-dependent cell-mediated cytotoxicity (17).

T cells

T cells are responsible for the coordination of many aspects of adaptive immunity. They play a key role in eliminating cells infected with intracellular parasites, mutated cells and in the maturation of B cells to memory B cells and plasma cells. The primary mediator of T cell activation is the T cell receptor (TCR). In addition, costimulatory signals are needed for T cell survival, proliferation, and differentiation (18). Maturation of T cells starts in the thymus, where T cell precursors undergo rearrangement of TCR receptor genes as well as the expression of TCR-associated proteins such as CD3 complex and co-receptors CD4 and CD8.

Interacting with the stroma of the thymus, T cell precursors undergo an initial phase of differentiation. After one week of development, they are called double-negative thymocytes. Despite expressing T cell-specific molecules such as CD2 or CD7, they still lack markers of mature T cells such as TCR:CD3 complex as well as CD4 and CD8 co-receptors. However, in this stage, two populations of more mature lineages can be differentiated from the main population – γδ T cells and type I NKT cells – both bearing TCR of minimal diversity and giving rise to a population of so-called

unconventional T cells, which lies on the border of the innate and adaptive immune system.

A critical step in the development of T cells is the TCR rearrangement. TCRs are heterodimers linked in most cases by disulfide bonds. Double-negative thymocytes first rearrange their β chains, which pair with the pre-T cell α chain forming the pre-T cell receptor. The interaction between pre-T cell α chain and conserved residues on β chains of other pre-T cell receptors triggers the expression of CD4 and CD8 co-receptors and rapid proliferation of these double positive thymocytes. When they stop proliferating, they become small double-positive thymocytes, and most of them successfully rearrange their α chains. At this moment, they undergo positive selection, ensuring that only T cells capable of recognizing self:peptide:self MHC molecular complexes survive. Thymocytes recognizing MHC class I lose expression of CD4, and those recognizing MHC class II lose expression of CD8 coreceptors. TCR expression increases and negative thymic selection begin to eliminate self-reactive cells. Only 2% of thymocytes pass the selection (1). T cells leave the thymus as CD4 or CD8 single positive naïve cells exhibiting $CD45RA^{+}CCR7^{+}$ phenotype (1).

Mature T cells then migrate to secondary lymphoid organs, many of which (Peyer's patches, mucosal lymph nodes, gut-associated lymphoid tissue, nasal-associated lymphoid tissue, and bronchus-associated lymphoid tissue) are associated with mucosal surfaces (19, 20). In addition, tertiary lymphoid tissues can form in mucosal tissue in case of infections or autoimmunity (20). In these specialized tissues, T cells encounter antigens presented on the MHC molecules of antigen-presenting cells (APCs) (21, 22). Naïve T cells, primed by antigens presented by APCs (primarily dendritic cells), expand and differentiate into effector and memory T cells and migrate to the site of the infection (21, 22). T cells in tissues might gain tissue-resident memory phenotype ($CCR7^{-}CD69^{+}$), which hinders their migration to the blood (23). These T cells may remain in tissues for years without recirculation (23, 24).

The process from encountering the pathogen for the first time to generating an efficient adaptive immune response takes up to seven days. However, it leads to the production of highly specific BCRs and TCRs and the immunological memory mediated by B and T memory cells lasts up to several decades and allows rapid response after repeated encounters with the same pathogen (25, 26).

MHC-restricted T cells

MHC-restricted T cells recognize antigens bound to MHC class I or MHC class II molecules. Their TCRs recognize complexes made by one MHC molecule and one peptide. MHC-restricted T cells represent the vast majority of circulating T cells in the human body and are the primary effectors of adaptive immunity.

MHC-restricted T cells are divided into two main populations based on the expression of CD4 and CD8 coreceptors. $CD8^+$ T cells recognize antigens bound to MHC class I molecules. MHC class I molecules are expressed by all nucleated cells and platelets and present short peptides (1). $CD8^+$ T cells are, therefore, necessary for tumor surveillance and the defense against intracellular pathogens. In response to stimulation by antigen, $CD8^+$ T cells rapidly proliferate and develop into effector cells producing IFN-γ and TNF-α and releasing cytotoxic granules containing granzymes and perforins (27, 28). The persistence and long-term memory of $CD8^+$ memory T cells depend on the activity of transcriptional factor eomesodermin. In contrast, committed short-term effector $CD8^+$ T cells to rely on the transcription factor T-bet (29).

$CD4^+$ T cells recognize antigens bound to MHC class II molecules. MHC class II molecules are expressed in large numbers only by professional APCs such as dendritic cells. These molecules bind peptides derived from engulfed and digested pathogens (1). The response of $CD4^+$ T cells following antigen encounter is less vigorous than in the $CD8^+$ T cells (28), and their further development is more complex. Most $CD4^+$ T cells are T helper cells, which can be divided into Th1, Th2, Th9, Th17, Th22, and Treg functionally different populations based on their cytokine production capacities coupled with the expression of specific transcription factors (**Fig.I-1**) (30, 31). Each of these $CD4^+$ T cell subsets has unique functional properties demonstrated mainly by the spectra of cytokines they can produce (**Fig.I-1**).

Th1 cells develop under the influence of IFN-γ and IL-12, express transcription factors T-bet and phosphorylated STAT4, and produce cytokines IL-2, IFN-γ, TNF-α, and lymphotoxin (31). They are efficient stimulators of cell-mediated immunity through activating $CD8^+$ T cells and macrophages (1).

Th2 cells develop under the influence of IL-4, a cytokine produced by activated Th2 cells but also mast cells, basophils, eosinophils, and TCR γδ cells (31, 32). They play an essential role in mucosal immunity, and their actions are highly influenced by interactions with epithelial cells and innate immune cells inhabiting mucosal tissues

(33). Th2-associated transcription factors are GATA3 and phosphorylated STAT6 (31), which trigger the expression of Th2 cytokines IL-4, IL-5, or IL-13.

Th17 cells develop under the influence of TGF-β, IL-6, IL-1, and IL-23, produce IL-17 cytokine family members such as IL-17, IL-22, IL-21, IL-25, and IL-26 as result of the transcriptional activity of RORγT and STAT3 (31). Th9 cell development requires a combination of IL-4 and TGF-β (34). The functions of Th9 cells are driven by high production of IL-9 mediated by the transcription factor PU.1 and IRF4 activity. IL-9 induces activation and proliferation of mast cells and eosinophils, making Th9 cells essential players in inflammatory processes in mucosal tissues (31, 35). In addition, Th22 cells were described as T helper cell subsets evolving under a combination of IL-6 and TNF-α, expressing the transcription factor AHR and producing high levels of IL-22 (31, 36). This cytokine acts primarily on non-immune cells, and Th22 cells play an essential role in several autoimmune diseases (37). Finally, Tregs represent the last functionally distinct population of T helper lymphocytes. They either differentiate already in the thymus or develop in the tissues under the influence of IL-2 and TGF-β (31, 38). Suppression of immune response is crucial for keeping immune reaction under control. Tregs contribute to this process by strong IL-10 production triggered by the expression of high levels of transcriptional factor FOXP3.

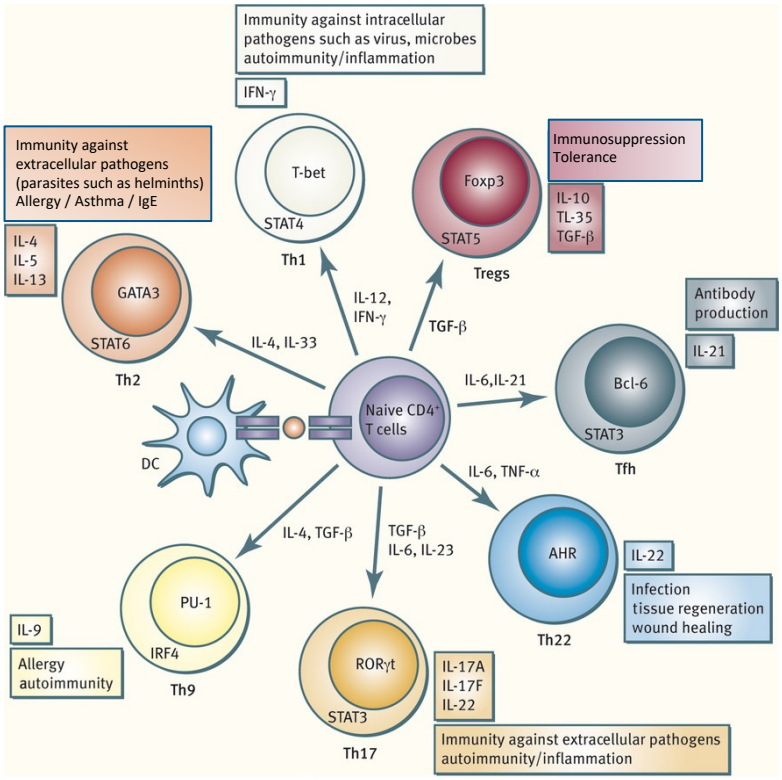

Figure I-1. CD4⁺ T cell subsets. The development of individual T helper cell subsets is driven by specific combinations of cytokines, inducing the activation of intracellular signaling molecules, which trigger the expression of transcriptional factors. These transcription factors are responsible for the functional properties of $CD4^+$ T cells. Each $CD4^+$ T cell subset is preferentially involved in different processes. Adapted from (39). AHR – aryl hydrocarbon receptor, BCL6 – B cell lymphoma 6, DC – dendritic cell, FOXP3 – forkhead box P3, GATA3 – GATA binding protein 3, IFN – interferon, RORγt – retinoid acid-related orphan receptor γ isoform t, IL – interleukin, STAT – signal transducer and activator of transcription, TGF-β – transforming growth factor β, Th – T helper.

The aging and functional maturation of classical T cells is connected with characteristic changes in the expression of surface proteins (40, 41). The most common classifications utilize expression of CD45RA and CCR7 to distinguish four main populations of T cells - naïve ($CCR7^+CD45RA^+$), T central memory (T_{CM}; $CCR7^+CD45RA^-$), T effector memory (T_{EM}; $CCR7^-CD45RA^-$) and terminally differentiated CD45RA re-expressing effector memory T cells (T_{EMRA}; $CCR7^-CD45RA^+$). Utilizing changes in telomere length during T cell aging, the expressions of CD31, CD27, CD28, KLRG1, PD1, and CD57 were shown to follow distinct trajectories during T cell development. They can therefore be utilized to track in a more detailed manner T cell proliferative history (**Fig. I-2**) (41).

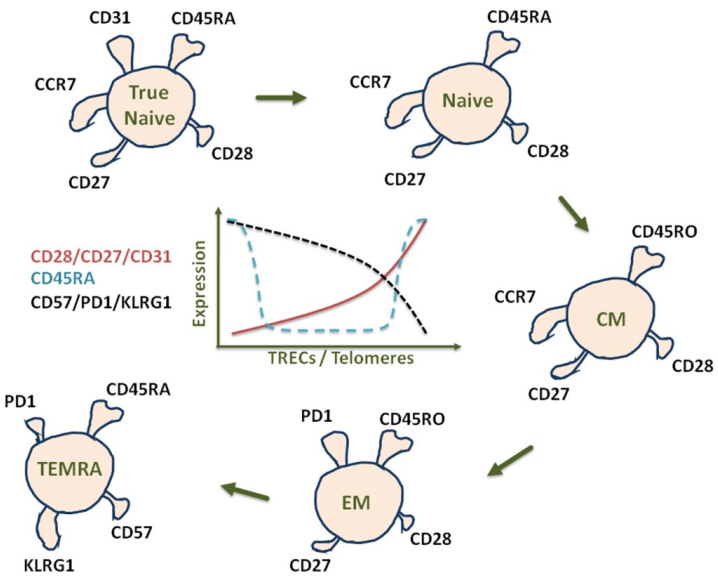

Figure I-2. Association of T cell surface markers expression with telomere length. Adapted from (41). CCR7 – C-C chemokine receptor 7, KLRG1 – killer cell

lectin like receptor G1, PD1 – programmed cell death protein 1, TRECs – T cell receptor excision circles.

Non-MHC-restricted T cells

Non-MHC-restricted T cells represent a heterogeneous group of T cells. They can be divided into cells restricted to CD1, MR1, or additional presenting molecules that are unknown. In rare cases, some TCRs can directly interact with the antigen (Ag) independently of a presenting molecule.

Mucosal-associated invariant T cells (MAIT cells), MR1T cells, γδ T cells, and CD1-restricted T cells. In some cases, the TCR heterogeneity of these cells is limited as they recognize a few Ags of microbial origin, which are shared among many microbes and therefore induce the expansion of T cells with unique TCR heterodimers. Due to their continuous interaction with microbial flora, they expand early in life and readily react to stimuli. Continuous Ag stimulation prevents the generation of memory cells resembling those observed after the recognition of microbial peptides. Furthermore, they release a series of cytokines involved in immediate defense. For all these reasons, they are frequently indicated as cells with functions of both innate and adaptive immunity (42).

CD1 restricted T cells

T cells recognizing lipids bound to antigen-presenting molecules from the CD1 family can be subdivided into invariant natural killer T cells (iNKT cells) and other T cells based on their Ag specificities.

CD1 glycoproteins present lipid antigens to T cells. There are four types of CD1 antigen-presenting molecules, CD1a, CD1b, CD1c, and CD1d divided into two groups: group I contains CD1a, CD1b, and CD1c while CD1d is the only member of group II (43). This classification is based on their protein homology. A fifth member of the CD1 family is CD1e, which promotes antigen processing (44) and presentation by other members of the CD1 family (45). While the group I CD1 expression is present only on professional APCs and thymocytes, CD1d is expressed on a broad range of cells throughout the tissues, including many cells without hematopoietic origin (46). The differences in the Ag-binding pockets of CD1 molecules result in the ability of each

CD1 antigen-presenting molecule to bind and present different lipid Ags as they all have unique sizes and antigen-binding cleft architecture (47, 48).

T cells restricted to the group I CD1 molecules have been studied in the context of their response to lipids derived from *Mycobacterium tuberculosis*. Several lipid antigens are recognized by T cells bearing a relatively broad TCR repertoire. However, the TCR repertoire specific for individual lipid antigens seems to be more limited, as demonstrated in the example of conserved TRAV1-2^{+}TRAJ9^{+} TCRs specific for mycobacterial glycolipid glucose monomycolate (49). Many CD1a and CD1c restricted T cells are also autoreactive (50, 51). Lipid antigens binding CD1 molecules are mostly amphipathic, with their lipidic tails anchored into CD1 and hydrophilic heads protruding for direct interaction with TCR (52). Another mechanism of CD1a-mediated T cell activation was described for squalene or neoantigens derived from the cleavage of amphipathic lipids. These molecules can bind deeply in the clefts of CD1a, change its conformation and allow effective binding of TCR without direct interaction between the CD1a ligand and TCR (53).

A population of T cells recognizing lipid antigens presented by CD1d is called invariant natural killer T cells (iNKT cells) (54). These cells express invariant TCRα chains made of TCR Vα24 and Jα18 chains paired to a limited number of TCRβ chains (54, 55). The second type of CD1d-restricted T cells also recognize lipidic antigens presented by CD1d, but their TCR usage is broad (48).

The first known antigen of type iNKT cells was a lipidic molecule α-galactosylceramide produced by bacteria colonizing the marine sponge *Agelas mauritianus* (56). Later it was reported that other glycosphingolipids produced by other bacteria and carrying an α-linked sugar or endogenous peroxisome-derived lipids might stimulate iNKT cells (45, 57, 58). Their importance is underscored by the fact that deficiency in type iNKT cells might contribute to the development of autoimmune diseases and increased risk of cancer (59).

Less is known about other lipid antigens stimulating CD1d restricted T cells that are not iNKT cells. Sulfatide has been shown to stimulate TCR αβ and TCR γδ cells (Most CD1d-sulfatide-specific T cells in human blood use a semi-invariant Vδ1 TCR) (45). In mice, non-iNKT cells seem associated with inhibition of anti-tumor immunity (60). In humans some CD1d-restricted T cells recognize lysophosphatidylcholine, which is present in increased concentrations in patients with multiple myeloma, but the direct link between these cells and the disease is not proven (61).

TCR γδ cells

TCR γδ T cells are a unique lymphocyte population preserved alongside TCR αβ cells for over the last 450 million years of vertebrate evolution (62). These cells are primarily defined by the expression of the TCR γδ and represent 0.2-20% of T cells in adult humans (63). The number of Vγ (14) and Vδ (8) genes is considerably lower than that of Vα (32) and Vβ (25) (64). Several Vγ genes are pseudogenes, so only six Vγ genes (2, 3, 4, 5, 8, and 9) encode functional proteins. The Vγ chains pair with different Vδ chains in a non-random fashion. Whether this is due to the unique chromosomal localization of Vδ genes, interspersed within the TCR Vα locus (64), or due to unique structural features of both chains remains to be investigated.

Each population of T cells bearing TCR with unique VγVδ chain pairs preferentially resides in a particular tissue, suggesting the existence of tissue-specific ligands for individual VγVδ combinations (65). A wide variety of heterogenous antigens and antigen-presenting molecules were already identified to stimulate TCR γδ cells (66). Notably, the activation of TCR γδ cells results in much faster and more vigorous responses than MHC-restricted T cells, resembling natural killer cells. Nevertheless, TCR γδ cells may release many different soluble factors (65). Some TCR γδ cells are also capable of TCR αβ cell priming, or facilitate IgE production by B cells or may contribute to dendritic cell maturation (65). Individual TCR γδ cells may provide local protection in some tissues and represent an immediate source of chemokines, cytokines, and other mediators and signals, which can significantly impact the activation of adaptive immunity.

The major population of the human peripheral blood TCR γδ cells expresses the TCR Vγ9Vδ2 (65). These cells are stimulated by phosphorylated metabolites generated in the mevalonate pathway of eukaryotic cells or the methyl erythritol pathway of bacteria and eukaryotes (66, 67). Activation of TCR Vγ9Vδ2 cells is mediated by binding these metabolites to the butyrophilin 3A proteins, which allows interaction with Vγ9Vδ2 TCR (68).

TCR Vδ1 cells are more prevalent in tissues, including mucosal surfaces. Vδ1 chain often pairs with the Vγ4 chain, which probably mediates the accumulation of TCR Vγ4Vδ1 cells in intestinal mucosa by interaction with butyrophilin-like molecule 3 (69).

TCR Vδ1 cells recognize broad spectra of antigen-presenting molecules such as CD1d, CD1c, or even specific MHC molecules presenting a heterogenous array of antigens (66). In many cases, these molecules and antigens are induced by stress (70). Stressed epithelial cells also express MHC class I-related molecules such as MICA, MICB, RAE1, H60, and ULBPs that bind NKG2D expressed on the surface of many TCR Vδ1 cells, influencing their activity in a TCR-independent manner (65, 66).

Mucosal-associated invariant T (MAIT) cells

MAIT cells represent a population of innate-like T-lymphocytes involved in anti-bacterial immunity. Porcelli *et al*. described in 1993 an increased usage of conserved TCRα chain gene comprised of TRAV1-2 joined to TRAJ33 among $CD4^-CD8^-$ T cells and suggested that T cells bearing this TCR might be restricted to nonpolymorphic antigen-presenting molecules (71). Preferential location of T cells bearing this TCRα chain in mucosal tissues led to naming those cells mucosal associated invariant T cells (72). *Tilloy et al.* also discovered that T cells with TRAV1-2 joined to TRAJ33 required the presence of β2M but not of known MHC class I-like antigen-presenting molecules, suggesting the involvement of a novel antigen-presenting molecule (73). This molecule was unraveled by discovering MAIT cell restriction to the MHC-related protein 1 (MR1) (72). It was later discovered that their TCR α chain pairs preferentially with a limited number of Vβ chains (74). Human MAIT cells also express high levels of CD161 (75), IL-18 receptor (76) and CD26 (77). Importantly, most of them express co-receptor CD8 (80%), only much smaller fraction is $CD4^-CD8^-$ (10-20%) and very few MAIT cells are $CD4^+$ or $CD4^+CD8^+$ (78). MAIT cells represent the most abundant innate-like T cell population in humans (79, 80), and their role in immune response remains only partially clarified.

MR1 is an evolutionarily highly conserved molecule resembling classical MHC class I molecules and consisting of three domains: the α1 and α2 domains determine an antigen-binding pocket, while the α3 domain interacts with β2M (81, 82). The gene encoding MR1 is ubiquitously transcribed in human cells (83), and the surface expression of the protein is often very low. The reason is that MR1 refolds as a stable protein and exits the endoplasmic reticulum in the presence of a ligand. It has been speculated that the low abundance of MR1 ligands limits its maturation and traffic to the plasma membrane (84, 85).

The MR1 ligands stimulating MAIT cells were first suggested to be of microbial origin, according to the observation that MAIT cells can be activated in an MR1-dependent manner by bacteria-infected APC (86, 87). Later it was found that only riboflavin-producing bacteria stimulate MAIT cells (82). These findings pointed out the potential role of MAIT cells in controlling microbial infections. This possibility is supported by the ability of MAIT cells to readily produce large amounts of pro-inflammatory cytokines (IFN-γ, TNF-α, IL-17) upon antigen recognition, as well as by the increased susceptibility of MR1-deficient mice to bacterial infections (87, 88). MAIT cells may also kill cells infected with specific bacteria species (74, 89). Their cytotoxic capacity is documented by an increase in the production of granzyme B and perforins after activation (90).

Metabolites derived from riboflavin and folic acid synthetic pathways were identified as MR1 ligands (82, 91). Importantly, MR1 ligands significantly differ in their ability to activate MAIT cells. The photosynthetic breakdown product of folic acid - 6-formyl pterin (6-FP) is non-stimulatory (82, 91). Others like 6, 7-dimethyl-8-D-ribityllumazine (RL-6, 7-diMe) can activate MAIT cells but with low potency, whereas pyrimidine-related 5-(2-oxoethylindenamino)-6-D-ribitylaminouracil (5-OE-RU) and 5-(2-oxopropilidenamino)-6-D-ribitylaminouracil (5-OP-RU) (92-95).

MAIT cells are scarce in the thymus, suggesting that they expand after migration to the mucosa or liver tissues and after encountering bacterial ligands presented by APCs (96, 97). Adult MAIT cells resemble effector memory T cells (express CDR45RO, IL7-Rα and low levels of CD62L), have distinct homing receptor profiles regulating their migration in mucosal tissues expressing often CXCR3, CCR5, CXCR1, CCR3, CXCR4 and CCR6 (98). The vast majority of MAIT cells also express the costimulatory molecules CD26, CD27, CD28, and CD150; tetraspanin family costimulatory molecules (CD53, CD63, CD81, and CD9) and receptors for IL-12, IL-18, and IL-23 (98). Interestingly, adult MAIT cells are less responsive to TCR stimulation than other T cell subsets (99), which could be overcome by co-activation with CD28 or IL12 addition (99). Transcriptomics profiling revealed that the mechanisms controlling TCR signaling in MAIT cells differ from those observed in anergic or exhausted T cells. Substantial MAIT cell activation was also reported in chronic viral infections, even though viruses and virus-infected cells do not produce

known MAIT cell ligands. In this case, a significant role may be played by cytokines IL-12, IL-15, and IL-18 released by infected cells (76).

MR1T cells

The fact that other MR1-restricted T cell populations than MAIT cells exist was discovered only recently when MR1-restricted TRAV1-2(-) T cells recognizing folate and riboflavin derivatives (100) and a TRAV12-2 clone reacting to riboflavin auxotroph *Streptococcus pyogenes* infected cells in MR1 dependent manner were described (101). Later a population of T cells, which do not react to microbial antigens or folate derivates and instead potently respond to various tumor cell lines, was discovered and named MR1T cells (102). MR1T cells are heterogenous, express a polyclonal TCR repertoire, and occur with frequencies comparable to peptide-specific T cells (<0.1%) (103, 104). While recognizing a broad range of tumor cell lines, at least some MR1T cells remain inert to nonmalignant cells (105). These observations suggest that MR1T cells might represent a population of unprecedented cancer fighters (104).

The immune system of the gastrointestinal tract

The primary role of the gastrointestinal tract is the digestion of food and the uptake of nutrients. Commensal bacteria play a crucial role in the functioning of the gastrointestinal tract, including the generation of metabolites required for metabolic and structural functions of the epithelial barrier (106). To protect the gastrointestinal tract against pathogenic bacteria, viruses, and potential food-derived compounds, an efficient mucosal immune system is needed, such as the mucosa-associated lymphoid tissues, which represent the largest mass of immune cells in the whole body (107, 108). Immune cells must dynamically interact with an epithelial barrier, microbiome, and luminal food antigens to ensure homeostasis in all parts of the gastrointestinal tract (109). Maintaining the balance between excessive and insufficient immune response in such environmental conditions is key to homeostasis in the intestine. When disrupted, chronic inflammatory conditions like Inflammatory bowel disease (IBD) or eosinophilic esophagitis (EoE) may develop.

Inflammatory bowel disease

Inflammatory bowel disease is an idiopathic, chronic remitting, and relapsing disease resulting from aberrant activation of the mucosal immune system (110). The peak onset of IBD is associated with early adulthood, but it also occurs in pediatric and geriatric populations (111). Familial occurrence of IBD has been observed (112, 113), and several allelic variants of genes and SNPs were identified to be associated with IBD development (110). IBD was originally a disease associated more commonly with Western countries; however, with the lifestyle changes also in developing countries, IBD incidence is rising worldwide (114). It suggests an important role of environmental factors in IBD pathogenesis. Interestingly, IBD development is rather connected with the dysregulation of commensal microbiome composition and activity than the presence of conventional pathogens (110, 115). IBD is traditionally dichotomized into Crohn's disease (CD) and Ulcerative colitis (UC).

Crohn's disease

Crohn's disease (CD) is a progressive and destructive transmural disease that can affect any part of the gastrointestinal tract. Approximately one-third of CD patients present with small-bowel, one-third with ileocolonic, and one-third with large-bowel manifestation or perianal manifestation (116). However, the involvement of the upper gastrointestinal tract (esophagus, stomach duodenum, jejunum) substantially differs among the studies (116). The etiology of CD remains unclear, although the contribution of genetic, epigenetic, immunological, and environmental factors has been identified (116). Genetic contribution to CD is relatively strong, with the concordance rate among monozygotic twins at 58.3% (113).

Several molecular mechanisms with important roles in CD pathogenesis are known (**Fig. I-3**). Initially, CD susceptibility was found to be associated with variants of NOD2 leucine-rich repeat domains responsible for increased activation of NF-κB in monocytes and macrophages (117). In genome-wide association studies, however, more than 200 other loci were identified to be associated with CD risk (118, 119). Most of these loci increase CD risk very modestly, are in regulatory regions of the genome, and the majority of them are shared by other immunological disorders (118-120). Nevertheless, a significant fraction of the heritable risk of CD development is explained

by the variability of variance in only several loci, including *NOD2*, *IL-23R*, or *ATG16L1* (118, 121-123). *NOD2* and *ATG16L1* mutations impair autophagy and bacteria recognition (121, 124). IL-23 receptor bind pro-inflammatory cytokine IL-23 leading to activation of innate and adaptive immune responses mediated mainly by STAT3 activation (125). Interestingly, some rare *IL23R* variants leading to the hypomorphic function of the protein are protective against IBD development (122). In general, only slightly over 13% of CD heritability is explained by genetic factors, which underscores the importance of epigenetic and environmental influence (116, 126).

Smoking and diet are among the most important environmental factors (127, 128). Other environmental factors associated with increased risk of CD development include early childhood exposure to antibiotics, oral contraceptives, aspirin, or nonsteroidal anti-inflammatory drugs and low dietary fiber content (129-131). Many of these risk factors influence the microbiome composition in the intestine or epithelial barrier function (115).

Changes in the microbiome seem to have an essential role in the development of CD (132). They are also likely connected with reported differences in the virome of CD patients, especially the increase of temporal phages (133). The alpha diversity of CD patients' fecal microbiome is significantly reduced (134, 135). Similarly, microbiome diversity is decreased in inflamed tissue compared to uninflamed tissue of the same patient (136). The decrease of gut microbiome diversity in CD is mainly associated with a reduction of diversity within bacteria from phylum Firmicutes (137), which generally represent most of the gut microbiota (138). Firmicutes are the leading producers of butyrate in the human colon, while propionate and acetate are produced more by Bacterioidetes (139). The abundance of many butyrate-producing species from phylum Firmicutes is reduced in CD (140-143). *Faecalibacterium prausnitzii* and several species from the genus *Roseburia* appeared in most of the studies as significantly decreased in CD (140-143). The lack of these bacteria is likely related to lower short-chain fatty acids (SCFAs) in the intestine and stool of patients with active CD (140). SCFAs are necessary for intestinal epithelial cell renewal (144). Butyrate represents the primary energy source for colonocytes (145) and has crucial anti-inflammatory functions (146). In addition, butyrate contributes to intestinal barrier function, and decreased presence of butyrate-producing bacteria might contribute to reduced gut barrier integrity in CD (146). Unlike butyrate-producing bacteria, *Enterobacteriaceae* (147), some particularly adherent-invasive *Escherichia coli* strains

(148) and mucolytic bacteria (149) are more abundant in the intestine of CD patients than in healthy people. Fecal microbial transplantation is in experimental use in IBD. In patients with UC, transplanting of the stool of donors with high microbial diversity improves clinical response (150). However, such data are currently missing for CD patients.

In a healthy gut epithelium, the mucous layer and the tight junction between adjacent epithelial cells collectively prevent the entrance of bacteria deeper into the tissue (1). Barrier function defects in CD allow bacterial penetration, which plays an essential role in the disease development (127). Paradoxically, despite the increased abundance of mucolytic bacteria, the mucus layer is thicker in CD than in healthy intestine (151). CD is the only inflammatory disease of the gut in which goblet cells are not depleted (152). MUC3, MUC4, and MUC5 expression is decreased in CD compared to healthy controls, and the expression of MUC1 is significantly reduced in inflamed areas compared to uninflamed areas of CD patient's intestine (153, 154). In contrast, the the expression of MUC2 is significantly increased in patients with severe CD (155). This suggests that an increase in mucus layer thickness might be associated with increased MUC2 production. The protective function of the mucus layer in CD can be potentially heavily impacted by reported abnormal glycosylation of mucins (155). Disruption of the mucus layer can be initiated by emulsifiers present in the western diet and might be also related to the mutations in the MUC2 gene (156, 157). Finally, an aberrant distribution and changes in the expression of claudins cause dysfunctional tight junctions and contribute to increased epithelial barrier permeability in CD (158). Neutrophil accumulation within the gut epithelium may also increase epithelial barrier permeability, further accelerating the inflammation (159).

Penetration of bacteria into tissue triggers an immediate vigorous immune response, primarily mediated by PRRs-induced activation of innate immune system. NOD2 is PRR that binds muramyl dipeptide found in all bacteria species. NOD2 variants leading to impaired bacteria recognition are the strongest genetic predisposition for CD development (121). NOD2 has important roles also on non-immune cells. Epithelial cells developed a mechanism preventing the dissemination of pathogens in healthy epithelium by destroying the dangerous content of cytoplasm in a lysosomal compartment in the process known as autophagy (160). Autophagy is significantly less efficient when people bear some allelic variants of NOD2 and ATG16L1 genes (121, 123, 124). Defective autophagy can also lead to increased endoplasmic reticulum

stress caused by the accumulation of unfolded proteins (161). The same allelic variants of NOD2 and ATG16L1 also alter the ability of Paneth's cells to produce antimicrobial proteins (162) and, in the case of NOD2, associate with low transcription of anti-inflammatory cytokine IL-10 (163).

Another change of epithelial cells in CD is decreased production of lymphopoietin, which conditions dendritic cells (DCs) to non-inflammatory phenotype (164). In line with increased bacterial infiltration, DCs in CD express markedly increased TLR levels, produce more IL-6 and IL-12, and express surface CCR7 which drives them to secondary lymphoid organs (165, 166). DCs from Peyer's patches imprints the gut tropism on T cells they activate (167). Leukocyte's ability to attach to intestinal epithelium depends on the expression of integrin α4β7, which bind MAdCAM1 molecules expressed on intestinal epithelial cells (168, 169).

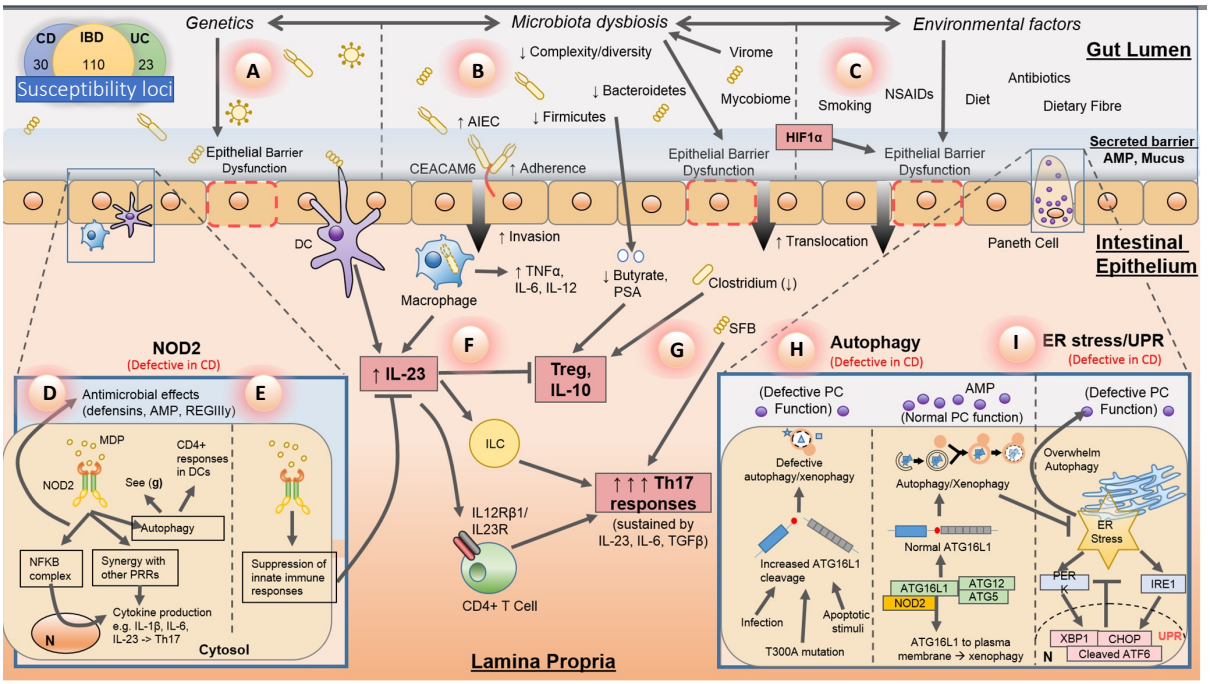

Figure I-3. Main molecular mechanisms in the pathogenesis of CD. A) CD is more likely to develop in people with genetic predispositions (such as NOD2 mutations) and **(B**) it is associated with microbial dysbiosis, decreased microbiome diversity and increased levels of AIEC. **C**) Environmental factors such as smoking and diet contribute to epithelial barrier disruption. **D**) There are two main theories about how defective NOD2 protein contributes to CD development. The first is based on the inability of defective NOD2 to efficiently trigger innate immune responses normally initiated by the binding of MDP to NOD2. This results in less efficient anti-bacterial responses and the persistence of intracellular bacteria. The second theory (**E**) is based on the inability of defective NOD2 to suppress cytokine effect (such as that of IL-23), which results in enhanced Th17 responses and inhibition of Tregs (**F**). **G**) Some microbes, such as SFB, preferentially induce Th17 responses, while others, like those

from genus *Clostridium* (reduced in CD) potently induce Treg cell responses. **H**) Mutated ATG16L1 leads to defective autophagy. **I**) Autophagy and UPR regulate ER stress as compensatory mechanisms. When autophagy is disrupted high ER stress can negatively affect functions of Paneth cells. Adapted from Boyapati et al. (170).
AIEC – adherent invasive *E. coli*, AMP – antimicrobial peptides, CD – Crohn's disease, ER – endoplasmic reticulum, MDP – muramyl dipeptide, N – nucleus, SFB – segmental filamentous bacteria, UPR – unfolded protein response, PC – Paneth cell, UC – Ulcerative colitis.

CD is associated with aberrantly increased responses of $CD4^+$ T cells, specifically of Th1 and Th17 cells (171, 172). Development, activation, and expansion of Th1 and Th17 cells in CD are triggered by IL-12- and IL-23-producing APCs and macrophages (116, 173, 174). Macrophages generally display an anergic signature in the gut mucosa, but in the CD, they display pro-inflammatory phenotype secreting IL-6, IL-23, and TNF-α (164). Th17 cells produce multiple cytokines, including IL-17 and IL-22 (175). Notably, IL-21 can further promote Th1 signaling and the production of IFN-γ (176). The pro-inflammatory cytokines IL-17, TNF-α, and IFN-γ increase inflammation by stimulating the production of IL-1, IL-6, IL-8, IL-12, and IL-18 by macrophages, monocytes, and epithelial cells (174). Finally, $CD4^+$ T cells with Treg phenotype and functional capacities are also expanded in the CD lesions (177). Although Tregs do not fully inhibit inflammation, they might prevent disease development and acceleration. Mutations in the gene for major Treg cytokine – IL-10 – and its receptor are associated with the early onset of IBD (178).

The proportion of $CD8^+$ T cells among intestinal intraepithelial lymphocytes is decreased, but among lamina propria lymphocytes is increased in CD (179). Analysis of heterogeneity of CD8 T cells in CD revealed that in CD patients, the transcriptional profile of $CD8^+$ T cells expressing gut residence marker CD103 is shifted towards a Th17-like (180). Concomitantly, the $KLRG1^+$ CD8 T cells proportion is higher in the intestine of CD patients than in healthy controls (180). And these cells show higher cytotoxic and proliferative potential compared to $KLRG1^-$ CD8 T cells (180). An increase of $CD8^+$ T cells expressing the cytotoxic molecules granzyme B and perforin was also documented in the blood of patients with active CD compared to those in remission and healthy controls, and they are associated with postoperative endoscopic recurrence (181). Finally, the importance of $CD8^+$ T cells in CD is well demonstrated by the ability of their gene expression profile to predict the prognosis of CD patients (182).

The involvement of TCR γδ cells in CD was studied regarding circulating as well as intestinal mucosa resident TCR γδ cells. Studies performed with a small number of patients (<10) documented an increase in TCR γδ cells in the blood of CD patients mainly driven by an increased presence of TCR Vδ1$^+$ cells (183, 184). A more recent study based on larger patient numbers (40 inflamed and 40 healthy) documented the exact opposite – a profound decrease in TCR γδ cells in the blood of CD patients (185). At the same time, according to Mann *et al*., TCR γδ cells isolated from the blood of CD patients express increased levels of the colon-homing chemokine receptor CCR9 (186).

Similarly contradictory are also the results from the studies of TCR γδ cells found in the intestinal mucosa. The first study mentioning TCR γδ cells in CD documented no differences in their proportion as compared to the control sample (187). On the contrary, later studies reported a decrease of TCR γδ (179) or specifically of TCR Vδ1 cells (184) in the inflamed intestinal mucosa of CD patients. Paradoxically, TCR Vδ1$^+$ cells expressing IFN-γ are more frequent in inflamed areas of CD patients' intestines than in non-inflamed areas (188). Recently it was demonstrated that the proportion of CD39$^+$TCR Vδ2$^-$TCR γδ cells decreases in inflamed regions of CD patient's intestine (189). These pieces of knowledge suggest that TCR γδ cells might play a role in CD pathogenesis, but more information is needed for its understanding.

Crohn's disease treatment

Currently, in patients with CD, corticosteroids, immunomodulators such as methotrexate or thiopurine, and biologics represent the main pillars of the drug treatment (190, 191). Numerous serious side effects of thiopurines and corticosteroids and limited success in achieving clinical remission stressed the importance of the development of novel, safer, and more efficient therapies.

The Association of increased TNF-α in mucosa and lamina propria with CD led to the development of the first targeted therapy and its successful test on 10 CD patients(192). This small study promoted the use of monoclonal antibodies against cytokines and their receptors involved in CD pathogenesis. Infliximab was the first broadly used anti-TNF-α antibody. In comparison with previous therapies, Infliximab was significantly safer and, if combined with the thiopurine drug azathioprine, induced higher remission rates in patients with CD (191, 193, 194). The drawback of this drug

is its immunogenicity in a small fraction of IBD patients. Meanwhile, other TNF-α blockers are approved for the treatment of patients with IBD (191, 195).
Understanding that the interaction of specific types of adhesion molecules on T cells with their ligands on the intestinal epithelium is needed for T cell migration to organs in the body suggested that blockage of such interaction might represent a successful strategy for the elimination of local inflammatory processes. Indeed, targeting gut homing α4β7 integrin showed some benefit even for patients with previous anti-TNF-α failure (196). Finally, the CD is a Th1 and Th17 mediated disease, and the development of T helper cells to Th1 and Th17 phenotype requires IL-12 and IL-23, produced mainly by myeloid cells. Inhibition of IL-12/IL-23 using the monoclonal antibody Ustekinumab resulted in safe and successful biological therapy for CD patients whose previous therapies failed (191, 197).

Eosinophilic esophagitis

Eosinophilic Esophagitis (EOE) is a chronic inflammatory Th2-mediated condition of the esophagus defined clinically by esophagus-related symptoms in combination with a dense esophageal eosinophilia (198). The first descriptions of the disease are dated to the late 1970 decade, reporting patients with achalasia connected with smooth muscle hypertrophy and eosinophilic infiltration of the esophagus (199). Patients often have allergic predispositions, and the immune reaction is in a significant fraction of them related to food allergens and only in a minor fraction to environmental antigens (200, 201). EoE has a worldwide increasing incidence (4.4-4.7/100000) and prevalence (43/ 100000) (202).
The inflammation in EoE is associated with impaired epithelial barrier integrity and the accumulation of many immune cell types (**Fig. I-4**) (203-205). The importance of esophageal barrier integrity for protection against EoE development is underscored by SNPs in genes involved in epithelial barrier function (filaggrin, calpain 14, desmoglein or periostin) associated with increased risk of developing EoE (206, 207). Recently, it was also shown that loss of esophageal epithelial barrier integrity through diminishing of filaggrin could be promoted by alterations in IL-20 subfamily cytokines production (208). In addition, the loss of esophageal epithelial barrier integrity can be further accelerated by a decrease of bacteria from phylum Firmicutes in EoE (209). These bacteria are an important source of butyrate, which can protect and restore the

esophageal epithelial barrier function (139, 210). Epithelial damage induces the expression of the TSLP gene encoding thymic stromal lymphopoietin, which is associated with atopy and Th2 cell activation and basophil mobilization (204, 211). Genetic variants of TSLP are also associated with an increased risk of developing EoE (211). Basophils presence is increased in EoE biopsies and contributes to eosinophil recruitment in mice model (212, 213). Barrier defect thus seems to significantly contribute to inflammation in EoE; however, whether it precedes the inflammation or is a consequence remains unknown.

Increased expression of IL-4, IL-5, or IL-13 in EoE biopsies suggests the involvement of Th2 cells in the disease (203). Th2 cells promote class switching from IgM to IgE, IgG2, or IgG4, and Th2 cytokines IL-4 and IL-13 have a significant role in these process (1, 214). Strikingly, despite IgE being the predominant antibody class in allergic responses, a substantial fraction of patients with EoE do not have increased levels of IgE (203). Possibly low importance of IgE in EoE pathogenesis was suggested by induction of experimental EoE in mice in the absence of IgE (212) or by failures of anti-IgE therapy in EoE treatment (215). A 45-fold increase of IgG4 in the homogenates of esophageal tissue in patients with active EoE compared to healthy tissue suggests that IgG4 might be an immunoglobulin class with high importance in EoE (215). This suggestion was recently supported by an observation that IgG4 levels are significantly higher in active EoE compared to Gastroesophageal reflux disease (GERD) (216).

Th2 cytokines are also crucial for the migration of eosinophils to the esophagus and their activation. IL-5 is essential for the maturation and differentiation of eosinophils in humans (217). IL-4 and IL-13 expression trigger STAT-6-dependent production of eotaxin by epithelial cells (204, 218). Eosinophils are usually absent in the healthy esophagus, and eotaxin is a ligand for CCR3 expressed in eosinophils. Therefore, Th2 cytokines-induced eotaxin production attracts eosinophils to the tissue. Migration of eosinophils to the esophagus is essential for EOE development. The distribution of eosinophils in the esophageal tissue of EoE patients is often patchy, but the granule proteins can be found distributed over the tissue even where no eosinophils occur (219-221). Eosinophils can also secrete a wide range of cytokines, chemokines, and growth factors influencing the inflammatory environment in the esophagus (204, 222). IL-9 produced by eosinophils increases mast cell influx in the murine model (223). Mast cells are abundant in EoE biopsies, and their activity results in smooth muscle

hypertrophy (224, 225). Importantly, eosinophils can serve as APCs for MHC-II restricted T cells, but whether they also can present antigens to other T cell types was not investigated until now (226).

Genetic predisposition and environmental factors may contribute to a dysfunctional epithelial-immune barrier, leading to increased exposure to environmental or food antigens and the development of an abnormal Th2 accumulation-associated inflammatory response in the esophagus. However, the interplay of different immune cell types in the esophagus of patients with EoE and many pathophysiological aspects of this chronic disorder remain largely unknown.

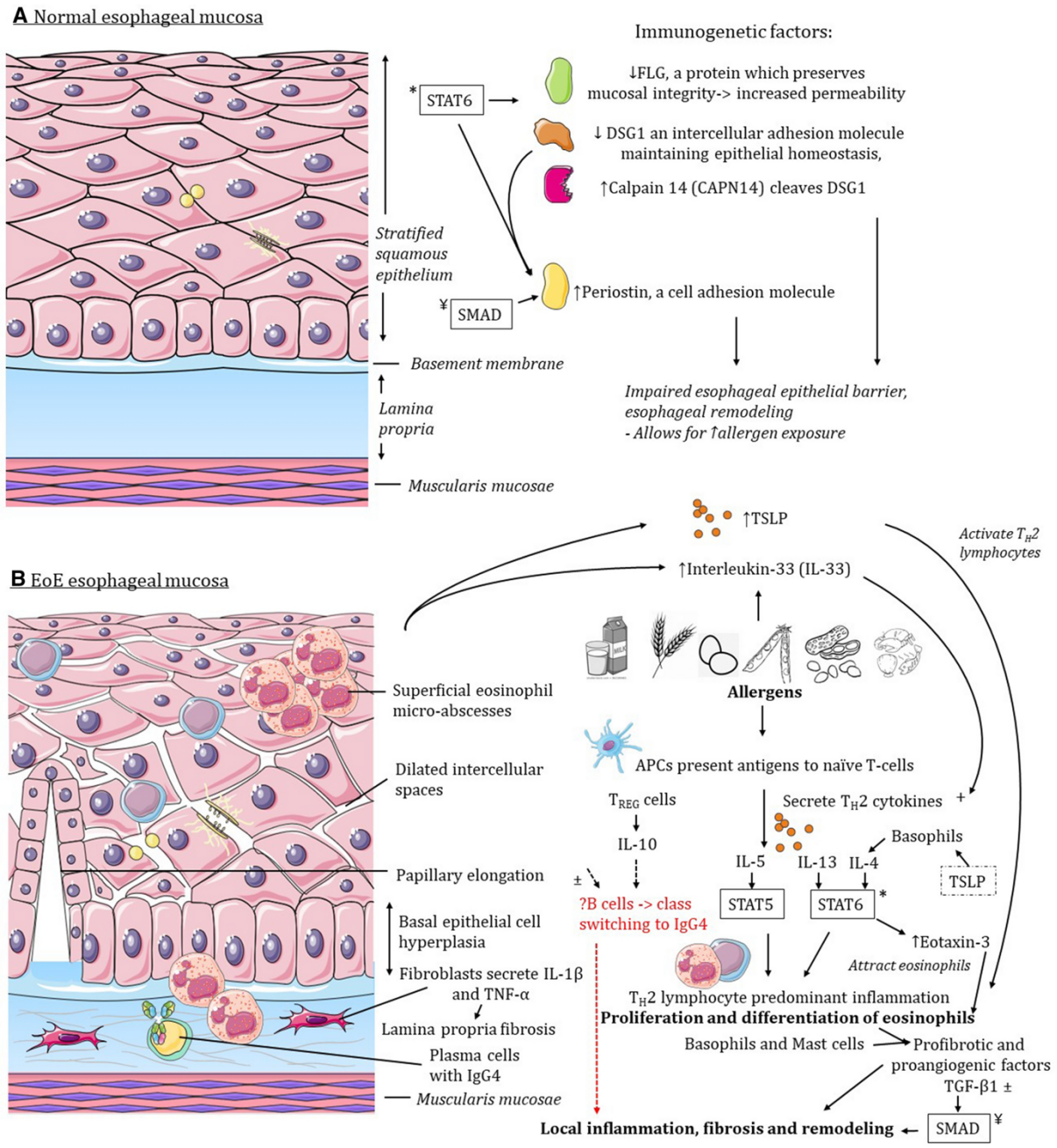

Figure I-4. **Main molecular mechanisms in the pathogenesis of EoE.** Schematic representation of: **A**) esophageal epithelium of person who does not suffer from EoE created by solid layer of stratified squamous epithelium. **B**) esophageal mucosa of person suffering from EoE. Epithelial barrier integrity is disrupted which triggers production of soluble factors such as IL-33 and TSLPs by injured epithelial cells. Disrupted epithelial layer increases the tissue exposure to food antigens. These changes promote Th2 mediated inflammation, eosinophil infiltration, esophageal inflammation, fibrosis and tissue remodeling. Adapted from (205).
CAPN14 – calpain 14, IL – interleukin, DSG1 – desmoglein 1, FLG – fillagrin, Treg - T regulatory cell, Th2 - T helper 2 cell, TSLP - thymic stromal lymphopoietin

Eosinophilic esophagitis treatment

EoE is driven by the activation of the immune system in the esophagus. The first treatment approaches, therefore, included suppression of the immune system using systemic and topical corticosteroids (202, 227). Initial usage of topical corticosteroid formulations designed for asthma was suboptimal for EoE treatment, but the introduction of orodispersible tablets with effervescent properties, as the first esophagus-targeted formulation, significantly improved their effects on EoE patients(228). Corticosteroids were able to cause remission in patients with EoE, which was, however, promptly relapsing after cessation of treatment (202). In addition, in some patients, EoE is refractory to steroid treatment. A fraction of EoE patients also suffer from gastric acid reflux to the esophagus (229). This condition can be treated by proton pump inhibitors (PPI). EoE patients can also benefit from PPI treatment, and interestingly, this is not restricted to those with concomitant gastroesophageal reflux disease (230). The therapeutic effect of Azathioprine and 6-mercaptopurine was observed only in a few cases of patients with EoE (231). Although these treatments reveal some efficacy, they are not routinely used in the clinical practice of the EoE (231).

Th2 profile of T cells activated in EoE and known food allergy background in a fraction of patients suggested that diet therapy might also be a successful approach for EoE treatment. Diet-based therapies' success underlies the importance of dietary antigens in EoE pathogenesis. Indeed, the meta-analysis revealed that exclusive feeding with amino acid-based elemental formulas proved high (90.8%) histological elimination of the disease (<15 eosinophils per high power field) (232). More common is to use a 6-food/4-food elimination diet approach (no wheat, milk, egg, nuts, soy, and fish/shellfish). Direct food elimination diet based on allergy tests resulted in histological remission in 70,2% *vs.* 45.5% of cases (232). The problem is that correctly identifying the allergen based on the allergy test result is not always warranted.

An increased understanding of disease pathogenesis might instruct attempts to develop targeted therapies. However, the development of successful targeted treatment for EoE remained an unmet goal for many years. It is mainly focused on targeting mast cells, eosinophils, and Th2 inflammatory pathways. Monoclonal antibodies directed against IL-5 (mepolizumab and reslizumab) and Siglec-8 (lirentelimab) demonstrated reduction of esophageal eosinophils or improvement of

endoscopic features, but no significant improvement in clinical symptoms was achieved (202, 233). Monoclonal antibodies against IL-13 (cendakimab) and IL-4 receptor alpha (dupilumab) lead to both histological improvement and improvement of symptoms (233). Importantly, in May 2022, dupilumab was approved in the US as the first biological therapy of EoE. A more accurate understanding of the disease pathogenesis might contribute to the development of novel and more successful therapies.

Materials and Methods

Human blood samples

Blood samples were obtained from IBD patients, EOE patients, patients with GERD, and healthy donors. Individual studies were approved by the local ethical review board (EKNZ PB_2016-02242; EKBB 2019–00273).

Peripheral blood mononuclear cells (PBMCs) were isolated by density gradient centrifugation using Lymphoprep (Stemcell). Isolated PBMCs were washed 2x in phosphate buffer saline (PBS) (Bio concept) and immediately used for experiments or viably cryopreserved in a solution containing 90% of heat-inactivated fetal calf serum (FCS) and 10% of dimethyl sulfoxide (DMSO). PBMCs were stored at -70°C for up to 3 days and then transferred to liquid nitrogen for long-term storage.

Granulocytes were isolated by density gradient centrifugation using lymphoprep (Stemcell). After aspirating the ring of PBMCs, all serum and lymphoprep were aspirated and trashed. Granulocytes and red blood cells were left in the tube and were resuspended in volume ratio 1:9 in ammonium chloride (Stemcell) and incubated on ice for 15min and washed twice in PBS containing 0.5% bovine serum albumin (BSA) and 1mM ethylenediaminetetraacetic acid (EDTA). Eosinophils were isolated from granulocytes by negative selection using an EasySep human eosinophil isolation kit (Stemcell). Monocytes were isolated from PBMCs by positive selection of CD14 expressing cells using EasySep human $CD14^+$ selection kit (Stemcell). B cells were isolated by negative selection using an EasySep human B cell enrichment kit (Stemcell). MAIT cell enriched subset of T cells was separated by negative enrichment of T cells using EasySep human T cell enrichment kit (Stemcell) followed by high-speed sorting of CD161 high (clone HP-3G10, APC, Biolegend) T cells on BD FACS Aria.

Human tissue samples

Patient samples were collected during regular gastroscopies at the Division of Gastroenterology and Hepatology at the University Hospital Basel (Basel, Switzerland).

Patient samples – Crohn's disease

Intestinal biopsies were collected from Crohn's disease patients and non-IBD donors suffering from diarrhea and predominant irritable bowel syndrome. Eight biopsies were obtained from each patient from inflamed or not inflamed segments, kept in physiological solution for transfer to the laboratory, and immediately processed. The project was approved by the ethical committee of the northwestern part of Switzerland (EKNZ PB_2016-02242). All patients involved provided written informed consent.

Patient samples – Eosinophilic esophagitis

Esophageal biopsies were collected from EoE patients, patients with GERD, and healthy donors. Five biopsies were obtained from each patient, kept in a physiological solution for transfer to the laboratory and immediately processed. The project was approved by the ethical committee of the northwestern part of Switzerland (EKBB 2019–00273). All patients involved provided written informed consent.

Intestinal and esophageal tissue processing

Tissue biopsies were cut into pieces of ± 0.5 mm in diameter using a sterile scalpel and incubated in 4 ml Gibco Roswell Park Memorial Institute 1640 media (Bioconcept) supplemented with 25mM HEPES (Cambrex), 200U collagenase IV (Sigma Aldrich), 0.5 mg/ml of DNAase I (Roche), 2,5 µg/ml of Amphotericin B (Life Technologies), 5 µg/ml of Vancomycin (Teva Pharma Ag), 30 µg/ml of Piperacillin/Tazobactam (mass ratio 8:1; Sandoz) and 10 µg/ml of Ciprofloxacin (Bayer) at 37°C for 2 hours.
Digested tissue was disrupted by pipetting, filtered through a 40 µm nylon strainer, washed 2x in PBS (Bioconcept), and viably cryopreserved in a solution containing 90% of heat-inactivated fetal calf serum (FCS) and 10% of dimethyl sulfoxide (DMSO). Samples were stored at -70°C for up to 3 days and then transferred to liquid nitrogen for long-term storage.

Flow cytometry analysis of surface markers on cells isolated from biopsies and blood

Cryopreserved cells were thawed in complete medium (RPMI media supplemented with 10 µg/ml of DNAase I, 10% heat-inactivated FCS, 100U/ml Kanamycin, 2mM stable glutamine, 1% of minimal essential medium [MEM] nonessential amino acids and 1mM sodium pyruvate [all from Bioconcept]) and immediately stained.

Screening of surface markers on IBD samples

Cells were stained with Zombie Aqua (Biolegend) diluted in PBS for 20 min at 21°C. All further steps of this protocol took 20 min each. They were performed at 4°C and with minimal exposure of cells to light. Cells were incubated and resuspended in a blocking buffer (50% PBS, 50% human AB serum). After washing in staining buffer (PBS containing 0.02% NaN3 and 0.5% bovine serum albumin), each biopsy was barcoded by staining with a combination of 1-3 anti-CD45 monoclonal antibodies (clone H30, Biolegend) conjugated with 5 different fluorochromes (**Tab. M-1**). Cells from all biopsies were pooled and stained with a combination of antibodies against surface lineage, activity and developmental markers (**Tab. M-1**). Cells were washed 2x and diluted in 5940 µl of staining buffer. 15 µl of cell suspension was added to each well of four 96-well U-bottom plates. Cells in each well were stained with different PE-conjugated antibody against one of the 360 surface markers contained in LEGENDScreen™ Human PE Kit (Biolegend) according to manufacturer recommendations. In addition, $1x10^5$ THP1 cells stained with Cell Trace Far Red (1:100; Biolegend) were added to each well after staining to decrease the loss of sample cells during washing. Cells were washed with staining buffer, fixed with fixation buffer (Biolegend), and analyzed using BD LSR Fortessa flow-cytometer with FACS Diva software (BD Biosciences).

Analysis of surface markers on immune cells from IBD and EOE biopsies and blood

Cells were stained with Zombie NIR (Biolegend) for 30 min at 21°C to exclude dead cells. Fc receptor blocking was done using Fc Receptor Binding Inhibitor Antibody (eBiosciences) at 4°C for 20 min. Staining of surface markers was performed by the mixture of monoclonal antibodies diluted in staining buffer at 4°C for 20 min (**Tab. M-2-4**). Cells were washed with staining buffer and immediately analyzed using Cytek Aurora flow-cytometer with SpectroFlo® Software (Cytek Biosciences). Autofluorescence of cells was treated as a separate fluorescence parameter to minimize its effect on the signal from fluorochromes. Quality control beads were run before each sample analysis to ensure the uniform performance of the machine.

Table M-1. Monoclonal antibodies used for the initial screening of surface markers on IBD samples.

specificity	clone	fluorochrome	ref. no	manufacturer
CD3	UCHT1	BV510	300448	Biolegend
CD137	4B4-1	PE-CY7	309818	Biolegend
CD14	M5-E2	PE-CY5	301864	Biolegend
CD161	HP-3G10	BV605	339916	Biolegend
CD19	H1B19	APC-CY7	302218	Biolegend
CD25	BC96	BV650	302634	Biolegend
CD28	CD28.2	AF700	302920	Biolegend
CD4	RPA-T4	PE-Dazzle 594	300548	Biolegend
CD45	HI30	APC	982304	Biolegend
CD45	HI30	APC-CY7	304037	Biolegend
CD45	HI30	BV711	304050	Biolegend
CD45	HI30	BB515	564586	BD Biosciences
CD45	HI30	BB700	746090	BD Biosciences
CD8	RPA-T8	PE-CY5.5	35-0088-42	Termo Fisher
CXCR3	1C6/CXCR3	BUV395	565223	BD Biosciences
KLRG1	14C2A07	BV421	368604	Biolegend
live/dead		Zombie Aqua	423102	Biolegend
γδ TCR	11F2	BV785	744743	BD Biosciences

Table M-2. Monoclonal antibodies used for the analysis of T cell populations defined by markers identified in screening of IBD samples.

specificity	clone	fluorochrome	ref. no	manufacturer
CCR7	GO43H7	AF647	353218	Biolegend
CD127	eBioRDR5	PE-CY5.5	35-1278-42	Termo Fisher
CD14	63D3	PE-Fire640	367154	Biolegend
CD155	SKII.4	PE- Dazzle 594	337616	Biolegend
CD161	DX1	BUV661	750382	BD Biosciences
CD162	KPL-1	PE-CY7	328816	Biolegend
CD19	HIB19	PE-CY5	302218	Biolegend
CD226	11A8	BV510	338330	Biolegend
CD25	CD25-3G10	PE-AF700	MHCD2524	Termo Fisher
CD27	M-T271	PE	356406	Biolegend
CD3	UCHT1	AF700	300424	Biolegend
CD357	108-17	BV421	371208	Biolegend
CD38	HIT2	APC-Fire 810	303550	Biolegend
CD39	A1	BV711	328228	Biolegend
CD4	SK3	Spark Blue	344656	Biolegend
CD45RA	HI-100	Spark NIR 685	304168	Biolegend
CD45RO	UCHL1	BV750	304262	Biolegend
CD49d	9F10	BV785	304344	Biolegend
CD49e	11A1	BUV737	741849	BD Biosciences
CD56	NCAM16.2	BUV563	612928	BD Biosciences
CD57	HNK-1	PerCP-Cy5.5	359622	Biolegend
CD71	CY164	BV650	334116	Biolegend
CD73	AD2	BUV805	748584	BD Biosciences
CD8	RPA-T8	BUV495	612943	BD Biosciences
KLRG1	13F12F2	PerCP-eFluor 710	46-9488-42	Termo Fisher
live/dead		Zombie NIR	423106	Biolegend
PD1	MIH4	BUV395	745619	BD Biosciences
TIGIT	A15153G	BV605	372712	Biolegend
Vα7.2 TCR	OF-5A12	BV480	749493	BD Biosciences
Vδ1TCR	TS-1	FITC	TCR2055	Termo Fisher
Vδ2 TCR	B6	Pacific Blue	331414	Biolegend
γδ TCR	11F2	BUV395	745681	BD Biosciences

Table M-3. Monoclonal antibodies used for the analysis of PBMCs of IBD patients and control subjects.

specificity	clone	fluorochrome	ref. no	manufacturer
CCR7	G043H7	Spark NIR 685	353258	Biolegend
CCR9	L053E8	APC	358908	Biolegend
CD103	Ber-ACT8	APC-Cy7	350228	Biolegend
CD127	eBioRDR5	PE-CY5.5	35-1278-42	Termo Fisher
CD14	63D3	PE-Fire640	367154	Biolegend
CD155	SKII.4	PE- Dazzle 594	337616	Biolegend
CD161	DX12	BUV661	750382	BD Biosciences
CD162	KPL-1	PE-CY7	328816	Biolegend
CD19	HIB19	Pe-Fire 640	302274	Biolegend
CD226	11A8	BV510	338330	Biolegend
CD25	CD25-3G10	PE-AF700	MHCD2524	Termo Fisher
CD3	UCHT1	AF700	300424	Biolegend
CD357	108-17	BV421	371208	Biolegend
CD38	HIT2	APC-Fire810	303550	Biolegend
CD39	A1	BV711	328228	Biolegend
CD4	SK3	Spark blue	344656	Biolegend
CD45RA	HI-100	Spark NIR 685	304168	Biolegend
CD45RO	UCHL1	BV750	304262	Biolegend
CD49d	9F10	BV785	304344	Biolegend
CD49e	11A1	BUV737	741849	BD Biosciences
CD56	NCAM16.2	BUV563	612928	BD Biosciences
CD57	HNK-1	PerCP-Cy5.5	359622	Biolegend
CD71	CY164	BV650	334116	Biolegend
CD73	AD2	BUV805	748584	BD Biosciences
CD8	RPA-T8	BUV495	612943	BD Biosciences
Integrin β7	FIB504	PE	321204	Biolegend
KLRG1	13F12F2	PerCP-eFluor710	46-9488-42	Termo Fisher
live/dead		Zombie NIR	423106	Biolegend
TIGIT	A15153G	BV605	372712	Biolegend
Vα7.2 TCR	OF-5A12	BV480	749493	BD Biosciences
Vδ1TCR	TS-1	FITC	TCR2055	Termo Fisher
Vδ2 TCR	B6	Pacific Blue	331414	Biolegend
γδ TCR	11F2	BUV395	745681	BD Biosciences

Table M-4. Monoclonal antibodies used for analysis of esophageal samples from patients with EoE, GERD and control subjects.

specificity	clone	fluorochrome	ref. no	manufacturer
CCR3	5E8	PE	310706	Biolegend
CD27	O323	BV510	302836	Biolegend
CCR7	HI-100	Spark NIR 685	353258	Biolegend
CD117	YB5.B8	BUV615	751618	BD Biosciences
CD11c	B-ly6	BUV805	741827	BD Biosciences
CD123	6H6	PE-CY7	306010	Biolegend
CD127	eBioRDR5	PE-Cy5.5	35-1278-42	Termo Fisher
CD14	TuK4	Pacific orange	MHCD1430	Termo Fisher
CD16	3G8	NF Blue 610-70S	H006T03B06	Termo Fisher
CD161	DX12	BUV737	748948	BD Biosciences
CD181	8F1/CXCR1	PerCP/Cy5.5	320622	Biolegend
CD19	HIB19	PE-Fire640	302274	Biolegend
CD203c	NP4D6	PE/Dazzle	324624	Biolegend
CD25	CD25-3G10	PE-AF700	MHCD2524	Termo Fisher
CD3	UCHT1	BV711	300464	Biolegend
CD38	HIT2	APC/Fire810	303510	Biolegend
TIGIT	A15153G	BV605	372712	Biolegend
CD4	SK3	Spark blue	344656	Biolegend
CD45	2D1	NF Blue 660-120S	H005T03B08	Termo Fisher
CD45RA	HI100	BUV661	741616	BD Biosciences
CD49d	9F10	BV785	304344	Biolegend
CD56	NCAM16.2	BUV563	612928	BD Biosciences
CD69	6B11	APC-CY7	310914	Biolegend
CD7	CD7-6B7	AF700	343126	Biolegend
CD8	RPA-T8	BUV495	612943	BD Biosciences
FcεR1	13F12F2	percp-efluor710	46-5898-82	Termo Fisher
HLADR	L203.rMAb	BV650	752489	BD Biosciences
IgA	IS11-8E10	APC	130-093-073	Miltenyi Biotec
IgD	11-26c.2a	Pacific blue	405712	Biolegend
KLRG1	2F1/KLRG1	PE-Fire810	138437	Biolegend
live/dead		Zombie NIR	423106	Biolegend
panγδ TCR	11F2	BUV395	745681	BD Biosciences
Siglec-8	837535	BV421	747875	BD Biosciences
Siglec-3	WM53	BV570	303417	Biolegend
TIM-3	F38-2E2	BV750	345056	Biolegend
Vα7.2 TCR	OF-5A12	BV480	749493	BD Biosciences
Vδ1 TCR	TS-1	FITC	TCR2055	Termo Fisher
Vδ2 TCR	B6	APC	331418	Biolegend

Cell culture

All cells were cultured at 37°C, 5% CO_2 and 95% humidity in Heracell 150i incubators (Termo Fisher). Stable tumor cell lines and freshly isolated eosinophils, B cells, and monocytes were cultured in complete RPMI media – RPMI media supplemented with 10% heat-inactivated FCS, 100U/ml Kanamycin, 2mM stable L-glutamine, 1% of minimal essential medium (MEM) nonessential amino acids and 1mM sodium pyruvate (all from Bioconcept). PCR analysis confirms the negativity of all used cell lines for mycoplasma. Transductants were generated by lentiviral transductions, and EGFP, and mCherry reporters or puromycin resistance were used to select successfully transduced cells. Expression of the transgene was, in each case, verified by flow cytometry.

T cells were expanded in RPMI media supplemented with 5% AB-positive human serum (Blutspendezentrum SRK beider Basel, Basel, Switzerland), 2mM stable L-glutamine, 1% of minimal essential medium (MEM) nonessential amino acids, 1mM sodium pyruvate (all from Bioconcept) and 100 U/ml recombinant human IL-2 (Peprotech). Functional assays with T cells were performed in the media used for stable tumor cell lines (no IL-2, no human serum), and in case surface marker expression was the readout of the assay, T cells were cultured in this media 24h prior to assay. Details of functional assays are later described separately for each experiment.

Analysis of T cells cytokine production by flow cytometry

Intracellular detection of cytokine production requires a relatively short (4-12h) incubation time, and blocking of cytokine excretion is also necessary. Protocols were optimized in regards to the type of stimulus and analyzed cytokines.

Stimulation of CD biopsies derived T cells for detection of cytokine production by intracellular staining

Cells isolated from intestinal tissue samples were thawed and cultivated in RPMI media supplemented with 10 µg/ml of DNAase I, 10% heat-inactivated FCS, 100U/ml

Kanamycin, 2mM stable glutamine, 1% of minimal essential medium (MEM) nonessential amino acids and 1mM sodium pyruvate (all from Bioconcept), 2,5 µg/ml of Amphotericin B (Life technologies), 5 µg/ml of Vancomycine (Teva Pharma Ag), 30 µg/ml of Piperacillin/Tazobactam (mass ratio 8:1; Sandoz) and 10 µg/ml of Ciprofloxacin (Bayer) at 37°C and 5% CO_2 for 12 hours. Cells were washed and resuspended in a complete medium containing PMA (50 ng/ml), calcium ionophore ionomycin (1 µg/ml), Brefeldin A (5 µg/ml), and Monensin (1mM) (all from Sigma-Aldrich) for 5 hours.

Stimulation of MAIT cells by 5-OP-RU pulsed eosinophils, monocytes, or B cells for detection of cytokine production by intracellular staining

Eosinophils, B cells, and monocytes (10^6/well of flat-bottom 96 well plates) isolated from blood were pulsed for 3h with serial dilution of 5-OP-RU. T cells (MAIT cell clone or MAIT enriched population [$CD161^{high}$ negatively enriched T cells] from blood) were added in APCs:T cells ratio 5:1 for 9h. After 1h of incubation, Brefeldin A (5 µg/ml; Sigma Aldrich) was added.

Intracellular staining of cytokines

Live/dead staining and surface receptor staining (**Tab. M5**) was performed as described above. Cells were subsequently washed with staining buffer, fixed with fixation buffer (Biolegend), and permeabilized using permeabilization buffer (Biolegend). Cytokine staining was performed on permeabilized cells (**Tab. M5**). Staining of surface markers downregulated on the surface after PMA/ionomycin stimulation (CD3, CD4, CD38, CD39, TCR Vδ1) was performed again also on permeabilized cells (**Tab. M5**). Cells were washed with staining buffer and immediately analyzed using Cytek Aurora flow-cytometer with SpectroFlo® Software (Cytek Biosciences).

Table M-5. Monoclonal antibodies used for experiments analyzing cytokine production

specificity	clone	fluorochrome	ref. no	manufacturer
Stimulation of T cells isolated from IBD biopsies				
CD14	63D3	PE-Fire640	367154	Biolegend
CD161	DX1	BUV661	750382	BD Biosciences
CD19	HIB19	PE-Fire 640	302274	Biolegend
CD3	UCHT1	AF700	300424	Biolegend
CD39	A1	BV605	328236	Biolegend
CD4	SK3	Spark Blue	344656	Biolegend
CD45RA	HI100	APC-CY7	304128	Biolegend
CD73	AD2	BUV805	748584	BD Biosciences
CD8	RPA-T8	BUV495	612943	BD Biosciences
IFN-γ	4S.B3	BUV737	612845	BD Biosciences
IL-10	JES3-9D7	PE	501404	Biolegend
IL-13	JES10-5A2	APC	501907	Biolegend
IL-17a	BL168	Pe- Dazzle 594	512336	Biolegend
IL-2	MQ1-17H12	BV650	564166	BD Biosciences
IL-21	3A3-N2	PerCP-Cy5.5	513012	Biolegend
IL-4	MP4-25D2	BV510	500836	Biolegend
IL-5	TRFK5	BV421	504311	Biolegend
IL-6	MQ2-13A5	PE-CY7	501120	Biolegend
IL-9	MH9D1	eFluor450	48-7098-42	Termo Fisher
live/dead		Zombie NIR	423106	Biolegend
TNF-α	Mab11	BV785	502948	Biolegend
Vδ1TCR	TS-1	FITC	TCR2055	Termo Fisher
Vδ2 TCR	B6	BV711	331412	Biolegend
γδ TCR	11F2	BUV395	745681	BD Biosciences
Stimulation of MAIT cells by 5-OP-RU treated eosinophils				
GM-CSF	BVD2-21C11	Pacific blue	502314	Biolegend
CD161	HP-3G10	APC	339912	Biolegend
CD3	UCHT1	AF700	300424	Biolegend
CD66b	6/40c	PE	392904	Biolegend
IFN-γ	4S.B3	BV605	502536	Biolegend
live/dead		Propidium Iodide	P1304MP	Termo Fisher
TNF-α	Mab11	PE-CY7	502930	Biolegend
Vα7.2 TCR	OF-5A12	BV480	749493	BD Biosciences

Activation of T cells for detection of surface markers expression changes and cytokine excretion

APCs were pulsed with tested compound for 3h, washed and co-cultured with T cells for 18h in ratio APCs:T cells 2:1. Cells were pelleted by centrifugation after incubation and stained for lineage and activation markers (**Tab. M-6**). The supernatant was used for the detection of cytokines by ELISA.

Table M-6. Monoclonal antibodies used for the analysis of changes in surface markers' expression after activation.

marker	clone	fluorochrome	Ref. No	Manufacturer
CD66b	6/40c	PE	392904	Biolegend
CD137	4B4-1	PE-CY7	309818	Biolegend
CD161	HP-3G10	APC	339912	Biolegend
CD3	UCHT1	BV421	300434	Biolegend
CD69	6B11	APC-CY7	310914	Biolegend
CD94	DX22	FITC	305504	Biolegend
live/dead		Propidium Iodide	P1304MP	Termo Fisher

Detection of cytokines by ELISA

Cytokine detection by ELISA was performed using direct sandwich ELISA on Maxisorp 96 or 384 well plates (all volumes used for 384 well plates are half of those for 96 well plates). In 96 well plates, 50 µl 2.5 µg/ml of PBS diluted anti-cytokine antibody (all from Biolegend) was added per well and incubated overnight at 4°C. The plate was washed, and 100 µl of 1% TOP BLOCK solution (diluted in PBS; Lubio Science) was added per well for 1h at room temperature. Plates were washed, and 50 µl of supernatant from the assay was added per well and incubated for 2h at room temperature. A standard curve was obtained using 1:2 serial dilution of recombinant cytokines (Peprotech). Plates were washed, and 50 µl of 0.5 µl/ml of biotinylated anti-cytokine antibody diluted in 1% TOP Block was added per well and incubated for 1h at room temperature. Plates were washed, and 50 µl of 0.25 µg/ml of horse radish peroxidase-conjugated streptavidin (Biolegend) diluted in 1% TOP Block was added per well and incubated for 1h at room temperature in the dark. Plates were washed, and the presence of cytokines was revealed by incubation with 100 µl of the solution of SIGMA FAST OPD (*o*-Phenylendiamin-dihydrochloride; Sigma-Aldrich) prepared

according to manufacturer recommendation and for the time optimized for each cytokine. The reaction was stopped by 10% H_2SO_4, and the absorbance was read at 490nm on Synergy H1 (Hybrid Reader, Biotek).

MR1 upregulation assay

Tumor cell lines were incubated with the tested compound for 3-6h in a complete medium. Cells were stained for 30min on ice with 2µg/ml of APC labeled anti-MR1 antibody (Biolegend) or respective isotype ctrl (Biolegend). Cells were washed with staining buffer, resuspended in 0.5µg/ml of DAPI in staining buffer, and immediately analyzed using BD LSR Fortessa flow-cytometer with FACS Diva software (BD Biosciences).

Analysis of ERK phosphorylation

APCs were pulsed with antigen for 3h and washed with RPMI (no serum). APCs were resuspended in 50 µl/well ($4x10^6$/ml) in U-bottom 96 well plate and incubated at 37°C for 5min. $4x10^4$ T cells in 20 µl of RPMI media were added per well and spun on short spin (10sec, max. acceleration) to settle down. Cells were incubated in a water bath for 2min. 200 µl/well of cold PBS was added, and plates were spun down in a pre-cooled centrifuge (4°C) for 2min at 400g. Cells were fixed by pre-warmed fixation buffer (Biolegend) for 10min at 37°C and permeabilized using permeabilization buffer (Biolegend) for 30 min on ice. Staining of phosphorylated ERK was done using an anti-pERK antibody (Biolegend, clone 6B8B69, PE) diluted in permeabilization buffer at room temperature for one hour. Cells were washed with staining buffer and immediately analyzed using BD LSR Fortessa flow-cytometer with FACS Diva software (BD Biosciences).

Analysis of TCR-mediated activation using activation assay of TCR-transduced Jurkat β2M-KO NFAT-Luciferase

10^5 APCs per resuspended in 50 µl of complete media and, if needed pulsed or pre-incubated with antigen were plated in the flat-bottom 96-well non-transparent plate (Costar). 10^5 TCR-transduced Jurkat β2mKO NFAT-Luciferase cells were added on top and incubated for 8h at 37°C. Cells are resuspended in 100 µl of Bio-Glo™ reagent and incubated at room temperature for 30min. The luminescence was read with gain 175 and 185 and exposure 1s on Synergy H1 (Hybrid Reader, Biotek).

Flow cytometry data analysis

Flow cytometry data were analyzed using FlowJo software (TreeStar) followed by Prism and R. Thresholds for single stained samples, and small panels were performed based on isotype control-stained samples. Determining thresholds for complex panels was done by FMO controls or a combination of isotype controls and computational deconvolution of Gaussian distributions.

Flow cytometry data analysis – IBD patient samples

Gating of positive cells for each marker, except that expression of which was bimodal with clearly separated populations (CD3, CD19, CD14, Vδ1 TCR, Vδ2 TCR, Vα7.2 TCR), was done based on a combination of fluorescence minus one controls (FMOs) and isotype controls performed on cells pooled from 5 intestinal biopsies.
We identified markers that could potentially discriminate between inflamed and not inflamed phenotypes in IBD biopsies from gated T cell flow-cytometry data. We reduced the data to counts of cells from each donor with positive and negative phenotypes for each marker in the screening. The fold change difference and significance of phenotype counts were determined with a binomial mixed effects model using the lme4 package in R (234). Processes enriched for proteins with significantly changed expression in inflamed tissue on analyzed cell subsets were identified using gene ontology enrichment by the topGo package in R (235).
In the screening validation experiments, we used the percentage of positive cells for individual markers in all analyzed T cell lineage subsets ($CD4^+$, $CD8^+$, Vδ1 TCR^+, Vδ2

TCR$^+$, Vδx TCR$^+$, [γδ TCR$^+$ & Vδ1 TCR$^-$ & Vδ2 TCR$^-$], MAIT cells [Vα7.2 TCR$^+$ & CD161$^+$]). These were analyzed in Prism using statistical tests suitable for each data set based on the study design, number of groups to compare, type, and data distribution. If multiple comparisons were performed, the results' significance was assessed based on the false discovery rate approach using Benjamini, Krieger, and Yekutieli method (236) and family-wise alpha threshold and confidence levels were set on 0.05.

For identifying unique populations in inflamed tissue, we utilized clustering through the R implementation of the Phenograph method(237). Markers associated with enriched cell populations were then used for functional characterization. To counteract the difference in available cells for each donor before the clustering, the data were down-sampled by randomly selecting 1000 cells for each donor in the CD4$^+$ T cells and 500 cells for each donor in the TCR Vδ1$^+$ cells. To perform clustering with Phenograph, we used the expression data for nine markers in the CD4$^+$ T cells (CD38, CD39, CD73, CD161, CD71, CD45RO, CD45RA, CCR7, CD25) and six markers for the TCR Vδ1$^+$ cells (CD45RA, CCR7, CD45RO, CD27, KLRG1, CD57). Clusters with similar marker expressions were manually merged. Enrichment for inflamed cells in each cluster was defined by comparing the distribution of the fractions of the cells of each donor present in the cluster between inflamed and healthy through a one-sided Mann–Whitney U test, performing multiple testing correction with the Benjamini Hochberg method (238) on all the clusters defined by Phenograph (237). To lessen the effect of sampling error, the downsampling and clustering steps were repeated five times for both the CD4 and the TCR Vδ1 dataset, selecting only clusters repeated in all the iterations.

Flow cytometry data analysis – EoE patient samples

Gating positive cells for each marker was done based on gaussian mixture modeling with the threshold set on gaining 5 % of the predicted false positivity (239). Isotype controls were also performed for control purposes, and all thresholds determined by computational modeling were higher than those specified by staining by isotype controls. All cells below the cutoff were assigned to 0 for that marker. Such an approach allowed staining of 2 markers by the same fluorochrome if their expression was lineage-specific (staining of IgA and TCR Vδ2 by antibodies

conjugated with APC [IgA is expressed on $CD19^+$, $CD3^-$ cells, TCR Vδ2 is expressed on $CD19^-$, $CD3^+$ cells]). Unmixing fluorochromes with similar spectra in the complex panel can in some cases lead to a diagonal spread of the negative population. Based on that observation, cells negative for marker A below the *ad hoc* threshold were assigned as negative also for marker B. We then conducted hyperbolic arcsine (arsinh) transformation on the raw data with a coefficient of 150. Clustering and differential cluster abundance analysis was performed using the functions provided by the diffcyt package, adapting the workflow described in Nowicka *et al*., 2019 (106, 240, 241).

We performed clustering for all $CD45^+$ cells and single subsets defined through pre-gating on the transformed data through FlowSOM (242), using specific marker panels for each subset (pan γδ TCR, CD8, CD56, CD117, CD161, CD11c, Siglec-8, IgD, Vα7.2 TCR, CD14, HLA-DR, CD3, α4 integrin, Vδ1 TCR, CD4, FCεR, CCR3, CD16, CD19, CD123, Vδ2 TCR, CD7, CD38, IgA and CD127). The number of clusters used for the clustering process was also determined according to the number of cells and markers. After unsupervised clustering, we conducted a step of the manual merging of clusters that presented high similarity and, in the case of the CD45 clustering, according to known immune cell subsets.

For each clustering instance, differential abundance analysis was conducted through the diffcyt implementation of the edgeR package (240, 241, 243), which fits models and calculates moderated tests at the cluster level, sharing information on variability across the clusters to account for the difference in the number of events for each donor and between conditions. In clustering $CD45^+$ cells, we used the trimmed mean of M-values (TMM) method from the edgeR package (Robinson and Oshlack, 2010) to calculate normalization factors and adjust for the skewed abundance between conditions in some clusters, according to the diffcyt documentation. The differential abundance analysis was conducted for all conditions compared to the active EoE state, and we performed multiple testing corrections through the Benjamini-Hochberg method (238) for each cluster between the p-values extracted from the analysis for each condition. We considered only the clusters that resulted in significantly different in healthy compared to active disease and added to them whether or not they also carried significant differences for remission compared to active disease or for GERD compared to active disease.

We also conducted a more supervised activation, inhibition and tissue residence markers-centered analysis and/or functional maturation markers-centered analysis for all subsets based on the markers suitable for each subset and through a similar differential abundance analysis methodology by defining each cell in the subset as either part of a positive cluster if they expressed the marker above cutoff or a negative cluster if they didn’t.

Aims

The studies described below had two aims:

1. Describe Crohn's disease-associated changes in the composition of immune cell subsets, focusing on T cells and their functional capabilities.
2. Describe changes in the esophageal immune cell population connected with EoE

Both studies were performed on tissue biopsies, in order to investigate the changes occurring in the tissue during disease.

T cells in Crohn's disease

Introduction

CD is associated with changes in the activity and the presence of T cell subsets usually present in intestinal mucosa. Aberrantly increased Th1 and Th17 responses leading to high secretion of IL-17, TNF-α and IFN-γ cytokines are a typical characteristic of the CD (244). Development of Th1 and Th17 cells requires the presence of IL-12- and IL-23-producing myeloid cells (173). Indeed, inhibition of TNF-α and IL-12/IL-23 with monoclonal antibodies resulted in successful biological therapies, as described above. Despite these successes, in many patients with CD, no response is observed during these treatments suggesting alternative pathophysiological mechanisms. In the near past, the role of other T cell subsets ($CD8^+$, $\gamma\delta$ TCR^+) in CD pathogenesis was discussed, and comprehensive screening-based studies revealed that immune cell subsets with unique plasticity and immune-regulatory properties accumulate in CD patients (182, 245-247).

Here, a flow-cytometry-based approach and *in vitro* stimulation assays were used to identify phenotypes and functional capacities of T cell populations enriched or diminished in inflamed intestinal tissue of patients with CD.

Patient characteristics

Patient samples were obtained from a total of 84 subjects; their characteristics are summarized in **Table 1-1**. From each patient with active Crohn's disease, bioptic tissue from areas with visible inflammation (defined as inflamed biopsies) and, if possible, from visually normal tissue (defined as not inflamed tissue) were collected. Finally, visually apparently normal tissue was collected from patients in clinical remission and healthy controls. No significant differences between patients with active disease, patients in remission, and healthy donors regarding age and gender were observed.

Table 1-1. Clinical and demographic data of patients included in the study of CD.

Variable	CD active (%) (n= 52)	CD in remission (%) (n = 19)	HC (%) (n = 13)
Male	36 (69.2%)	9 (47.4%)	8 (61.5%)
Median age at sample,	41 (17-67)	53 (19-70)	42 (19-61)
Median age at diagnosis, y, (range)	23.5 (10-64)	28 (8-43)	-
Smoker, current	19 (36.5%)	3 (15.8%)	5 (38.5%)
Montreal Class			
A1	9 (17.3%)	2 (10.5%)	-
A2	33 (63.5%)	12 (63.2%)	-
A3	10 (19.2%)	5 (26.3%)	-
B1	33 (63.5%)	12 (63.2%)	-
B2	8 (15.4%)	6 (31.6%)	-
B3	7 (13.5%)	-	-
B3p	3 (5.8%)	1 (5.3%)	-
L1	7 (13.5%)	4 (21.1%)	-
L2	12 (23.1%)	2 (10.5%)	-
L3	33 (63.5%)	13 (68.4%)	-
L4*	11 (21.2%)	-	-
HBI Score			
Remission (0-4)	22 (42.3%)	17 (89.5%)	-
Mild (5-7)	16 (30.8%)	2 (10.5%)	-
Moderate (8-16)	11 (21.2%)	-	-
Severe (>16)	3 (5.8%)	-	-
Medications			
Steroids (oral)	5 (9.6%)	-	-
Anti-IL-12 IL-23	2 (3.8%)	1 (5.3%)	-
Azathioprine	7 (13.5%)	4 (21.1%)	-
Anti-TNF-α Antibody	28 (53.8%)	11 (57.9%)	-
No treatment	15 (28.8%)	3 (15.8%)	-
Extraintestinal Manifestations	24 (46.2%)	7 (36.8%)	-
Previous surgery, intra-abdominal	16 (30.8%)	8 (42.1%)	-

CD, Crohn's Disease; HC, healthy control; TNF, tumor necrosis factor.

Among active CD, 44 samples were paired inflamed and not inflamed tissue and 8 samples only from inflamed tissue

L4* concomitant upper gastrointestinal disease

Expression of surface markers involved in T cell regulation is altered in inflamed mucosa

To identify differentially expressed markers on the surface of immune cells isolated from inflamed and not inflamed areas of the CD patient's intestine, these cells were stained with 360 monoclonal antibodies specific for different surface markers. Cells were labeled with a panel of 12 monoclonal antibodies (mAbs) specific for seven cell lineages (CD3, TCR $\gamma\delta$, CD14, CD19, CD4, CD8, and CD161), two activation markers (CD25, CD137) and three functional maturation markers (CD28, KLRG1, CXCR3). To simultaneously follow the presence and the expression level of hundreds of markers on the small number of cells isolated from intestinal biopsies (on average 10^5 cells were recovered from each tissue sample), a barcoding multicolor flow cytometry-based assay was established. Pre-staining of biopsies with combinations of 5 anti-CD45 mAbs allowed analysis of cells of hematopoietic origin from up to 24 biopsies in one tube (**Fig.1-1A**), followed by demultiplexing using analytical software. This approach, in combination with the use of 360 PE-labelled mAbs, enabled the assessment of multiple samples simultaneously in the same tube (Material and Methods section for a detailed description of the method). The first round of screening performed on ten pairs of biopsies from inflamed (I) and not inflamed (NI) tissue identified 131 markers enriched in I or NI tissue. The second round of screening compared ten additional paired samples from inflamed and not inflamed tissue of patients with active disease. This second screening was performed to validate the 131 markers using the same multiplexing technique. Significant changes were confirmed for 87 markers on at least one of the analyzed immune cell subsets (monocytes, B cells, $CD4^+$ T cells, $CD8^+$ T cells, TCR $\gamma\delta$ cells) (**Tab.1-2**).

Table 1-2. Proteins with significantly different expression in at least one out of investigated immune cell lineages (B cells, monocytes, $CD4^+$ T cells, $CD8^+$ T cells, TCR $\gamma\delta^+$ T cells) in the second round of the screening.

Negl2fc – negative binary logarithm of fold change between expression of protein in inflamed and uninflamed tissue; Neglfdr – negative decadic logarithm of false discovery rate.

Names of proteins chosen for further analysis are highlighted in bold. All significant FDR (negative decadic logarithm of FDR > 1.33) are highlighted in bold.

		B cells		monocytes		$CD4^+$ T cells		$CD8^+$ T cells		TCR $\gamma\delta^+$ T cells	
	marker	negl2fc	neglfdr	negl2fc	neglfdr	negl2fc	neglfdr	negl2fc	neglfdr	negl2fc	neglfdr
1	CCR8	0.29	**1.89**	-0.04	0.02	0.55	**6.32**	0.21	0.41	0.22	0.14
2	CD100	-0.64	**1.95**	-0.87	0.38	-0.03	0.03	0.01	0.01	-0.13	0.06
3	CD119	-0.40	**1.35**	-0.04	0.01	-0.21	0.34	-0.65	0.24	1.05	0.82
4	CD11C	-0.38	0.77	0.77	1.03	-0.19	0.38	-1.01	**3.06**	-0.54	0.43
5	**CD127**	-0.40	**0.04**	0.25	0.07	-0.66	**5.72**	0.15	0.19	0.59	0.62
6	CD129	0.41	0.66	-0.36	0.29	1.14	**5.01**	0.66	0.41	-0.30	0.05
7	CD134	-0.19	0.10	-1.21	0.57	0.92	**9.31**	0.04	0.01	0.96	0.62
8	CD158	0.91	0.65	-2.70	**2.25**	0.88	0.59	0.52	0.32	1.19	0.27
9	**CD162**	2.33	**3.89**	0.53	0.19	0.75	**3.15**	0.45	0.26	0.74	0.51
10	CD163	0.78	**8.90**	-0.03	0.01	0.39	**1.80**	0.67	**1.48**	0.79	0.65
11	CD191	-1.17	**3.25**	NA	NA	1.67	**2.71**	0.27	0.06	1.58	0.28
12	CD192	-1.09	**24.91**	1.99	**4.28**	-0.97	**19.59**	-0.49	**1.80**	-0.10	0.05
13	CD194	0.61	**4.67**	-0.41	0.16	0.72	**7.82**	0.61	1.23	1.66	**2.96**
14	CD195	-0.01	0.01	0.69	0.25	-0.87	**6.81**	-0.34	0.38	-1.13	0.84
15	CD196	-0.70	**8.39**	-0.30	0.18	-0.29	1.21	0.34	0.25	1.05	0.74
16	**CD197**	0.10	0.20	-0.55	0.25	0.11	0.24	0.77	**2.73**	-0.25	0.14
17	CD1B	1.58	0.89	-1.42	0.64	0.92	**1.50**	0.37	0.06	NA	NA
18	CD200	-0.05	0.08	-2.18	1.10	0.72	**4.14**	0.21	0.04	-0.55	0.20
19	CD203C	0.84	**2.50**	-1.60	**1.76**	-0.65	**6.32**	-1.39	**6.53**	-0.44	0.40
20	CD207	NA	NA	NA	NA	2.54	**5.44**	1.06	0.13	2.48	1.17
21	CD213A1	0.55	**1.64**	-1.24	0.15	0.35	0.28	-1.34	0.47	1.46	0.31
22	CD220	-1.27	**20.03**	-0.46	0.20	-0.14	0.05	1.92	**1.40**	1.69	0.13
23	**CD226**	0.77	**1.54**	-0.47	0.16	-0.90	**11.81**	-1.42	**9.96**	0.23	0.14
24	CD227	1.62	**4.88**	-0.31	0.10	0.05	0.02	0.41	0.14	0.91	0.36
25	CD231	-0.25	0.14	0.16	0.03	0.90	**1.68**	0.91	0.67	1.51	0.48
26	CD24	0.60	**7.68**	-0.06	0.03	0.47	**1.60**	0.17	0.31	0.65	0.32
27	CD258	-0.14	0.06	-2.91	**4.36**	0.07	0.02	1.11	0.62	-0.42	0.04
28	CD261	2.04	1.22	-0.22	0.03	1.08	**1.69**	0.32	0.12	1.27	0.64
29	CD269	-0.37	0.44	-0.54	0.26	1.12	0.89	0.66	**2.29**	1.01	0.30

		B cells		monocytes		CD4⁺ T cells		CD8⁺ T cells		TCR γδ⁺ T cells	
	marker	negl2fc	neglfdr	negl2fc	neglfdr	negl2fc	neglfdr	negl2fc	neglfdr	negl2fc	neglfdr
30	CD276	-0.88	**3.14**	-1.00	0.61	0.76	**1.99**	0.32	0.14	0.26	0.07
31	CD278	-0.69	0.29	-2.12	**3.26**	0.32	0.59	-0.07	0.06	0.00	0.00
32	CD279	-1.23	0.39	-2.02	**2.63**	-0.10	0.17	-0.03	0.02	-0.16	0.06
33	CD300C	1.00	**8.95**	1.04	0.65	0.71	**4.73**	1.10	**2.27**	0.82	0.63
34	CD301	0.33	**2.09**	1.29	**2.27**	0.10	0.20	-0.03	0.03	0.24	0.14
35	CD314	0.01	0.01	0.52	0.31	0.58	**2.13**	-0.31	0.34	-0.04	0.02
36	CD317	0.08	0.13	0.47	0.18	0.43	**1.46**	0.20	0.13	0.48	0.33
37	CD35	0.76	**6.45**	2.70	**4.20**	0.37	0.36	0.37	0.14	0.60	0.19
38	**CD357**	-1.38	**14.26**	-0.43	0.13	1.27	**14.59**	-0.09	0.09	0.45	0.35
39	CD36L1	-0.08	0.10	-1.27	0.33	1.14	**1.99**	1.49	1.12	3.00	**1.70**
40	**CD39**	0.14	0.11	2.08	**2.65**	0.48	**3.06**	-0.36	0.56	-0.97	1.08
41	**CD49d**	-1.10	**4.01**	-0.34	0.10	-0.81	**6.61**	-0.91	**2.27**	-0.75	0.44
42	**CD49e**	-0.68	**3.04**	1.67	**5.17**	0.02	0.03	0.97	**5.80**	0.92	**1.37**
43	CD49F	-0.56	**6.59**	0.91	1.27	0.87	**19.67**	0.93	**6.84**	0.69	0.98
44	CD54	0.26	0.56	2.06	**2.59**	0.05	0.08	-0.30	0.48	-0.10	0.04
45	**CD57**	-0.41	0.31	-1.71	0.77	0.54	**1.59**	0.53	1.12	-0.51	0.29
46	CD62E	-0.24	0.34	NA	NA	1.54	**3.73**	0.44	0.22	0.05	0.01
47	CD64	-0.23	0.14	3.03	**6.15**	0.46	1.05	1.12	0.74	2.15	0.40
48	CD69	-0.73	**5.99**	-1.74	**1.62**	0.03	0.03	0.14	0.12	0.66	0.36
49	CD7	-0.53	0.42	-1.32	**1.63**	0.45	1.21	0.45	0.06	-0.35	0.04
50	**CD71**	-0.04	0.09	0.13	0.05	1.22	**22.82**	2.39	**7.75**	1.99	**4.57**
51	**CD73**	-0.60	**4.34**	-0.22	0.07	-0.55	**3.04**	-0.19	0.28	1.00	**1.42**
52	CD74	-0.49	**3.16**	1.31	**1.64**	0.34	0.54	0.02	0.01	0.80	0.44
53	CD83	0.33	**1.62**	-0.97	1.13	0.18	0.31	-0.24	0.20	0.94	0.70
54	CD85A	-5.02	0.67	-0.03	0.01	1.43	**1.81**	0.22	0.10	1.06	0.15
55	CD85D	0.15	0.34	0.71	0.76	0.44	**1.56**	0.76	**2.51**	1.70	**1.43**
56	CD85H	-0.08	0.02	0.93	0.53	1.20	**1.80**	0.86	0.60	-3.49	1.26
57	CD85J	-1.09	**18.61**	2.11	**6.64**	0.58	1.03	1.21	**1.97**	0.55	0.20
58	CD87	-0.23	0.16	1.31	**1.52**	-0.10	0.09	0.09	0.04	0.03	0.01

		B cells		monocytes		CD4⁺ T cells		CD8⁺ T cells		TCR γδ⁺ T cells	
	marker	negl2fc	**neglfdr**	negl2fc	**neglfdr**	negl2fc	**neglfdr**	negl2fc	**neglfdr**	negl2fc	**neglfdr**
59	CD88	-0.36	0.25	0.98	1.22	0.85	**1.70**	0.07	0.02	1.20	0.47
60	CD89	-0.71	**6.42**	1.87	**2.91**	0.25	0.45	0.41	0.77	0.43	0.19
61	CD90	-0.02	0.00	-0.11	0.02	-1.10	**6.22**	0.19	0.08	0.57	0.10
62	CD92	-0.71	**8.48**	1.49	**2.53**	-0.42	**1.57**	0.32	0.35	0.02	0.01
63	CD93	0.42	0.14	0.28	0.12	0.89	**1.67**	0.71	0.84	0.62	0.18
64	CD99	-0.89	**6.94**	0.41	0.22	-0.64	**4.45**	-0.50	0.89	0.91	0.24
65	CXCR1	-0.55	0.42	0.47	0.26	0.41	1.16	0.44	0.72	-1.29	**1.83**
66	CXCR7	-0.12	0.11	-1.10	**2.16**	0.47	0.90	1.82	**4.95**	-0.09	0.01
67	DOP	0.60	0.58	-0.92	1.09	0.65	**3.40**	1.48	**2.53**	-0.37	0.08
68	EGFR	-2.02	**14.31**	-3.79	0.48	2.08	**16.71**	1.03	0.77	0.86	0.80
69	GPR19	-0.01	0.00	-0.37	0.06	0.91	**3.26**	0.37	0.25	0.88	0.33
70	GPR83	0.10	0.31	-0.13	0.07	0.26	**1.40**	0.43	0.94	0.75	1.03
71	IFN-γRB	-0.38	0.40	-1.14	0.98	0.71	**2.90**	0.99	0.83	0.24	0.08
72	IL15R	0.64	0.69	-0.18	0.08	0.40	0.30	1.48	**5.27**	1.07	1.28
73	IL21R	0.16	0.06	-0.85	0.34	1.40	**2.38**	0.22	0.21	1.07	0.25
74	**KLGR1**	1.02	**1.37**	-0.82	0.66	-0.32	**1.79**	1.28	**12.68**	1.05	**3.13**
75	LTBR	1.06	1.19	0.37	0.26	0.28	0.46	1.37	**4.09**	1.77	0.95
76	MERTK	-0.02	0.02	-0.52	0.40	0.62	0.83	0.86	**2.92**	-0.51	0.08
77	MRGX2	0.43	0.46	-0.25	0.12	0.66	1.08	1.41	**1.70**	-0.22	0.03
78	MUC13	-0.67	**1.52**	-1.34	0.98	0.14	0.11	0.19	0.24	-0.08	0.02
79	NOTCH1	-0.46	0.38	-2.57	**1.56**	0.81	**1.52**	0.49	0.93	0.56	0.27
80	NOTCH2	0.33	0.19	0.33	0.13	0.98	**5.34**	0.72	0.55	1.15	**1.39**
81	PDPN	-0.04	0.00	-2.93	**1.62**	1.31	1.19	0.72	0.31	-0.85	0.10
82	SIGLEC7	0.46	0.28	1.92	**1.99**	0.47	0.72	-0.03	0.02	-0.97	0.35
83	SIGLEC10	-0.14	0.25	-1.19	0.98	0.58	**1.51**	0.22	0.20	-0.15	0.04
84	SLAMF6	-0.49	**3.31**	0.13	0.05	0.66	**1.38**	-0.13	0.15	0.34	0.12
85	**TIGIT**	-0.23	0.05	-1.05	0.65	1.04	**27.57**	0.70	**3.15**	0.04	0.02
86	TMEM8A	0.21	0.09	0.24	0.09	1.23	**2.47**	0.68	0.74	-0.20	0.03
87	XCR1	0.07	0.13	-0.27	0.16	0.57	**1.99**	0.96	**3.57**	0.69	0.34

Gene ontology enrichment revealed that proteins involved in regulating leukocyte proliferation are the most significantly enriched on $CD4^+$ T cells (**Tab.1-3**). Similarly, proteins involved in endocytosis were most enriched among $CD8^+$ T cells, those involved in the chemokine-mediated signaling pathway among $CD161^+$ T cells, and those involved in the cellular defense response among TCR γδ cells (**Tab. 1-3**). Proteins involved in the regulation of TCR αβ cell activation were among the most significantly enriched in both B cells and $CD14^+$ cells, revealing the importance of T cells in Crohn's disease (**Tab. 1-3**).

Table 1-3. Two processes (defined by GO Terms) the most significantly enriched for proteins with significantly changed expression in inflamed tissue are depicted for each investigated immune cell subset (B cells, $CD14^+$ cells, $CD4^+$ T cells, $CD8^+$ T cells, TCR $\gamma\delta^+$ T cells).

Cell subset	GO ID	GO Term	pval
$CD4^+$ T cells	GO:0070663	regulation of leukocyte proliferation	0.035
	GO:0006968	cellular defense response	0.037
$CD8^+$ T cells	GO:0006897	endocytosis	0.012
	GO:0098657	import into cell	0.012
TCR $\gamma\delta^+$ cells	GO:0006968	cellular defense response	0.005
	GO:0002377	immunoglobulin production	0.006
B cells	GO:0002460	adaptive immune response based on somatic hypermutations	0.004
	GO:0046631	alpha-beta T cell activation	0.006
monocytes	GO:0050865	regulation of cell activation	0.017
	GO:0046634	regulation of alpha-beta T cell activation	0.023

Further studies were thus focused on T cells, and the relevant markers differentially expressed in at least one T cell lineage ($CD4^+$, $CD8^+$, or TCR $\gamma\delta^+$ cells) are depicted in **Fig. 1B**. Inflammation was associated with an increased proportion of T cells expressing CD71 independently of T cell lineage subset (**Fig. 1B**). CD71 is transferrin receptor, and its increased presence on T cells is associated with increased iron usage, DNA synthesis and ultimately T cell proliferation (248). $CD4^+$ T cells showed increased expression of receptors for IL-9, IL-21, EGFR, IFN-γ and opioid peptides

(IL-9R, IL-21R, EGFR, IFN-γ-R, DOP) in inflamed tissue, which pointed to increased responsiveness of $CD4^+$ T cells to these soluble factors (**Fig. 1-1B**). $CD4^+$ T cells in inflamed tissue also showed increased expression of the activation marker molecule CD357, chemokine receptors CCR8 and CCR4, inhibitory molecule CD57, and the ectonucleotidase CD39. The expression of these markers is associated with TCR-mediated activation (249). None of these markers were significantly increased in other T cell populations (**Fig. 1-1B, Tab.1-2**). The same analysis also showed a significant reduction in the $CD4^+$ T cells expressing the ectonucleotidase CD73 and the chemokine receptors CD192 and CD195. A significant decrease in CD127 and KLRG1 suggested a decrease of terminally differentiated as well as naïve and/or central memory $CD4^+$ T cells.

$CD8^+$ T cells in inflamed tissue express lymphotoxin receptor (LTBR) and IL-15 receptor more often, which is in line with the known role of these cytokines in inflammation (**Fig. 1-1B**). This observation underlines the differences in cytokine sensitivity between $CD4^+$ and $CD8^+$ cells. $CD8^+$ T cells also expressed more CCR7, TIGIT, and KLRG1, pointing to their increased activation and increased presence of terminally differentiated $CD8^+$ T cells. They also expressed more CD49e, and surprisingly in inflamed tissue, also CXCR7 (**Fig. 1-1B**).

TCR γδ cells showed an increase in CCR4-positive subset and increased expression of KLRG1 (**Fig. 1-1B**). Importantly, changes in the expression of ectonucleotidases CD73 and CD39 were opposite to those observed in $CD4^+$ T cells. $CD73^+$ subset of TCR γδ cells was enriched in inflamed tissue. In contrast, $CD39^+$ TCR γδ cells were almost half in inflamed tissue, although this difference did not reach statistical significance (**Fig. 1-1B**).

Based on their association with the expression of activation or exhaustion markers observed in the screening or based on their expected roles in mucosal T cell immunity, 13 significantly changed T cell surface proteins, including immunosuppressive ectonucleotidases (CD39, CD73), proteins related to cell migration (CD162, CD49d, CD49e), T cell activation (CD71, CD226, TIGIT, CD357) and functional maturation (CCR7, CD127, KLRG1, CD57) (**Fig. 1-1C**) were chosen for further studies. These 13 markers were used together with 18 lineage, activation, and functional maturation markers (**Tab. M-2**) to evaluate the phenotypic heterogeneity and functional maturation stages of T cells in CD biopsies.

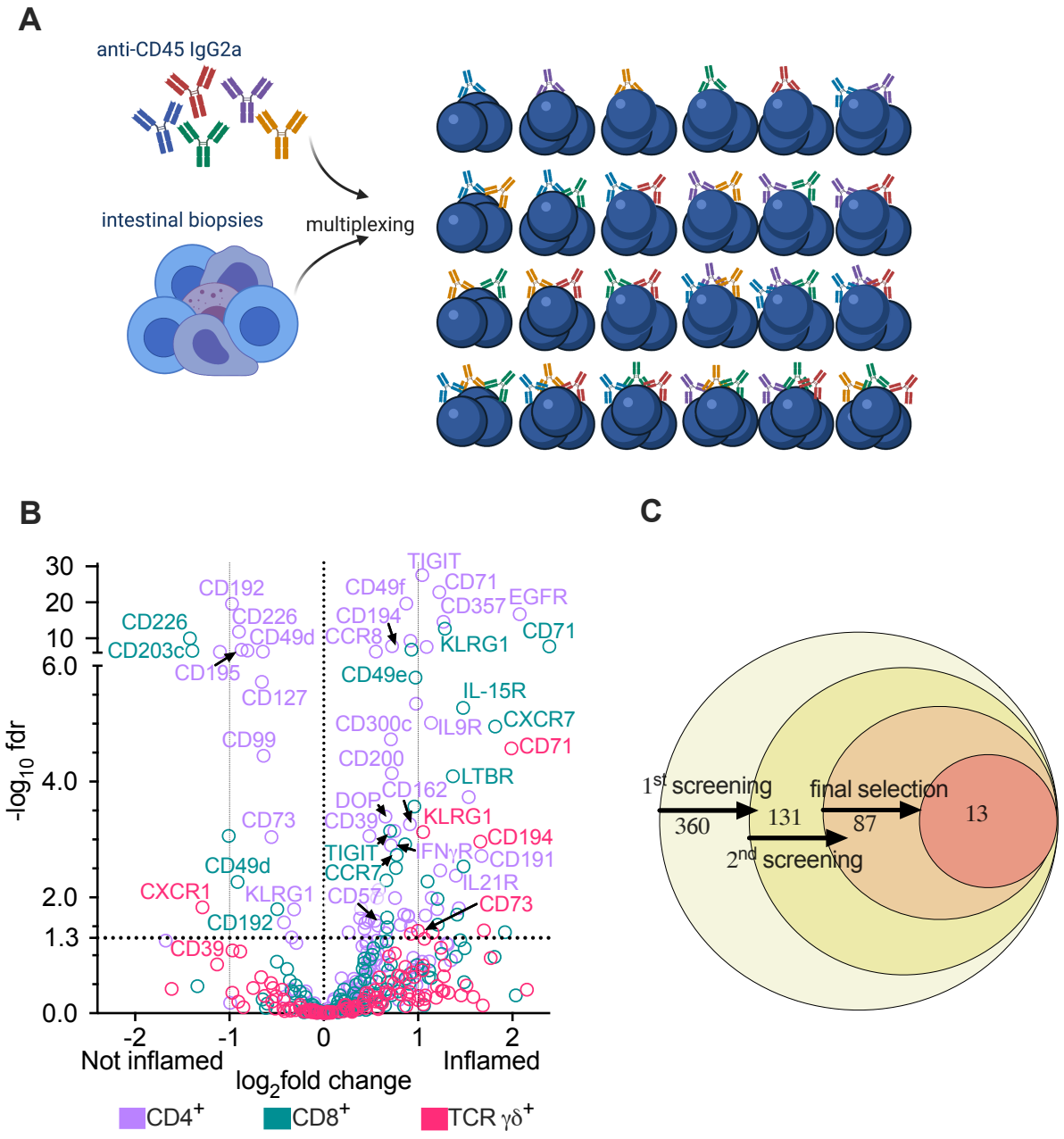

Figure 1-1. Screening and marker selection. A) Labelling of cells isolated from biopsies using differently labeled anti-CD45 mAbs was performed using a unique combination for each patient, thus allowing donor identification. **B**) Log2 fold change of the estimated probability of expression between inflamed and not inflamed tissue (x-axis) and -$\log_{10}$ of FDR corrected *p*-values (y-axis) of 131 proteins analyzed in the 2nd screening on CD4$^+$, CD8$^+$, and TCR $\gamma\delta^+$ T cells from 10 paired (inflamed / not inflamed) CD biopsies. **C**) Scheme of screening steps up to the final selection of 16 markers. Each screening was performed on different patient cohorts.

Accumulation of $CD4^+$ and proportional decrease of Vδ1 TCR^+ cells accompany CD-associated inflammation

The above-mentioned combination of markers was used to compare T cells in inflamed (I) tissue with those in not inflamed (NI) tissue, and also in tissue isolated from biopsies of patients in remission (R), and with the biopsies from healthy donors (H). Changes in the proportion of T cell lineages are expected in CD because of its well-studied association with increased activity and the presence of $CD4^+$ T cells. Indeed, the proportion of $CD4^+$ T cells was significantly increased in I and R compared to NI and H. On the contrary, $CD8^+$ cells were slightly but not significantly reduced in I *vs*. NI and H, and no significant changes were found in MAIT cell frequencies (**Fig.1-2**). Vδ1 TCR^+ cells showed a significant decrease in R, NI, and I tissue compared to H. In I tissue we also observed decreased frequency of TCR Vδ1 cells as compared to NI (**Fig.1-2**). The frequencies of TCR Vδ2 cells were unchanged among conditions. Cells expressing a TCR γδ with Vδ chains different from Vδ1 and Vδ2, named here Vδx were decreased in R, NI, and I tissue compared to the H, but their frequency was not further reduced in I compared to NI (**Fig.1-2**).

In summary, $CD4^+$ T cells were proportionally increased in inflamed intestinal tissue of CD patients, whereas a marginal decrease in $CD8^+$ T cells and several fold decrease in the proportions of Vδ1 and Vδx TCR^+ cells were detected.

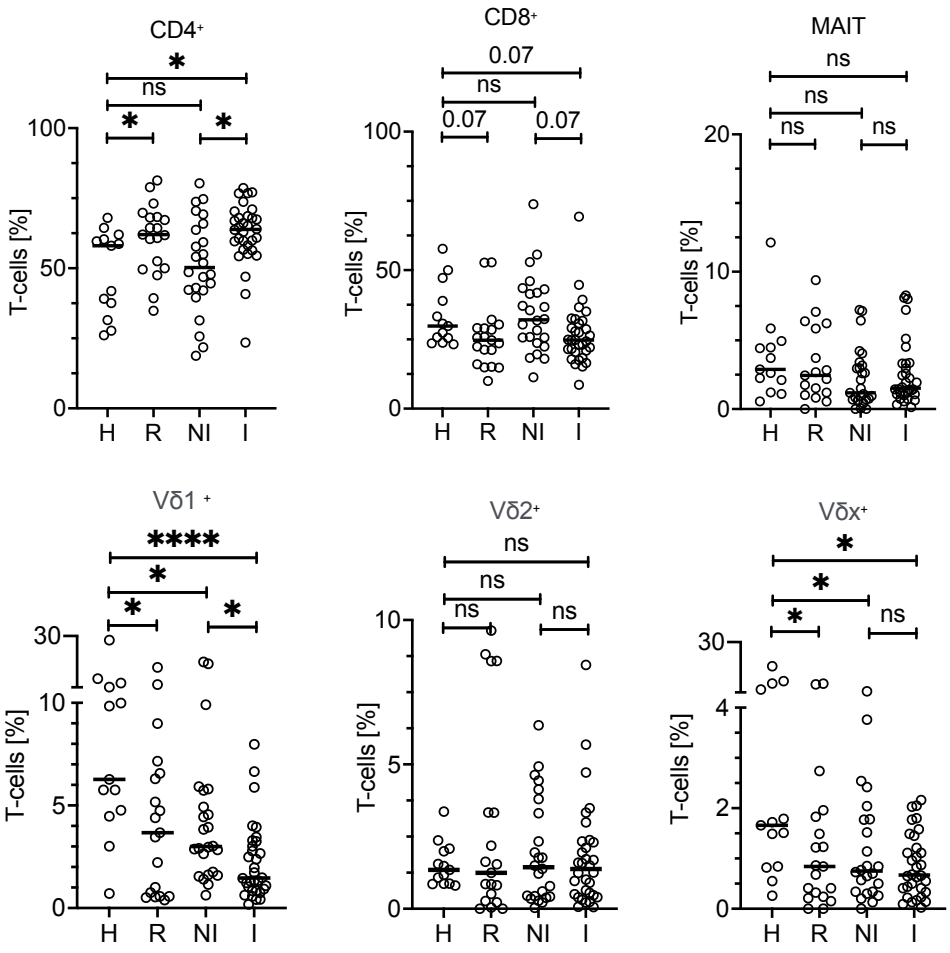

Figure 1-2. Analysis of T cell populations proportions in intestinal tissue of inflamed lesions, not inflamed areas, tissue of patients in clinical remission, and healthy controls. Horizontal bars represent median values. *=*qval*<0.05, ****=*qval*<0.0001. 24 paired (I / NI), 8 unpaired I, 19 R, and 13 H samples were used for the analysis.

Inflammation is associated with the accumulation of TEMRA T cells

The functional maturation stage of T cells strongly influences their capacity to perform effector functions and to proliferate. Primary functional maturation stages of T cells (Naïve, T_{CM}, T_{EM}, T_{EMRA}) can be determined by the expression of CD45 isoforms (CD45RO, CD45RA) and CCR7 (**Fig. I-1**) (41). The comparison of functional maturation within main T cell lineages revealed a significant increase of T_{EMRA} $CD4^+$ T cells in inflamed tissue and a decrease of T_{EM} cells $CD8^+$ T cells balanced by the rise of T_{CM} and T_{EMRA} $CD8^+$ T cells (**Fig.1-3A**). Vδ1 TCR^+ cells showed a massive decrease in $CD45RO^+$ memory populations in I balanced by the concomitant increase in both naïve and T_{EMRA} populations. Strikingly, the T_{EMRA} population was very large and represented almost half of total Vδ1 TCR^+ cells in I (**Fig.1-3B**). Vδ2 TCR^+ cells also showed a significant decrease in T_{EM} populations in I but only compared to NI and not to H and with lower fold change compared to Vδ1 TCR^+ cells (**Fig.1-3B**). There is a significant increase of TEM Vδ2 TCR+ cells in NI tissue compared to both H and I (**Fig.1-3B**). Naïve and T_{CM} Vδ2 TCR^+ cells proportion are marginally increased in I compared to NI (**Fig.1-3B**). T_{CM} Vδ2 TCR^+ are also decreased in both NI and R compared to H. Overall, no differences in functional maturation of Vδ2 TCR^+ cells were observed between I and H tissue, but NI and R are different from both I and H. Vδx TCR^+ cells show similar differences among I and NI as Vδ2 TCR^+ cells (**Fig.1-3B**). In I tissue there was increased T_{CM} and naïve Vδx TCR^+ cells frequencies compared to NI (**Fig.1-3B**). Median frequencies of Vδ2 TCR^+ and Vδx TCR^+ TEMRA cells were increased in I, but this increase was not statistically significant (**Fig.1-3B**). The increased presence of T_{EMRA} cells in several T cell subsets likely reflects their intense stimulation associated with inflammatory processes. Whether these differences are also associated with concomitant changes in the other investigated markers and the phenotypical characteristics of T cell subpopulations enriched in inflamed tissue was investigated in the following analysis.

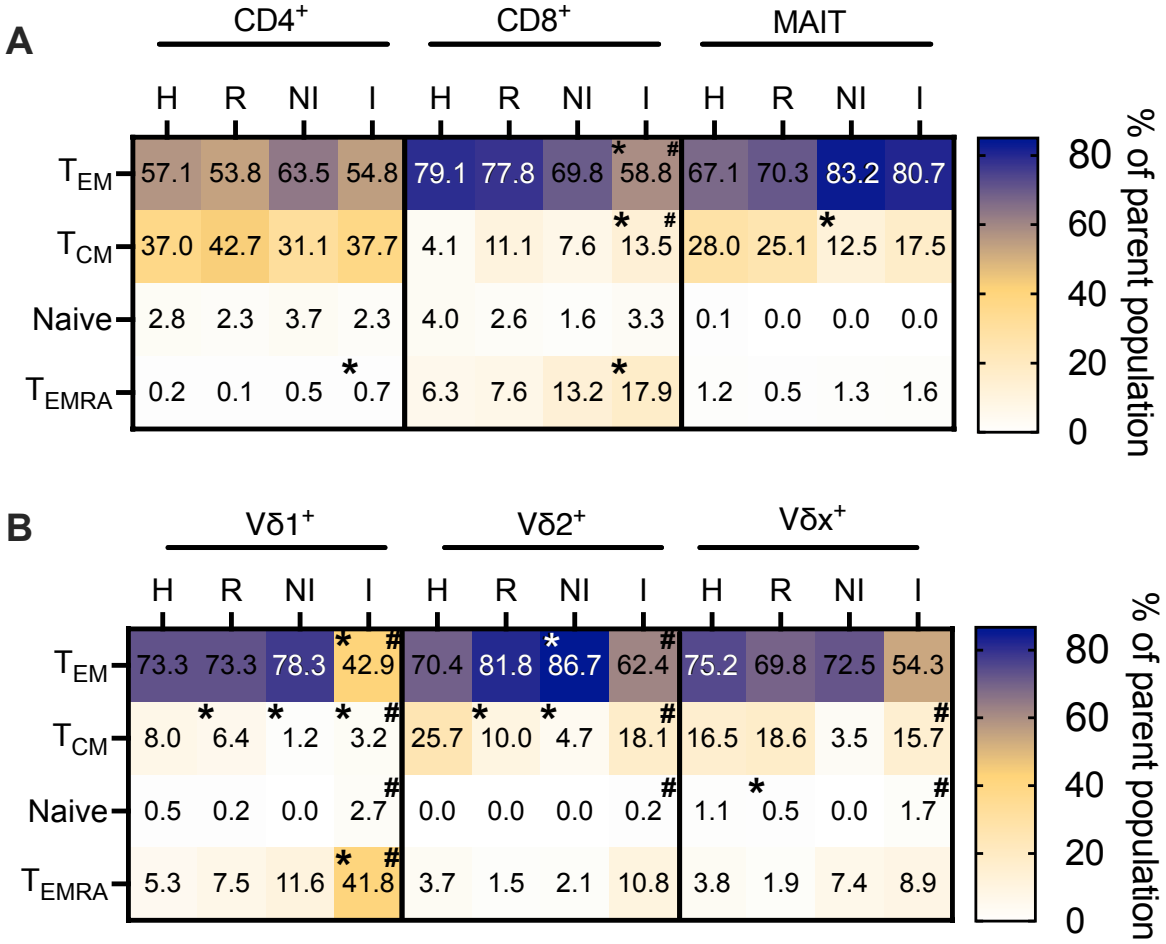

Figure 1-3. **Differences in functional maturation stages of T cell**. Median proportions of T cells of individual lineage subsets in different functional maturation stages (naive, T_{CM}, T_{EM}, T_{EMRA}) derived from I and NI tissue of patients with active disease, from R and H. **A**) CD4, CD8 and MAIT cells **B**) TCR Vδ1$^+$, TCR Vδ2$^+$ and TCR Vδx$^+$ cells.
I, NI and R were compared to healthy, and a significant difference (qval <0.05) is marked by * at the left upper corner. NI was also compared to I, and a significant difference (qval <0.05) is marked by # in the upper right corner. Twenty-four paired (I/NI), eight unpaired I, 19 R, and 13 H samples were used for the analysis.

Markers with expression changes on individual T cell subsets related to the presence and activity of CD were compared in R, NI, and I to H and in NI to I (**Fig.1-4**, **Fig.1-7**). Clusters of T cells enriched explicitly in inflamed or healthy tissue were revealed using the phenograph clustering-based method (**Fig.1-5)**. Data were spitted into two subsets for easier orientation. First, CD4$^+$, CD8$^+$, and MAIT cells were investigated (**Fig.1-4-6**), and subsequently γδ T cells (**Fig.1-7-9**).

Activated T_{EM} $CD39^{+}CD73^{-}$ $CD4^{+}$ T cells are enriched in inflamed tissue

Identifying surface proteins uniquely enriched in inflamed tissue represented the basis to reveal phenotypically distinct populations which accumulate or decrease in the tissue during disease.

In $CD4^{+}$ T cells: i) comparing I and H tissues, CD357, CD27, CD71, CD57, and KLRG1 were more abundantly expressed in I whereas CD161, CD127, and CD73 were more abundantly expressed in H; ii) comparing I and NI, CD357, CD39, CD71, and CD49e were increased in I, whereas $CD161^{+}$ and $CD127^{+}$ cells were more frequent among in NI (**Fig.1-4**).

In $CD8^{+}$ cells: i) comparing I and H, CCR7, CD27, CD71, CD57, KLRG1, and CD45RA were more abundantly expressed in I, whereas CD226 in H; ii) comparing I and NI, CCR7, CD27, CD71, CD49e, and KLRG1 were increased in I, whereas $CD226^{+}$ cells were more frequent among $CD8^{+}$ T cells in NI (**Fig.1-4**).

Finally, in MAIT cells i) comparing I and H, CCR7, CD71, and KLRG1 were more abundantly expressed in I, whereas TIGIT, CD226, CD73, and CD155 in H; ii) comparing I and NI, CCR7, CD71, CD25 and KLRG1 were increased in I, whereas $CD226^{+}$ cells were more frequent in NI (**Fig.1-4**).

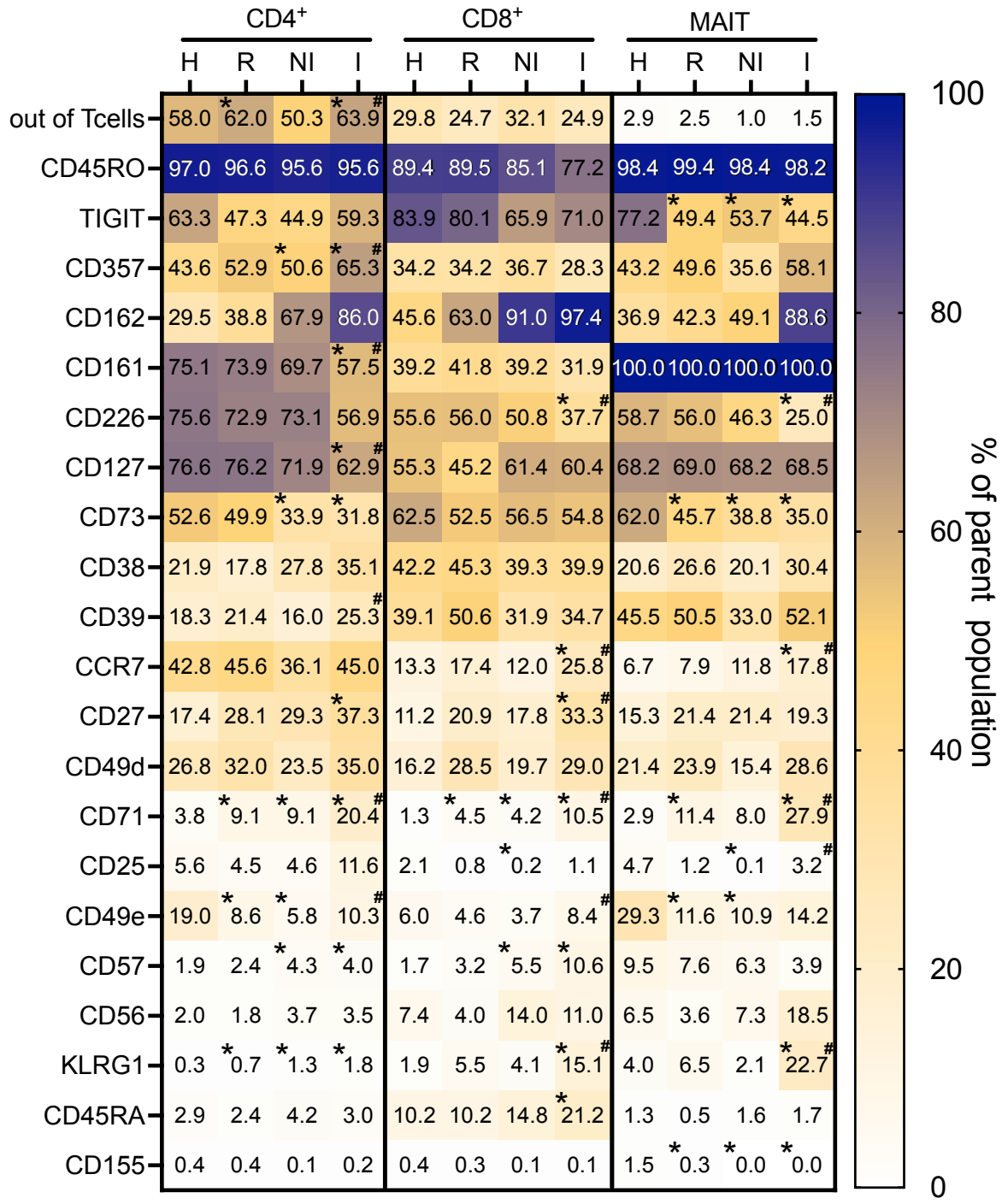

Figure 1-4. Differences in proportions of CD4⁺ T cells, CD8⁺ T cells, and MAIT cell populations expressing surface markers were identified by screening in CD patients and healthy donors. Heatmap represents median proportions. I, NI and R were compared to H, and a significant difference (qval <0.05) is marked by * at the left upper corner. NI was also compared to I; a significant difference (qval <0.05) is marked by # in the upper right corner. Twenty-four paired (I /NI), eight unpaired I, 19 R, and 13 H samples were used for the analysis.

$CD4^+$ T cells were considered the subset with the most striking changes when looking at frequency, functional maturation, and surface marker expression (**Fig.1-2, Fig.1-3, Fig.1-4**). Therefore, an analysis of surface maker co-expression was performed based on the functional maturation markers (CD45RA, CCR7, and CD45RO), the activation markers (CD38 and CD25), and other surface proteins (CD161, CD73, CD39, and CD71) considered potentially relevant based on the previous analysis to reveal the phenotype of clusters accumulating in I resp. H tissue (**Fig.1-5A**). Ten clusters were significantly more frequent in H compared to I, NI, and R (**Fig.1-5A**). From the perspective of functional maturation, more than half (6) of these represented transitional stages between TEM and TEMRA cells, which is demonstrated by the co-expression of CD45RA and CD45RO and the absence of CCR7 (**Fig.1-5A**). Similarly, 7 out of ten clusters were positive for ectonucleotidase CD73 (**Fig.1-5A**). Eight clusters were more frequent in I vs. H, 2 clusters in I vs. H and NI, 1 in I vs. H and R, and 3 in I *vs*. H, R, and NI. Most of these clusters (11) represent TEM cells, and there was no cluster co-expressing CD45RA and CD45RO. The CD161 marker (**Fig.1-5A, B)**, which was previously shown to be present in pro-inflammatory intralesional $CD4^+$ cells in CD patients(250), was also frequent (in 8 clusters). Only 2 clusters expressed CD73, while several expressed the activation markers CD71 or CD25. Clusters 13, 19, 20, 21, 22, and 23 were significantly enriched in I compared to H and also NI and/or R. These observations indicated that they represent cells specifically enriched in sites of mucosal inflammation. Five out of these 6 clusters (19, 20, 21, 22 and 23) were phenotypically similar (**Fig.1-5A, B**) and were the only clusters expressing the proliferation marker CD71 (**Fig.1-5A, B**). When we compared the expression of two ectonucleotidases (CD39 and CD73), most of these cells were $CD39^+$, and all did not express CD73.

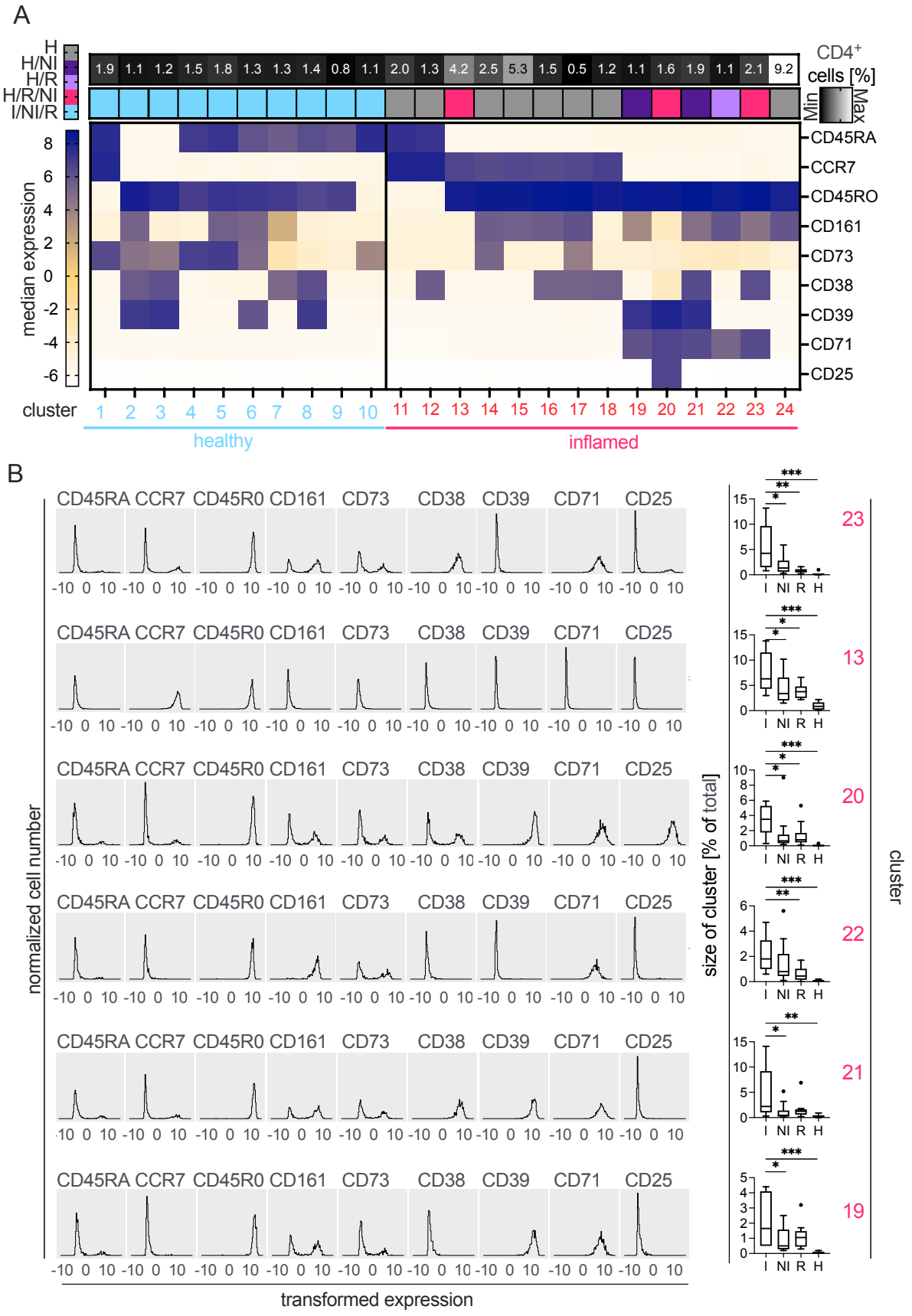
A
H
H/NI
H/R
H/R/NI
I/NI/R
1.9 1.1 1.2 1.5 1.8 1.3 1.3 1.4 0.8 1.1 2.0 1.3 4.2 2.5 5.3 1.5 0.5 1.2 1.1 1.6 1.9 1.1 2.1 9.2
CD4+ cells [%]
Min
Max
median expression
8
6
4
2
0
-2
-4
-6
CD45RA
CCR7
CD45RO
CD161
CD73
CD38
CD39
CD71
CD25
cluster
1 2 3 4 5 6 7 8 9 10 11 12 13 14 15 16 17 18 19 20 21 22 23 24
healthy
inflamed
B
CD45RA CCR7 CD45R0 CD161 CD73 CD38 CD39 CD71 CD25
-10 0 10
normalized cell number
transformed expression
size of cluster [% of total]
I NI R H
23
13
20
22
21
19
cluster

Figure 1-5. **Unique CD4$^+$ T_{EM} populations appear in the inflamed intestinal tissue of CD patients. A**) Arsinh transformed median expression of CD45RA, CCR7, CD45RO, CD161, CD73, CD38, CD39, CD71, and CD25 on the Phenograph clusters (defined by the expression of these molecules) significantly enriched (qval <0.05) for healthy (H) (1-10) or inflamed (I) (11-24) tissue. **B**) Histograms of CD45RA, CCR7, CD45RO, CD161, CD73, CD38, CD39, CD71, and CD25 expression and boxplots showing the fraction of each condition (I, not inflamed [NI], remission [R], H) represented by the cluster for the clusters significantly enriched for I tissue compared to H, R, and NI (23, 13 20), H and R (22) or H and NI (21, 19). *= qval <0.05. ** = qval<0.01. 10 I, 10 NI, 10 R, and 10 H samples were used for the analysis.

As these two ectonucleotidases were expressed in an almost mutually exclusive manner in all conditions (**Fig.1-6A**), they can be used to identify different CD4$^+$ cell populations. Indeed, single positive CD39 or CD73 populations showed highly significant differential expression of CD45RO, CD357, TIGIT, CD27, CD38, CD71, CD25, CD45RA, KLRG1, CCR7, CD161, CD226 and CD127 (**Fig.1-6B**). Notably, CD39$^+$ cells expressed markers compatible with T_{EM} phenotype, whereas CD73$^+$ cells expressed markers compatible with all T cell maturation stages (**Fig.1-6B**).

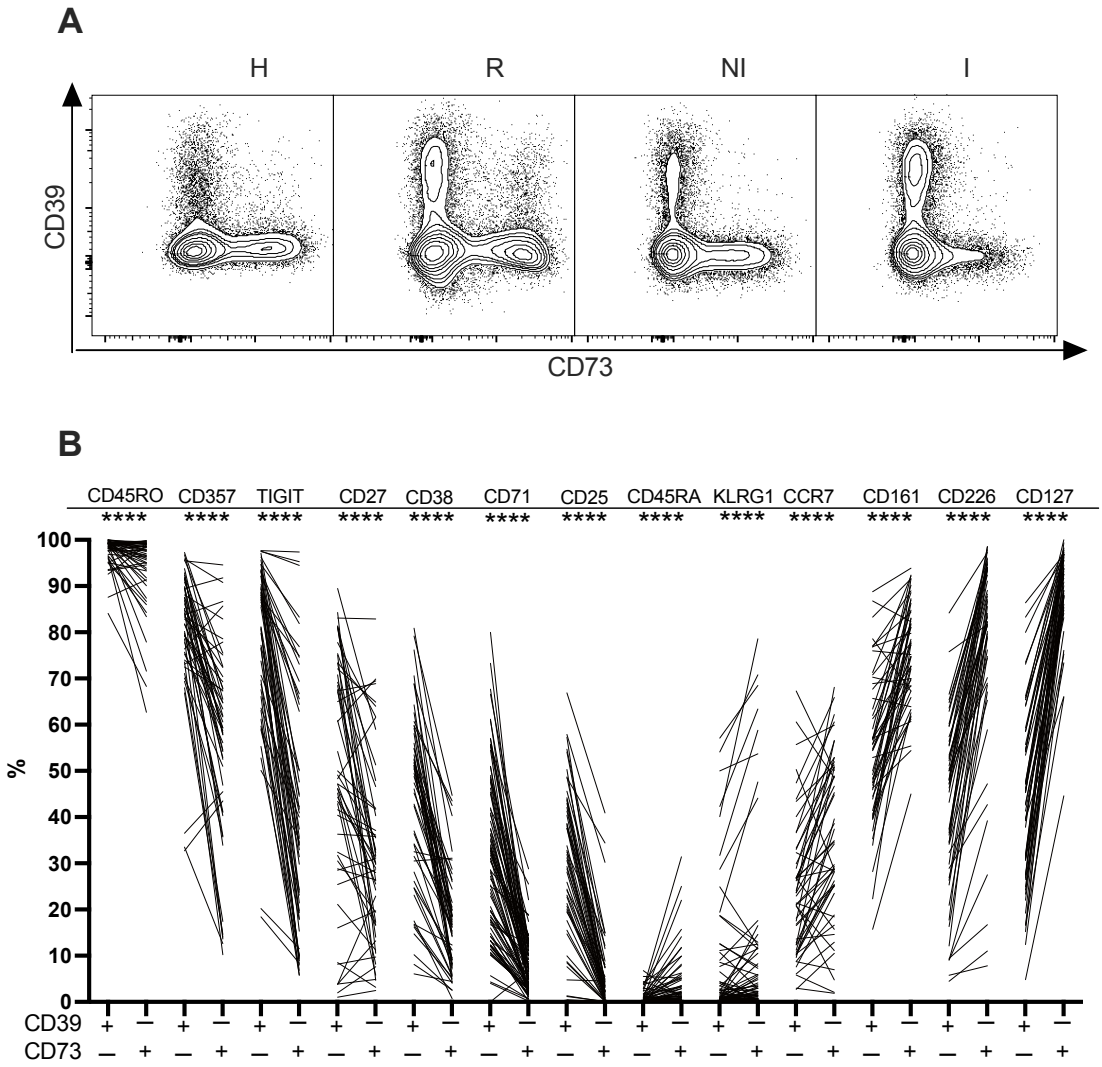

Figure 1-6. **CD39⁺ and CD73⁺ CD4⁺ T cells represent distinct and phenotypically highly different cell subsets. A**) Expression of CD39 and CD73 on concatenated CD4⁺ T cells from all analyzed biopsies from inflamed (I), not inflamed (NI), remission (R), and healthy (H) tissue. **B**) Comparison of surface markers expression between CD39⁺ CD73⁻ and CD39⁻ CD73⁺ CD4⁺ T cell subsets. *=qval<0.05, **=qval<0.01, ***= qval <0.001, ****= qval <0.0001. Twenty-four paired (I/NI), eight unpaired I, 19 R, and 13 H samples were used for the analysis.

CD39⁺ T_{EM} Vδ1 TCR are diminished in the inflamed tissue while CD39⁻ TEMRA cells proportion is increased

Analogous analysis was also performed for TCR γδ cell subsets. The abnormal increase of T_{EMRA} Vδ1⁺ cells in inflamed tissue (41.8% in I vs. 5.3 % in H; **Fig.1-3**) was associated with significantly increased expression of CD27, CD71, CD57, KLRG1, and CD45RA on these T cells (**Fig.1-7**). Furthermore, Vδ1⁺ cells in inflamed tissue

expressed less CD45RO, CD38, CD39, and CD25 (**Fig.1-9**). Vδx⁺ and Vδ2⁺ cells showed increased expression of CD71 as compared to cells in H tissue, suggesting that also these populations are activated and are proliferating in inflamed tissue.

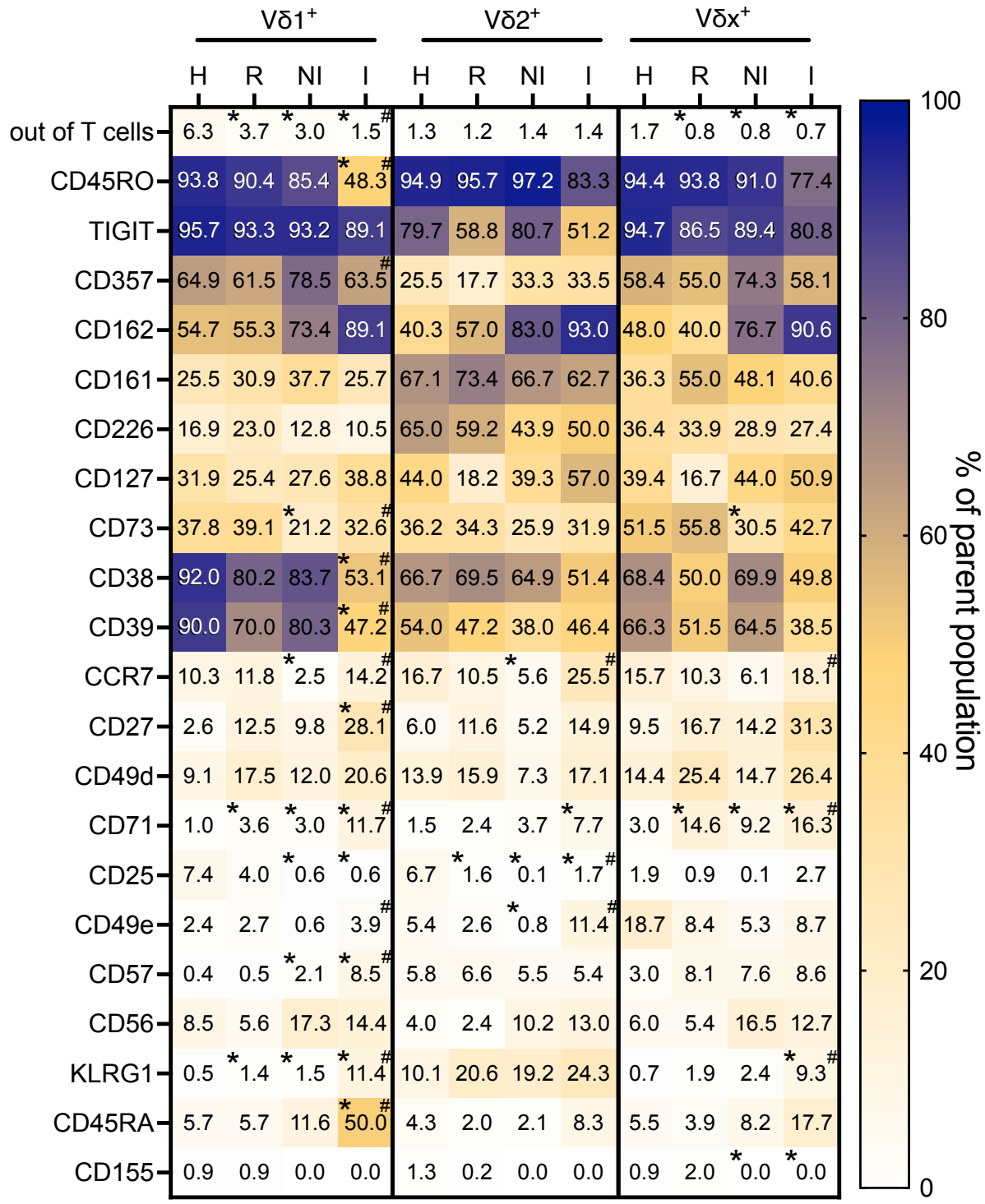

Figure 1-7. Differences in proportions TCR Vδ1$^+$, TCR Vδ2$^+$, and TCR Vδx$^+$ T cell populations positive for surface markers identified by screening in CD patients and healthy donors. Heatmap represents median proportions. I, NI and R were compared to H, and a significant difference (qval <0.05) is marked by * at the left upper corner. NI was also compared to I; a significant difference (qval <0.05) is marked by $^{\#}$ in the upper right corner. Twenty-four paired (I /NI), eight unpaired I, nineteen R, and thirteen H samples were used for the analysis.

Numerous significant changes of Vδ1$^+$ cells in terms of their proportion, functional maturation as well as surface markers expression stressed the importance of identification of phenotypically distinct populations enriched in inflamed and healthy tissue. Cluster analysis based on proteins related to the functional maturation of T cells (CD45RA, CD45RO, CCR7, CD27, KLRG1, and CD57) was used for that purpose (**Fig.1-8A**). Two clusters (1 and 2) were significantly enriched in healthy tissue, whereas seven clusters (3-9) were significantly enriched in I *vs*. H (**Fig.1-8A, Fig.1-8B**). Vδ1$^+$ cells enriched in H (clusters 1 and 2) represent almost 50% of all Vδ1$^+$ cells (**Fig.1-8A**). Cluster 1 (5 % of Vδ1$^+$ cells) represented TCM cells while cluster 2 (45% of Vδ1$^+$ cells) represented T_{EM} cells (**Fig.1-8A**). Both clusters enriched in healthy tissue were CD38$^+$CD39$^+$CD45RO$^+$CD45RA$^-$ and no similar phenotype was found among those enriched in inflamed tissue. Instead, in the same inflamed tissue, CD45RA was expressed by all cells in 6 of 7 clusters, KLRG1 in 5 / 7, CCR7 in 2 / 7, and CD57 in 2 / 7 clusters (**Fig.1-8C**). These findings demonstrated that most of the Vδ1$^+$ cells enriched in I are T_{EMRA} cells. Intriguingly, a subpopulation of CD45RA$^+$ cells expressed very low levels of CCR7 (**Fig.1-8D**), possibly representing cells in which CCR7 was transiently upregulated upon TCR engagement(251). Indeed, true CD4$^+$ naïve (CD45RA$^+$CCR7$^+$) cells expressed much higher levels of CCR7 than Vδ1$^+$ cells (**Fig.1-8E**). Therefore, the overactivation of Vδ1$^+$ cells in inflamed tissue might cause their transition from T_{EM} to T_{EMRA} phenotype. Strikingly, in not inflamed tissue, T_{EMRA}-like Vδ1$^+$ cells were only a minor fraction (11.6%) (**Fig.1-3B**), probably due to reduced chronic activation.

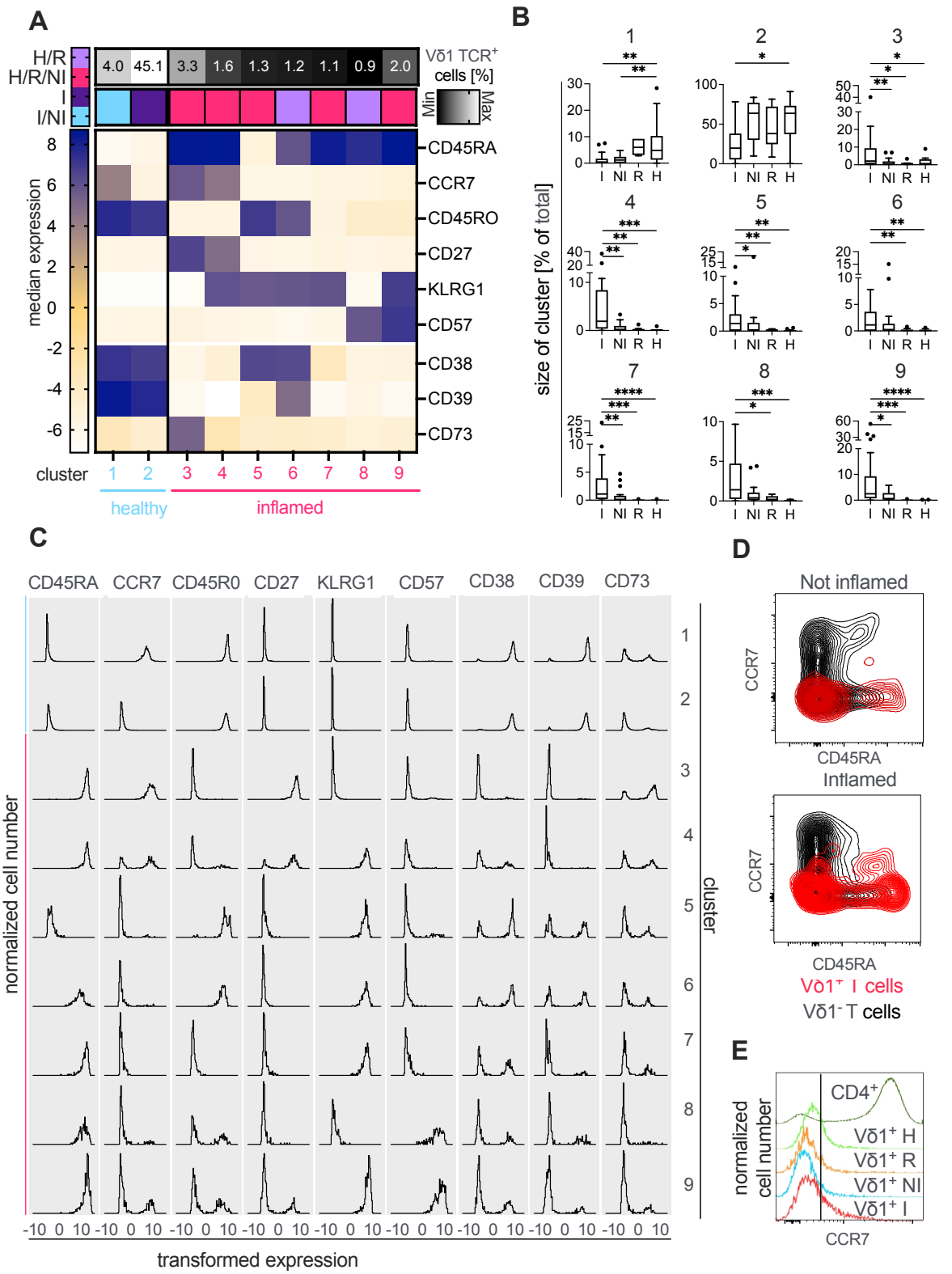
A
H/R
H/R/NI
I
I/NI
4.0
45.1
3.3
1.6
1.3
1.2
1.1
0.9
2.0
Vδ1 TCR+ cells [%]
Min
Max
median expression
CD45RA
CCR7
CD45RO
CD27
KLRG1
CD57
CD38
CD39
CD73
cluster
healthy
inflamed
B
size of cluster [% of total]
I NI R H
C
normalized cell number
transformed expression
cluster
D
Not inflamed
Inflamed
CCR7
CD45RA
Vδ1+ I cells
Vδ1- T cells
E
normalized cell number
CD4+
Vδ1+ H
Vδ1+ R
Vδ1+ NI
Vδ1+ I
CCR7

Figure 1-8. **T_{EMRA} TCR Vδ1$^+$ cell population is enriched in the inflamed intestinal tissue of CD patients. A**) Arcsinh transformed median expression of CD45RA, CCR7, CD45RO, CD27, KLRG1, CD57, CD38, CD39, and CD73 on the Phenograph clusters (defined by the expression of CD45RA, CCR7, CD45RO, CD27, KLRG1, CD57) significantly enriched (qval <0.05) for healthy (H) (1, 2) or inflamed (I) (3-9) tissue. **B**) Boxplots showing fractions of each condition (I, not inflamed [NI], remission [R], H) represented by the clusters significantly enriched for I (1, 2) or H (3-9). *Cluster 2 was stably present in all five iterations of clustering we performed (see methods), but the q-value between the H and I condition for this cluster varies between 0.04-0.06 depending on the iteration. **C**) Histograms of CD45RA, CCR7, CD45RO, CD27, KLRG1 CD57, CD38, CD39, and CD73 expression in the clusters significantly enriched for I (1, 2) or H (3-9). **D**) Representative example of changes in the CCR7 and CD45RA expression between I and NI tissue of the same CD patient. **E**) Comparison of CCR7 expression levels on concatenated CD45RA$^+$ TCR Vδ1$^+$ cells from H, R NI and I tissue and on total CD45RA$^+$ CD4$^+$ T cells. *=qval<0.05, **=qval<0.01. 10 I, 10 NI, 10 R, and 10 H samples were used for the analysis in A, B, and C. 24 paired (I/NI), eight unpaired I, 19 R and 13 H samples were used for the analysis in E.

The association of CD45RA expression with clusters enriched in I and CD39 with those increased in H prompted the analysis of their co-expression. Notably, these two markers were largely expressed in a non-overlapping manner (**Fig.1-9A**), thus identifying different cell populations. CD45RA and CD39 populations also differed in the expression of many other surface markers, as shown in **Fig.1-9B**.

These findings suggested further studies to investigate whether phenotypically distinct CD4 and Vδ1$^+$ cell populations were also functionally distinct.

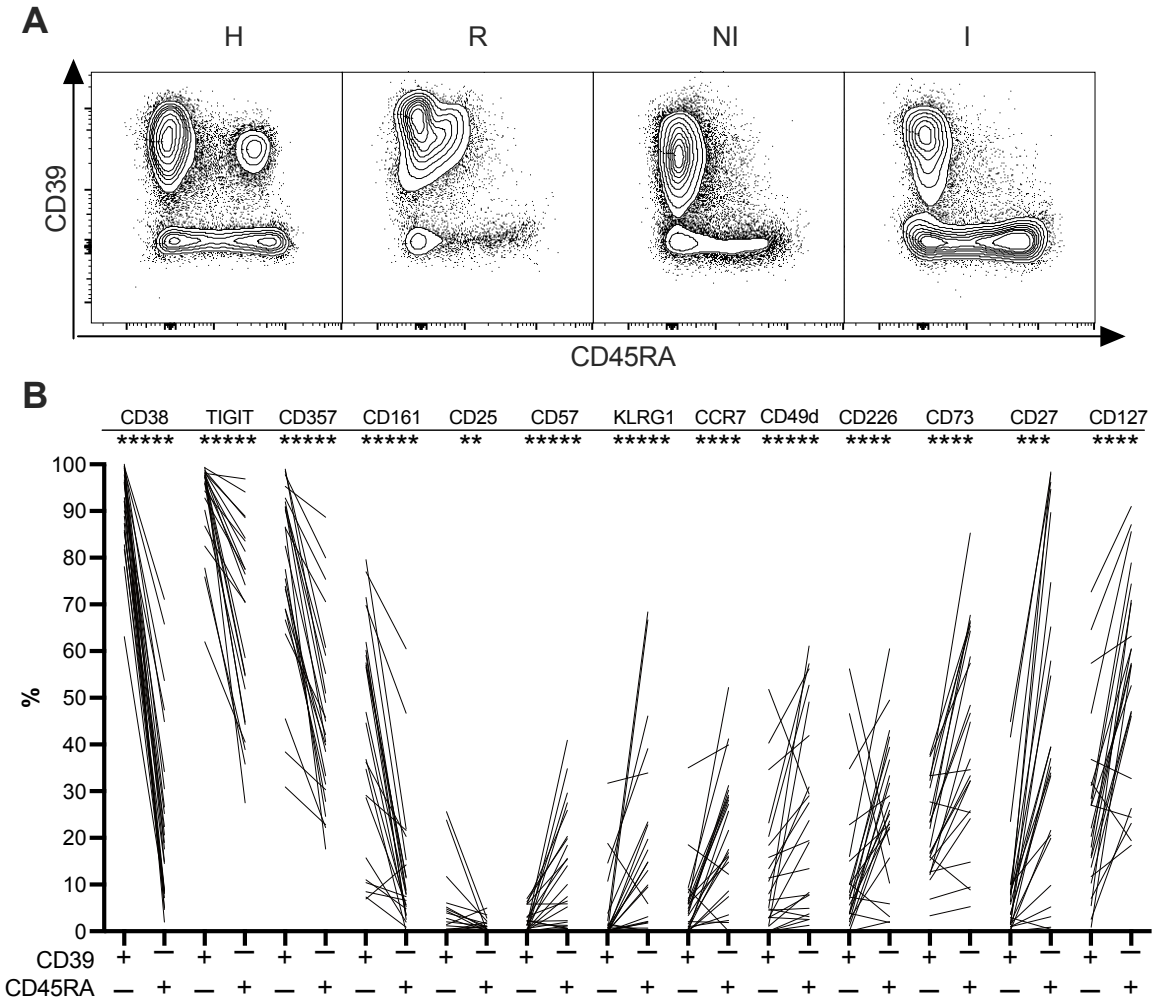

Figure 1-9. **CD39⁺ and CD45RA⁺ TCR Vδ1⁺ cells represent distinct and phenotypically highly different cell subsets. A**) Expression of CD39 and 45RA on concatenated TCR Vδ1⁺ cells from all analyzed biopsies from inflamed (I), not inflamed (NI), remission (R), and healthy (H) tissue. **B**) Comparison of surface markers expression between CD39⁺CD45RA⁻ and CD39⁻CD45RA⁺ Vδ1 TCR⁺ cells subsets. *=qval<0.05, **=qval<0.01, ***=qval<0.001, ****=qval<0.0001. Twenty-four paired (I/NI), eight unpaired I, 19 R, and 13 H samples were used for the analysis. In B, samples with less than 50 living cells for any of the compared subsets (CD39⁺ TCR Vδ1⁺ cells, CD45RA⁺ TCR Vδ1⁺ cells) were excluded from the analysis.

Unique clusters of CD4$^+$ and TCR Vδ1$^+$ cells in PBMCs of patients with active CD

Next studies were performed with circulating T cells to investigate whether there was a difference in the gut-homing potential of CD4$^+$ and TCR Vδ1$^+$ cells in patients with active disease and healthy donors. We stained PBMCs with a flow-cytometry panel containing antibodies against CD103 (αE integrin), CD49d (α4 integrin), CD49e (α5 integrin), CCR9, β7 integrin, and additional 23 lineage markers, activation markers, functional maturation markers and markers considered relevant based on tissue analysis. Clustering based on the CD103, CD49d, CD49e, CCR9, β7 integrin, and activation marker CD71 revealed the presence of 1 CD4$^+$ and 3 TCR Vδ1$^+$ cells clusters significantly enriched in the blood of CD patients (**Fig.1-10B, Fig.1-11B**). A cluster of CD4$^+$ cells consisted of cells expressing CD49d, β7 integrin, CD49e, and CD71 (**Fig.1-10A, C**). In addition, these cells are primarily CD45RO$^+$ and CD127$^+$, a significant part of them expressed CCR7, and almost none express KLRG1 (**Fig.1-10D**). This cluster consists of activated T_{CM} and T_{EM} cells with gut-homing potential. All cells in TCR Vδ1$^+$ clusters enriched in the blood of CD patients express CD49d and CD49e (**Fig.1-10E-G**). Cluster 1 was also co-expressing β7 integrin and CD71, cluster 2 only CD71 and cluster 3 was negative for both (**Fig.1-10E-G**). Cells in all 3 clusters were mostly CD45RO$^-$, CD127$^-$, CCR7$^-$, and KLRG1$^+$(**Fig.1-1-10H**). Cluster 1, therefore, represents activated T_{EMRA} cells with gut-homing potential. The homing potential of cells in clusters 2 and 3 remain to be investigated with other markers.

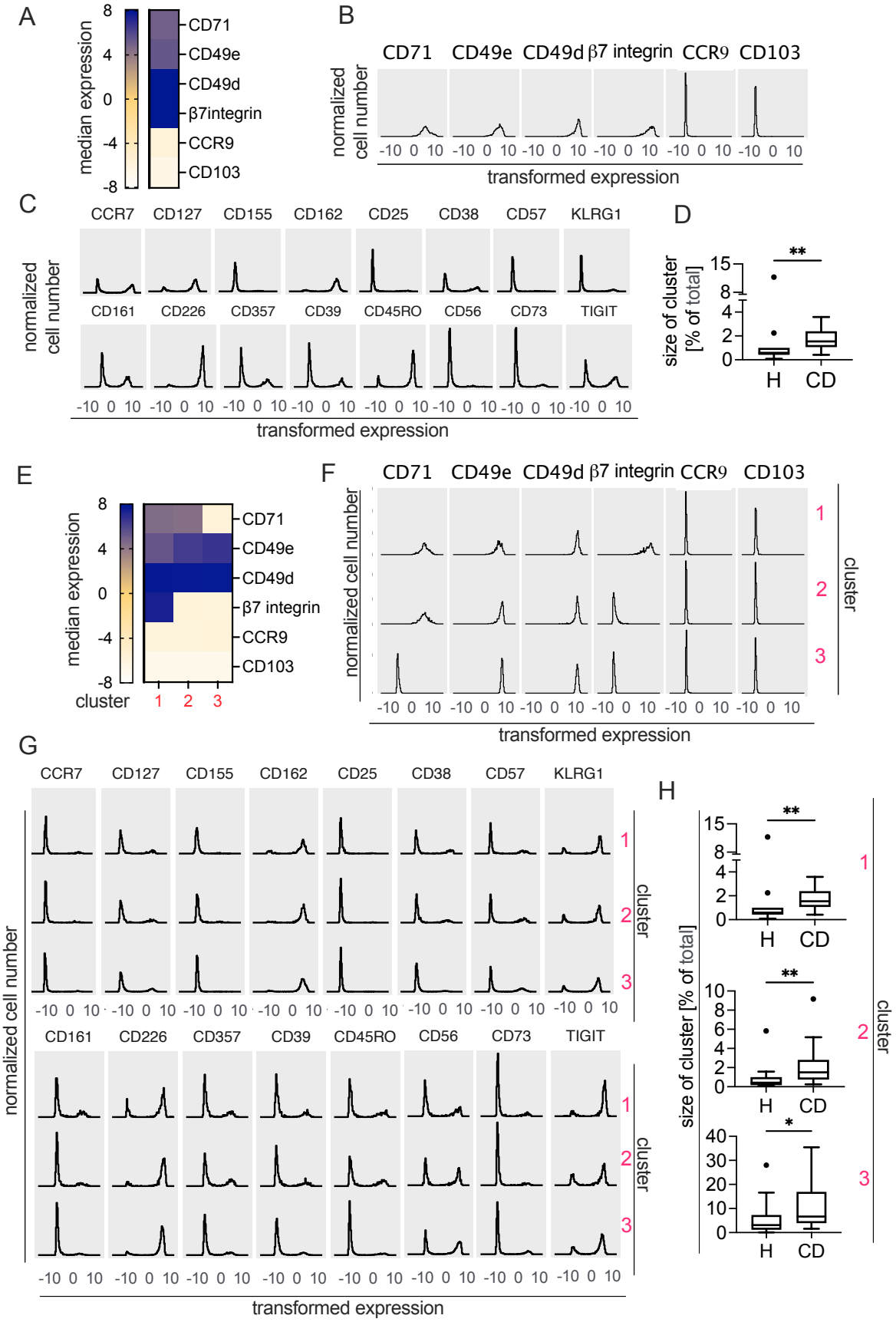
A
median expression
8
4
0
-4
-8
CD71
CD49e
CD49d
β7integrin
CCR9
CD103
B
CD71 CD49e CD49d β7 integrin CCR9 CD103
normalized cell number
-10 0 10
transformed expression
C
CCR7 CD127 CD155 CD162 CD25 CD38 CD57 KLRG1
CD161 CD226 CD357 CD39 CD45RO CD56 CD73 TIGIT
normalized cell number
-10 0 10
transformed expression
D
size of cluster [% of total]
15
8
4
2
0
**
H
CD
E
median expression
8
4
0
-4
-8
cluster
1 2 3
CD71
CD49e
CD49d
β7 integrin
CCR9
CD103
F
CD71 CD49e CD49d β7 integrin CCR9 CD103
normalized cell number
1
2
3
cluster
-10 0 10
transformed expression
G
CCR7 CD127 CD155 CD162 CD25 CD38 CD57 KLRG1
CD161 CD226 CD357 CD39 CD45RO CD56 CD73 TIGIT
normalized cell number
1
2
3
cluster
-10 0 10
transformed expression
H
size of cluster [% of total]
15
8
4
2
0
10
8
6
4
2
0
40
30
20
10
0
**
*
H
CD
1
2
3
cluster

Figure 1-10. **Clusters of activated T_{EM}/T_{CM} $CD4^+$ T cells and activated T_{EMRA} TCR V$\delta1^+$ cells with gut-homing potential are enriched in the blood of patients with active CD**. **A**) Phenotype of $CD4^+$ T cells in cluster enriched in patients with the active disease described by arcsinh transformed median expression of CD71, CD49e, CD49d, $\beta7$ integrin, CCR9, and CD103 **B**) Histograms of CD71, CD49e, CD49d, $\beta7$ integrin, CCR9, and CD103 on $CD4^+$ T cells from cluster shown in A. **C**) Histograms of CCR7, CD127, CD155, CD162, CD25, CD38, CD57, KLRG1, CD161, CD226, CD357, CD39, CD45RO, CD56, CD73 and TIGIT expression on $CD4^+$ T cells from cluster shown in A. **D**) Boxplot showing fractions of both conditions (CD, H) represented by the cluster of $CD4^+$ T cells shown in A. **E**) Phenotypes of TCR V$\delta1^+$ cells in clusters enriched in patients with the active disease described by arcsinh transformed median expression of CD71, CD49e, CD49d, $\beta7$ integrin, CCR9, and CD103. **F**) Histograms of CD71, CD49e, CD49d, $\beta7$ integrin, CCR9, and CD103 expression on TCR V$\delta1^+$ cells from clusters shown in E. **G**) Histograms of CCR7, CD127, CD155, CD162, CD25, CD38, CD57, KLRG1, CD161, CD226, CD357, CD39, CD45RO, CD56, CD73 and TIGIT expression on TCR V$\delta1^+$ cells from clusters shown in E. **H**) Boxplots showing fractions of both conditions (CD, H) represented by the clusters of TCR V$\delta1^+$ cells shown in E. *=qval<0.05; **=qval<0.01. 20 CD patients and 20 H donors were used for the analysis

$CD4^+$ T cells populations enriched in inflamed tissue are Th17 cells

T cells in the intestine are stimulated by antigens presented on antigen-presenting molecules (CD1, MHCI, MHCII, MR1, Butyrophilins), by molecules with PAMPs, which trigger PRRs expressed on T cells or by cytokines and other soluble factors released by T and B lymphocytes, by cells of the innate immune system or by adjacent nonimmune cells. Upon their activation, T cells release a plethora of soluble factors which determine their effector functions. To assess the functional capability of T cells in tissue, we activated T cells isolated from inflamed CD lesions with PMA/ionomycin. The cytokines produced by functionally mature T cells are determined by the expression of transcription factors (EOMES [CD8-cytotoxic T cell], T-bet [Th1 cell], GATA3 [Th2 cell], PU.1 [Th9], RORγT [TH17 cell]. The panel of investigated cytokines included Th1 (IL-2, TNF-α, and IFN-γ), Th2 (IL-4, IL-5, IL-6 and IL-13), Th17 (IL-17, IL-21), Th9 (IL-9) and Treg cytokine (IL-10), and cover cytokines released by all major Th cells populations. In line with current knowledge of CD pathogenesis, we found that T cells producing Th1 and Th17 cytokines were the most common, while those expressing Th2 were rare (**Fig.1-11**).

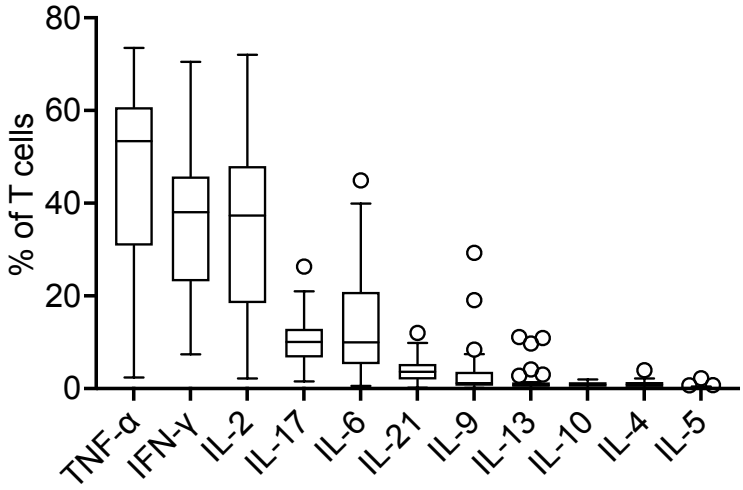

Figure 1-11. Intestinal T cells from patients with active CD express mostly Th1 and Th17 cytokines. Twenty-eight samples of patients with active CD were used for the analysis.

Investigation of $CD4^+$ tSNE clustering based on CD38, CD39, CD73, CD45RA, and CD161 showed that IL-21 expression paralleled CD39 expression and was almost absent in $CD73^+$ cells (**Fig.1-12A**). Conversely, $CD73^+$ cells produced TNF-α, IFN-γ, IL-2, and IL-6 (**Fig.1-12A**). Paired analysis showed that $CD39^+$ cells produced more IL-21 and IL-17 in most donors than $CD73^+$ cells (**Fig.1-12B**). Furthermore, $CD73^+$ cells produced more IFN-γ, TNF-α, IL-2, and IL-6 (**Fig.1-12B**). These findings suggested that the $CD4^+$ T cells population enriched in the inflamed mucosal tissue of CD patients is represented by $CD39^+CD73^-CD45RA^-$ Th-17 cells.

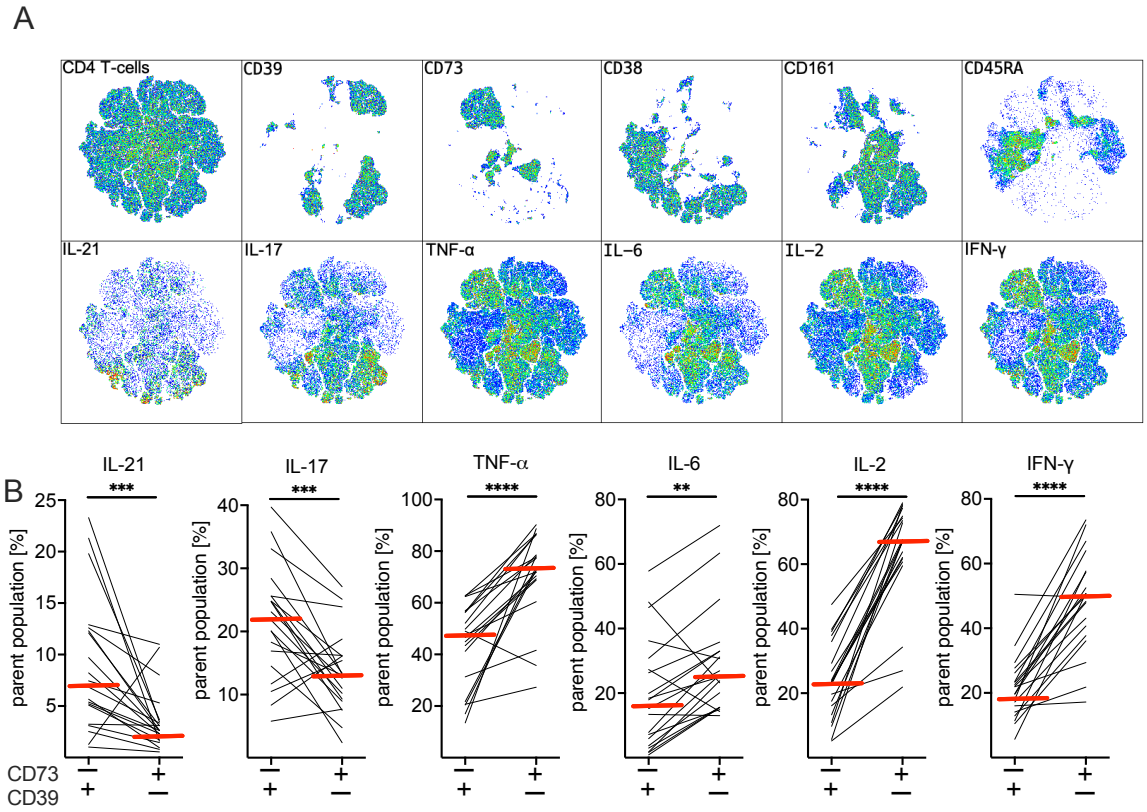

Figure 1-12. Cytokine expression by CD39⁺ and CD73⁺ CD4⁺ T cells A) tSNE clustering plot of CD4⁺ T cells based on the expression of CD39, CD73, CD38, CD161, and CD45RA. Cells expressing markers used for tSNE clustering (top row) and cells expressing cytokines IL-21, IL-17, TNF-α, IL-6, IL-2, and IFN-γ (bottom row) are shown. **B**) Comparison of proportion of IL-21, IL-17, TNF-α, IL-6, IL-2, and IFN-γ producing CD4⁺ T cells on population defined by CD39 and CD73 expression. ***=qval<0.001, ****=qval<0.0001. Twenty-eight samples of patients with active CD were used for the analysis. In B, samples with less than 50 living cells for any of the compared subsets here or in figure 1-13 (CD39⁺ CD4⁺ T cells, CD73⁺ CD4⁺ T cells, CD39⁺ TCR Vδ1⁺ cells, CD45RA⁺ TCR Vδ1⁺ cells) were excluded from the analysis.

TEM TCR Vδ1⁺ cells express IL-9, IL-6, and IL-17, while TEMRA-like TCR Vδ1⁺ cells produce Th1 cytokines

Cytokine expression was also investigated in TCR Vδ1⁺ cells. tSNE clustering confirmed that CD39 and CD45RA are mutually exclusively expressed and revealed that they identify cells with differential cytokine production (**Fig.1-13A**). CD39⁺ cells expressed more IL-9, IL-6, IL-17, and IL-2 than CD45RA⁺ cells. These cytokines are often co-produced by the same cells. Strikingly, no IL-9, IL-6, and IL-17 expression were detected in CD45⁺ TCR Vδ1⁺ cells, which produced more IFN-γ and TNF-α

(**Fig.1-13B**). IL-9 expression by TCR Vδ1⁺ cells was the highest among analyzed T cell subsets suggesting that loss of IL-9 secreting TCR Vδ1⁺ cells might have a serious impact on processes induced by IL-9, such as mucin secretion (252) and intestinal barrier function through modulation of claudin expression (253). Analysis of cytokine co-production showed that TEMRA-like cells often co-produced pro-inflammatory cytokines IFN-γ and TNF-α and that expression of other cytokines was minimal.

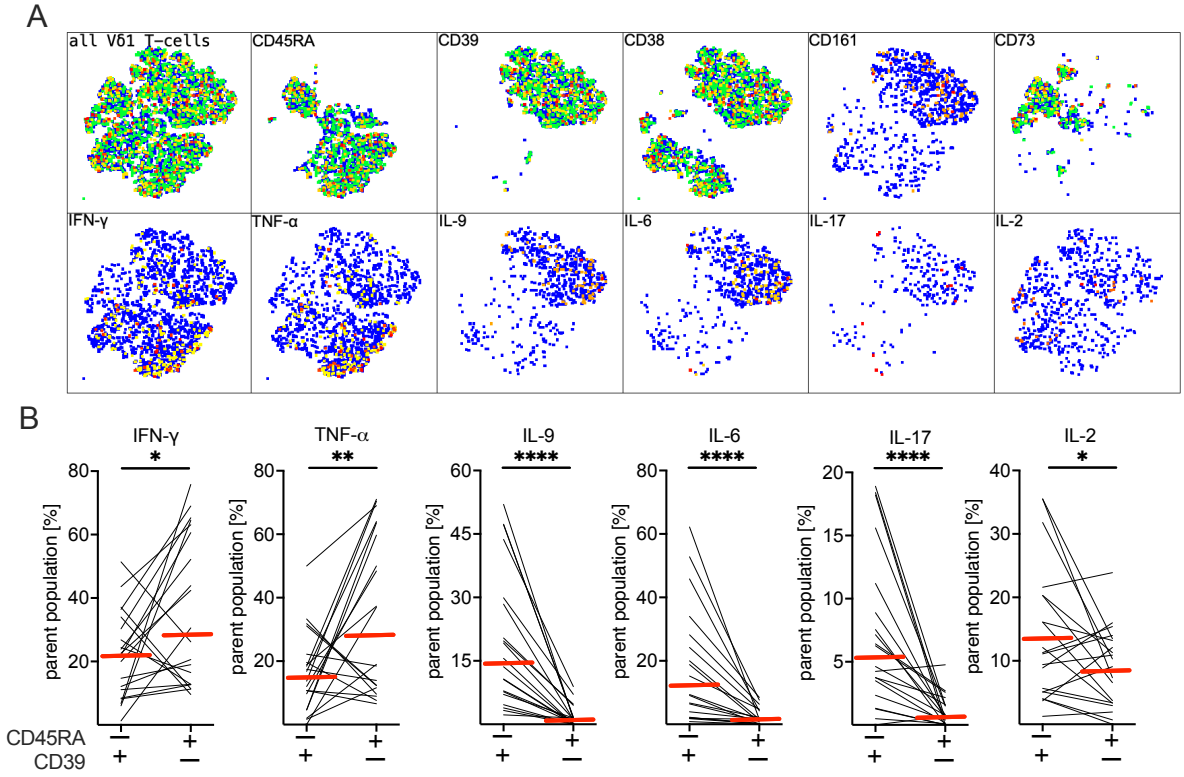

Figure 1-13. The expression of CD39 and CD45RA defines cytokine expression by TCR Vδ1⁺ cells. A) tSNE clustering plot of TCR Vδ1⁺ cells based on the expression of CD45RA, CD39, CD38, CD161, and CD73. Cells expressing markers used for tSNE clustering (top row) and cells expressing cytokines IFN-γ, TNF-α, IL-9, IL-6, IL-17, and IL-2 (bottom row) are shown. **B**) Comparison of proportion of IFN-γ, TNF-α, IL-9, IL-6, IL-17, and IL-2 producing TCR Vδ1⁺ cells on populations defined by CD39 and CD45RA expression. *=qval<0.05, **=qval<0.01, ****=qval<0.0001. Twenty-eight samples of patients with active CD were used for the analysis. In B, samples with less than 50 living cells for any of the compared subsets here or in Figure 1-12 (CD39⁺ CD4⁺ T cells, CD73⁺ CD4⁺ T cells, CD39⁺ TCR Vδ1⁺ cells, CD45RA⁺ TCR Vδ1⁺ cells) were excluded from the analysis.

Discussion

This study revealed alterations in the composition and activity of T cell populations in patients with Crohn's disease. It also identified and functionally characterized various T cell subsets proportions, which are the most significantly altered in inflamed areas. Using a CD45 antibody-based barcoding approach and multidimensional flow cytometry, we screened 360 surface markers and identified and validated markers differentially expressed in $CD14^+$ cells, B cells, and T cells ($CD4^+$, $CD8^+$, TCR $\gamma\delta^+$). Analysis of gene ontology enrichment of differentially expressed proteins revealed that proteins involved in regulating T cell activation are the most enriched group in B cells and CD14+ cells, pointing to the central role of T cells in the CD. Markers identified as differentially expressed in T cells and individual T cells lineage subsets are involved in T cell activation, cytokine and chemokine signaling, and cellular adhesion. Only some of our validated markers were previously identified using single-cell transcriptomics (179, 254) and mass spectrometry studies (255) performed on CD bioptic tissue. Thus, our approach led to the identification of unique T cell phenotypes accumulating in inflamed intestinal tissue of patients with active Crohn's disease.

Comparison of T cell lineage proportions revealed accumulation of $CD4^+$ T cells in inflamed tissue compared to uninflamed tissue and tissue from healthy donors. This increase might be related to the increased proportion of the population of proliferative ($CD71^+$) $CD4^+$ T cells with gut homing ($\alpha4\beta7$ $integrin^+$) potential that we observed in the blood of CD patients compared to healthy donors (169, 248, 256). In the intestinal tissue, we observed that $CD4^+$ T cells in patients with active disease expressed more activation markers (CD71, CD357) and the functional maturation markers KLRG1 and CD57 compared to healthy tissue indicating sustained stimulation and progression toward terminal maturation (41). T cells of patients with active disease also showed decreased expression of CD73 ectonucleotidase. Interestingly, the expression of another functionally related ectonucleotidase, CD39, was increased in inflamed tissue compared to the not inflamed and indeed, these two molecules define two not-overlapping cell populations that also differed in the expression of activation (CD71, CD25, CD357, TIGIT, CD38) and functional maturation (CD127, CCR7, CD45RO, CD45RA, KLRG1) markers. Clustering analysis of $CD4^+$ T cells revealed that cells in the clusters enriched for inflamed tissue showed features of recently stimulated cells

(CD45RO$^+$, CD71$^+$, and CD25$^+$), thus supporting the hypothesis of local antigen stimulation.

The functional analysis that we performed also showed that distinct effector functions distinguish these two populations. Indeed, CD4$^+$ CD39$^+$ T cells expressed significantly more IL-21 and IL-17, whereas CD4$^+$ CD73$^+$ T cells expressed more IFN-γ, TNF-α, IL-2, and IL-6. Such dichotomy might indicate that the two CD4$^+$ T cell populations undergo functional maturation in different microenvironments and in the presence of other soluble factors. IL-17 and IL-21 are produced by Th17 cells (257). T helper cells polarize to Th17 under the influence of TGF-β, IL1β, and either IL-6, IL-21, or IL-23 (258). Intestinal immune cells produce such Th17-polarizing cytokines in response to stimulation by microbiota (259, 260). Thus, the accumulation of CD4$^+$CD39$^+$ T cells in inflamed tissue might result from response to unique microbial flora. Indeed, microbial dysbiosis has been associated with CD (115).

The ability of IL-21 to induce Th17 development was demonstrated in mice, and whether such an autocrine amplification loop of Th17 development also exists in humans remains to be investigated (261). Involvement of IL-21 in CD was previously suggested when IL-21 was observed by western blot in all investigated CD tissue samples and was higher than in ulcerative colitis (UC) and control tissues (262). Enhanced IL-21 was detected in both ileal and colonic CD and fibrostenosing and nonfibrostenosing disease, thus indicating a role independent of tissue localization and type of lesions (262). In addition, IL-21 might also contribute to the accumulation of T cells in intestinal mucosa by promoting the secretion of the chemoattractant MIP-3α by epithelial cells (263).

To sum up, the accumulation of Th17-like CD4$^+$CD39$^+$CD73$^-$ T cells in inflamed intestinal tissue of CD patients can contribute to chronic inflammation of the tissue in several ways. If Th17 development bypasses the need of IL-23 by developing in the presence of IL-21, as was demonstrated in mice, they cannot be efficiently targeted by any immunobiological therapy currently in use. Despite the probable involvement of microbiota, the exact type of antigen specificity that drives development, activation and expansion of CD4$^+$CD39$^+$CD73$^-$ T cells remains to be investigated.

The analyses of TCR $\gamma\delta$ cell populations showed a significant decrease in the proportion of TCR Vδ1$^+$ cells in CD patients, which was more pronounced in patients with active disease and the strongest in the inflamed areas of the intestine. This was

driven by a massive decrease of TEM (CD45RO+CCR7-) TCR Vδ1$^+$ T cells and an increase of T_{EMRA} (CD45RA$^+$CCR7$^-$) TCR Vδ1$^+$ T cells. T_{EMRA} cells represented up to 42% of total TCR Vδ1$^+$ in inflamed tissue. These cells also often co-expressed the CD57 and KLRG1 markers, identifying cells undergoing chronic stimulation. It was previously demonstrated that T cells could develop into T_{EMRA} phenotype under the influence of homeostatic cytokines even in the absence of an antigen (264). In this latter case, the analysis of the TCR sequences of T_{EMRA} (CD45RA$^+$CCR7$^-$) TCR Vδ1$^+$ T cells may reveal if their expansion is oligoclonal (antigen-driven) or polyclonal (non-specifically induced by other factors).

Interestingly, we observed that T_{EMRA} TCR Vδ1$^+$ T cells expressing gut homing markers (α4β7 integrin$^+$) are increased in the blood of CD patients with active disease (169, 256). The fact that these TCR Vδ1$^+$ cells exhibit T_{EMRA} phenotype in the blood suggests that they might also shift to this stage under the influence of soluble factors before they reach the tissue. T_{EMRA} cells have a lower proliferative capacity (41, 264), which might result in the decreased proportion of TCR Vδ1$^+$ T cells in the inflamed intestine. Alternatively, the presence of these cells in the blood can result from the recirculation of tissue-resident cells. It was previously demonstrated that CD4$^+$ T cells residing in the skin also migrate out of their organ of residence and are detectable in the blood of healthy individuals (265). Tissue egress of resident T cells was also thoroughly described in a mice model (266). Lymphocytic choriomeningitis virus-specific tissue-resident CD8$^+$ T cells were able to egress tissue and home to lymph nodes, where they became a source of secondary lymphoid organ tissue-resident memory cells (266). Notably, while activation molecules typical for tissue-resident memory cells, such as CD69, are rapidly downregulated after tissue egress, the expression of some tissue homing molecules remains high for up to a hundred days (266). Whether similar protein expression occurs also in human cells remains to be studied.

TCR Vδ1$^+$ cells are the largest population of TCR γδ in the human gut (267), and they co-express several inhibitory molecules (268), which probably counterbalance their activation in the gut. So far, the antigens that stimulate TCR γδ cells in the human gut remain unknown and different mechanisms might contribute to their local activation. Exceptional use of the TRDJ3 gene segment in T cells expressing the TRDV1 and TRDV3 genes was found in CD patients and not in patients with other chronic

inflammatory diseases of the colon, thus implicating recognition of specific ligands driving their expansion (269). In addition to antigen recognition, other mechanisms might promote the activation of TCR Vδ1$^+$ cells. As TCR Vδ1$^+$ cells in the human gut frequently co-express the Vγ4 chain, the interaction of this TCR Vγ chain with the butyrophilin-like 3 (BTNL3) and butyrophilin-like 8 (BTNL8) dimers expressed on gut epithelial cells (69, 270) might facilitate their activation and functional maturation. An increase in methylated BTNL3 gene has been reported in the gut of IBD patients (271). In patients with coeliac disease, a decreased expression of the BTNL8 gene has been reported and is associated with a dramatic reduction of TCR Vγ4$^+$Vδ1$^+$ tissue resident cells (272). If increased methylation decreases BTNL3 and BTNL8 expression in IBD, it might represent a potential reason for decreased TCR Vδ1$^+$ proportion in the tissue. Another non-alternative possibility is that TCR Vδ1$^+$ cells co-express activating natural cytotoxicity receptors (NCRs) that promote their stimulation in a TCR-independent manner. Indeed, the NCR NKp30 was recently found to be expressed by TCR γδ cells from CD patients in almost 50% of TCR γδ$^+$ Vδ2$^-$ cells (179). Another study showed the expression of NCRs NKp46 and/or NKp44 on a vast majority of Vδ1$^+$ intraepithelial cells in coeliac disease patients (272), further underlining the potential NCR-dependent stimulation of this cell population in the gut.

The functional analysis of TCR Vδ1$^+$ cells showed strikingly different effector capacities of the CD39$^-$T$_{EMRA}$ cells accumulating in inflamed lesions and CD39$^+$T$_{EM}$ cells, which are strongly reduced in sites of inflammation. CD39$^+$T$_{EM}$ cells produced IL-9, IL-17, and IL-6, while their IFN-γ and TNFα production was reduced. IL-9 expression by TCR Vδ1$^+$ cells was the highest among analyzed T cell subsets suggesting that loss of IL-9 secreting TCR Vδ1$^+$ cells might have a severe impact on processes induced by IL-9 such as mucin secretion (252) and maintaining the intestinal barrier function through modulation of claudin expression (253).

The second population, represented by CD39$^-$T$_{EMRA}$-like Vδ1$^+$ T cells, was strongly stained only with IFN-γ and TNFα-specific mAbs, resembling the Vδ1$^+$ T cell populations found in patients with esophageal adenocarcinoma (273). Thus, T$_{EMRA}$-like TCR Vδ1$^+$ cells probably exert a pro-inflammatory role. Whether some T$_{EMRA}$-like TCR Vδ1$^+$ cells have homeostatic activities and promote local integrity of the epithelial barrier remains to be determined. Such a function was elegantly suggested by studies

conducted in mice in which TCR γδ cells were found to promote barrier surveillance proactively through recognition of tissue ligands that remained unknown at that time and were predicted to be expressed in the steady state and modulated by cellular stress (274). A significant increase in inflamed tissue of T_{EMRA} TCR Vδ1$^+$ cells releasing pro-inflammatory cytokines represents a novel aspect of IBD immunopathology. Understanding the immunological role of TCR γδ cells in intestinal inflammation might reveal unknown pathogenetic mechanisms in CD.

In conclusion, our data indicate a profound alteration in the T cell populations in the inflamed colon areas of CD patients. Significant changes affect T_{EM} Th17 cells, T_{EM} TCR Vδ1$^+$ cells producing IL-9, and T_{EMRA} TCR Vδ1$^+$ cells producing IFN-γ and TNF-α. Understanding the mechanisms leading to these alterations of intestinal immune system composition may provide the basis for future IBD therapeutic options.

Changes in the esophageal immune cell population associated with Eosinophilic esophagitis

Introduction

EoE is associated with esophageal eosinophilic infiltration and abnormal Th2 accumulation-associated inflammatory response in the esophagus (198, 204). A dysfunctional epithelial-immune barrier leading to increased exposure to environmental or food antigens is a potential reason for this condition's development. The epithelial-immune barrier's function is influenced by genetic predisposition and environmental factors. The interplay of different immune cell types in the esophagus of patients with EoE and many pathophysiological aspects of this chronic disorder remain largely unknown. A detailed description of the immune cell composition of the esophagus in EoE may be instrumental in understanding the pathophysiologic mechanisms involved in this disease. Until now, the cellular composition and inflammation-dependent changes of the mucosal immune system in the esophagus are largely unknown (201).

To describe the cellular composition of the immune system in esophageal mucosa and simultaneously reveal its changes during active EoE, we applied a multicolor flow cytometry-based analysis on the cells isolated from esophageal biopsies of patients with active EoE, EoE in remission, gastroesophageal reflux disease (GERD) and healthy donors. We provided the first extensive description of EoE-associated changes in immune cells in the human esophagus and described changes in all major immune cell subsets' presence, activity, and functional maturation. In addition, we described the ability of eosinophils to activate MAIT cells, which leads to the production of cytokines able to attract and activate eosinophils. Such a mechanism might contribute to chronic inflammation in EoE.

Patient characteristics

Patient samples were obtained from a total of 70 subjects, and their characteristics are summarized in **Table 2-1**. From each donor, bioptic tissue was collected during an endoscopic procedure. No significant differences between patients with active disease, patients in remission, and healthy donors regarding age and gender were observed.

Table 2-1. Clinical and demographic data of patients included in the study of EoE.

Variable	EoE active (%) (n= 21)	EoE in remission (%) (n = 20)	GERD (%) (n = 11)	Healthy (%) (n = 18)
Male	13/21 (61.9%)	13 (65.0%)	7 (63.6%)	11 (61.1%)
Median age at sample, y, (range)	41.5 (25-71)	39 (25-85)	44 (25-74)	42.5 (22-57)
Median age at EoE diagnosis, y, (range)	34 (19-69)	37 (19-81)	-	-
Median weight (kg), y, (range)	79 (56-130)	76.5 (51-94)	83 (67-103)	71 (55-111)
Edema	9 (42.9%)	1 (5.0%)	0 (0.0%)	1 (5.6%)
Exudates	17 (81.0%)	2 (10.0%)	1 (9.0%)	1 (5.6%)
Furrows	19 (90.5%)	7 (35.0%)	0 (0.0%)	3 (16.7%)
Rings	13 (61.9%)	9 (45.0%)	0 (0.0%)	1 (5.6%)
Stricture	4 (19.0%)	0 (0.0%)	0 (0.0%)	0 (0.0%)
Moderate to severe signs	21 (100.0%)	14 (70.0%)	1 (9.0%)	4 (22.2%)
Atopic history	14 (66.7%)	14 (70.0%)	4 (36.4%)	8 (44.4%)
Alergic asthma	4 (19.0%)	4 (20.0%)	2 (18.2%)	3 (16.7%)
Food allergies	4 (19.0%)	6 (30.0%)	0 (0.0%)	2 (11.1%)
Dysphagia	21 (100%)	11 (55.0%)	6 (54.5%)	11 (61.1%)
Food impaction	18 (85.7%)	9 (45.0%)	4 (36.4%)	4 (22.2%)
Reflux	2 (9.5%)	4 (20.0%)	6 (54.5%)	9 (50.0%)
Median peak of eosinophils / hpf, y, (range)	76 (25-170)	1 (0-14)	0 (0-10)	0 (0-0)
Treatments				
Diet	1 (4.8%)	1 (5.0%)	0 (0.0%)	0 (0.0%)
Steroids	4 (19.0%)	7 (35.0%)	0 (0.0%)	0 (0.0%)
Steroids / Diet	1 (4.8%)	0 (0.0%)	0 (0.0%)	0 (0.0%)
Steroids /PPI	0 (0.0%)	6 (30.0%)	0 (0.0%)	0 (0.0%)
PPI	3 (14.3%)	4 (20.0%)	5 (45.5%)	10 (55.6%)
Other	0 (0.0%)	1 (5.0%)	1 (9.0%)	0 (0.0%)

Immune cells accumulate in the esophageal mucosa of EoE patients

A healthy esophagus is sparsely infiltrated by immune cells ($CD45^+$). We investigated the changes in the infiltration of immune cells to the esophageal tissue by comparing the ratio of $CD45^+$ and $CD45^-$ cells in the biopsies. This comparison revealed that the immune cells are more frequent in the biopsies from the esophageal mucosa of patients with active EoE compared to patients with gastroesophageal reflux disease (GERD), EoE patients in remission (R), and healthy donors (H) (**Fig.2-1**). Simultaneously, the relative abundance of $CD45^+$ cells was significantly higher in healthy donors than in patients in remission and patients with GERD.

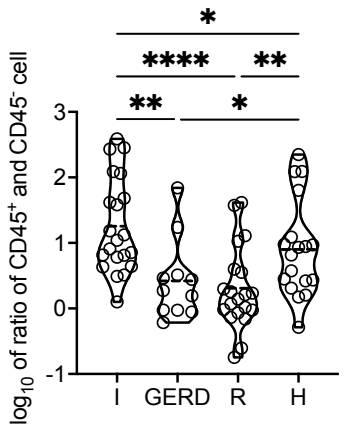

Figure 2-1. Comparison of $CD45^+$ and $CD45^-$ cells ratio between esophageal biopsies of patients with active EoE (I), gastroesophageal reflux disease (GERD), EoE in remission (R), and healthy donors (H). Horizontal line represents mean. *=qval<0.05, **=qval<0.01, ****=qval<0.0001

Phenotypic characterization of major immune subsets infiltrating EOE biopsies

Phenotypic characterization of cells isolated from esophageal biopsies was done by spectral flow cytometry-based immunophenotyping panel, which allowed recognition of all major immune cell populations in the esophageal biopsies (**Fig.2-2**).

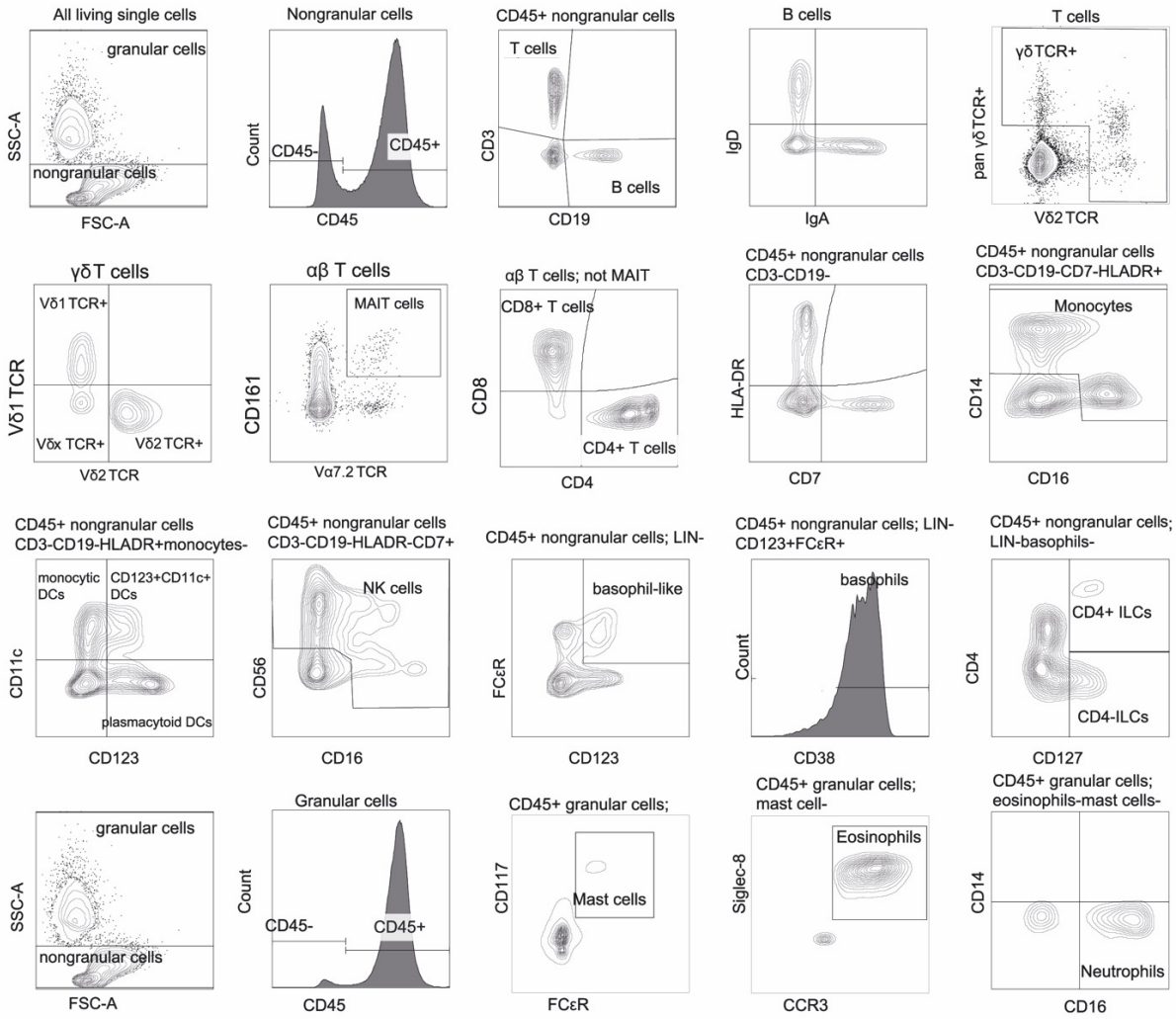

Figure 2-2. Gating strategy used for separation of immune cell lineage subsets. Data shown here represent concatenated living single cells from 70 esophageal biopsies.

FlowSOM clustering analysis of $CD45^+$ cells was performed based on the expression of the following markers (CD3, CD4, CD8, pan γδ TCR, Vδ1 TCR, Vδ2 TCR, Vα7.2 TCR, CD161, CD56, CD127, CD19, IgA, IgD, HLA-DR, CD11c, CD123, CD14, CD38, CD117, FcεR, CCR3, Siglec-8, α4 integrin). Manual merging of clusters corresponding to the same immune cell subset allowed comparing relative abundances of immune cell subsets ($CD4^+$αβ T cells, $CD8^+$αβ T cells, $CD4^+CD8^+$αβ T cells, $CD4^-CD8^-$ T cells, MAIT cells, TCR $Vδ1^+$ T cells, TCR $Vδ2^+$ T cells, $CD56^+$ NK cells, $CD16^+$ NK cells, $CD16^+CD56^+$ NK cells, ILCs, IgA^-IgD^- B cells, IgA^+ B cells, IgD^+ B cells, plasmacytoid dendritic cells, myeloid dendritic cells, classical monocytes, intermediate monocytes, nonclassical monocytes, basophils, mast cells, eosinophils, neutrophils) between active EoE and other investigated conditions (**Fig.2-3A**). Only 4.7 % of cells were

attached to clusters which were impossible to classify into any of these categories (**Fig.2-3A**).

Eosinophils were significantly more frequent in active EoE than in healthy subjects, patients with EoE in remission, and patients with GERD (**Fig.2-3A, B**). Their presence in the esophagus is a diagnostic criterium for EoE, and we, therefore, normalize our data for this to be able to observe changes in the other immune cell populations. We revealed an increase in the abundance of mast cells and basophils in patients with active EoE compared to healthy donors. In addition, all B cell subsets were significantly more abundant in active EoE than healthy and $IgD^{-}IgA^{-}$ and IgA^{+} B cells compared to patients in remission (**Fig.2-3A, B**). Neutrophils were significantly more frequent in healthy patients than in patients with active EoE (**Fig.2-3A**). As expected, the viability of neutrophils isolated from EoE biopsies was insufficient; therefore, we did not investigate them any deeper in this study. $CD4^{+}$αβ T cells are considered critical mediators of EoE (203) but they were not more frequent in EoE tissue than in healthy tissue (**Fig.2-3A, B**).

Median expression of 11 activation and functional maturation markers, which were not used for clustering, provided deeper information about individual immune cell subsets. On most T cell populations high expression of CD69 suggested their activation typically observed for tissue-resident T cells (**Fig.2-3A**). Interestingly, TCR $Vδ2^{+}$ cells did not express CD69 but were highly positive for KLRG1 and negative for TIGIT (**Fig.2-3A**). Our previous analysis of intestinal samples and blood showed that this is a typical profile of circulating TCR $Vδ2^{+}$ cells in the blood. In contrast, TCR $Vδ2^{+}$ cells residing in the intestinal mucosa express TIGIT and lose KLRG1 (**Fig.1-7**). Thereby, it is probable that TCR $Vδ2^{+}$ cells in the esophageal biopsies represent the population of blood cells perfusing inflamed tissue and not tissue-resident cells. In clusters corresponding to unconventional T cells, expression of CD45RA was the highest. Their concomitant lack of CCR7 and expression of CD57 and KLRG1 markers indicated a high proportion of T_{EMRA} in these subsets (41) (**Fig.2-3A**).

Expression of CD45RA on the B cell subsets was highest in IgD-expressing B cells which were also negative for CD27 and CD38 (**Fig.2-3A**). This finding aligns with current knowledge of B cell development since IgD is expressed immediately after B cell maturation. In this developmental stage, B cells do not express CD38 neither CD27 (275). CD45RA expression on B cells is also the highest in early developmental stages, and transition to CD45RO occurs with differentiation to plasma cells (276).

Accordingly, IgA-expressing B cells are dim for CD45RA and express high levels of CD27 and CD38, suggesting they are plasma cells (**Fig.2-3A**) (275). We also found that the inhibitory receptor TIGIT was expressed mainly by T cells and monocytes, with the highest expression by TCR Vδ1^{+} cells (**Fig.2-3A**). The adhesion molecule Siglec-3 and the inhibitory molecule TIM3 were predominantly expressed by cells of the innate immune system (**Fig.2-3A**). The expression of IL-2 receptor CD25 was mainly detected on CD4^{+} T cells, CD56^{+} NK cells, ILCs, and basophils (**Fig.2-3A**). The expression of the adhesion molecule CXCR1 – CD181 - was rare on all analyzed cell subsets, with the highest proportion of positive cells on ILCs (**Fig.2-3A**). Autofluorescence of cells was the strongest in dendritic cells, monocytes, and granulocytes, with the highest signal in eosinophils, which also represented the smallest and the most granular cell subset (**Fig.2-3A**).

Taken together, this analysis showed an association of active EoE with the higher relative abundance of eosinophils, mast cells, basophils, and B cell subsets and provided information on investigated surface markers expression by major immune cell subsets in the esophagus.

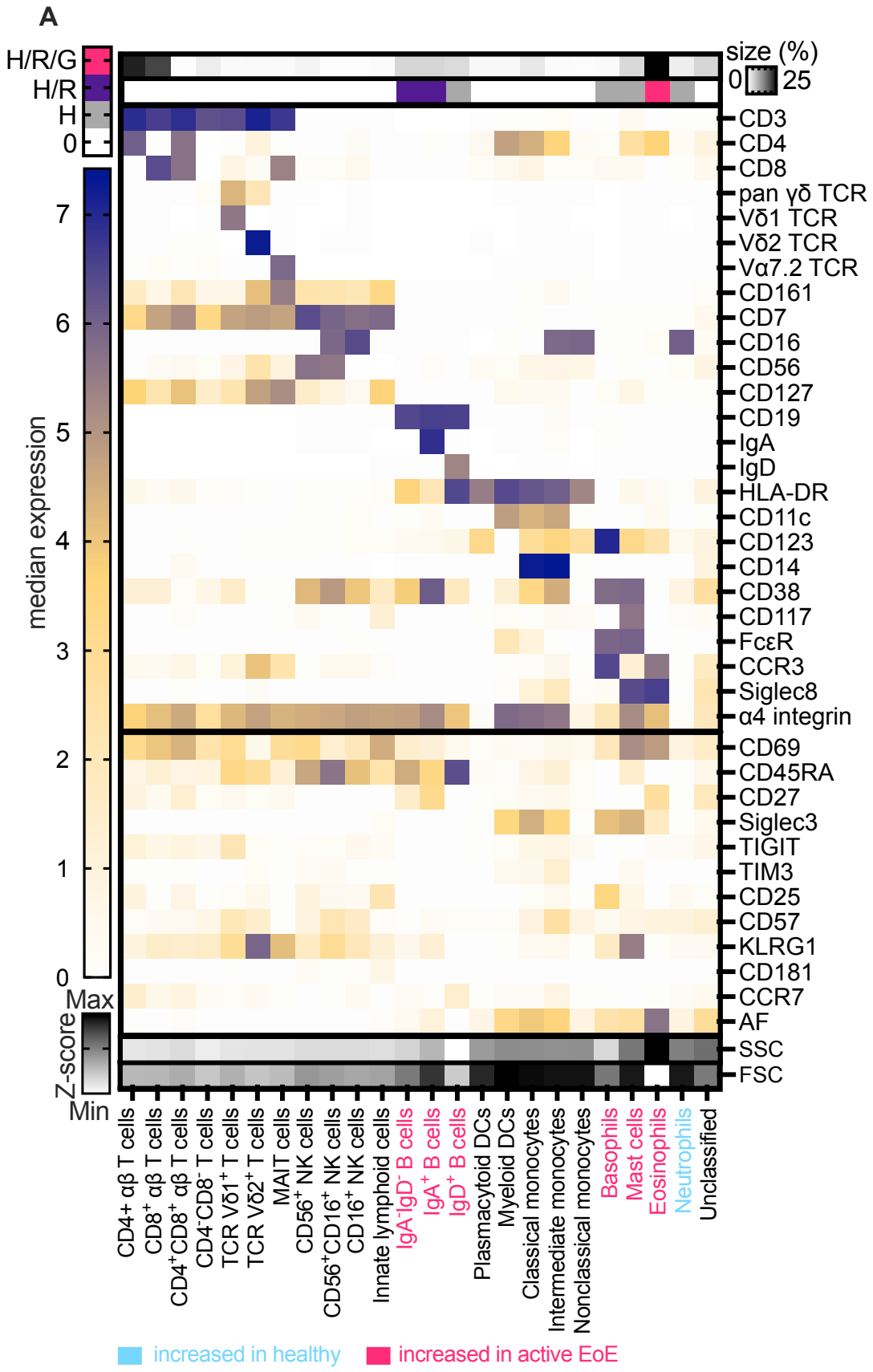
A
H/R/G
H/R
H
0
median expression
7
6
5
4
3
2
1
0
Max
Z-score
Min
size (%)
0
25
CD3
CD4
CD8
pan γδ TCR
Vδ1 TCR
Vδ2 TCR
Vα7.2 TCR
CD161
CD7
CD16
CD56
CD127
CD19
IgA
IgD
HLA-DR
CD11c
CD123
CD14
CD38
CD117
FcεR
CCR3
Siglec8
α4 integrin
CD69
CD45RA
CD27
Siglec3
TIGIT
TIM3
CD25
CD57
KLRG1
CD181
CCR7
AF
SSC
FSC
CD4+ αβ T cells
CD8+ αβ T cells
CD4+CD8+ αβ T cells
CD4-CD8- T cells
TCR Vδ1+ T cells
TCR Vδ2+ T cells
MAIT cells
CD56+ NK cells
CD56+CD16+ NK cells
CD16+ NK cells
Innate lymphoid cells
IgA-IgD- B cells
IgA+ B cells
IgD+ B cells
Plasmacytoid DCs
Myeloid DCs
Classical monocytes
Intermediate monocytes
Nonclassical monocytes
Basophils
Mast cells
Eosinophils
Neutrophils
Unclassified
increased in healthy
increased in active EoE

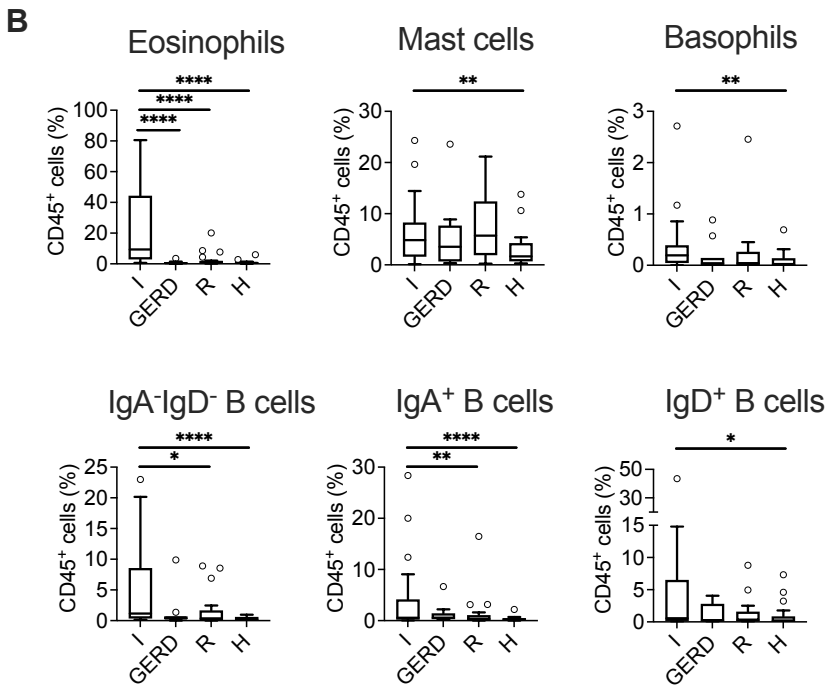

Figure 2-3. Changes in the abundance of immune cell subsets associated with EoE. A) Heat map shows arcsinh transformed median expression of all markers used for the analysis. Twenty-four proteins used to cluster the immune cell subsets are listed above the black horizontal line. The Z-score of FSC-A and SSC-A represent differences in the size and granularity of cells. The horizontal bar on top represents the size of the cluster (size in %); the second from the top shows whether the abundance of the cluster is significantly different between healthy subjects (H), patients with EoE in remission (R and patients with gastroesophageal reflux disease (GERD) compared to patients with active disease (I); AF – autofluorescence of cells; SSC –side scatter detected by blue laser (represent granularity of cell); FSC-A – forward scatter detected by blue laser (represent the size of a cell). **B**) Changes in the proportions of eosinophils, mast cells, basophils, IgA^-IgD^- B cells, IgA^+ B cells, and IgD^+ B cells in patients with active EoE (I), gastroesophageal reflux disease (GERD), EoE in remission (R), and healthy donors (H). Major immune cell subsets with significantly different abundance in I compared to H are shown. *=qval<0.05, **=qval <0.01, ***=qval<0.001, ****=qval<0.0001

Eosinophils and basophils in the esophagus of patients with active EoE are activated cells

Our flow-cytometry investigation of EoE biopsies was supportive of the clinical diagnosis, showing highly increased eosinophil abundance in patients with active EoE (**Fig. 2-3B**). Low counts of eosinophils in the esophagus of patients with EoE in remission, patients with GERD, and healthy donors do not allow for comparing subsets of eosinophils among these conditions. We, therefore, decided to investigate the activation status of eosinophils in the esophagus of patients with the active disease by utilizing the expression of five known eosinophil activation markers (CD4, CD69, CD38, CD123, HLA-DR). We found that CD4 (median = 60.5%) and CD69 (median = 70.8%) were the most frequently expressed activation markers on eosinophils. A smaller number of eosinophils expressed CD123 (median = 29.3%), HLA-DR (median = 2.1%), and CD38 (median = 0.9%) (**Fig. 2-4A**).

Most eosinophils expressed two or more activation markers suggesting that eosinophils infiltrating the esophagus of patients with active EoE are activated (**Fig. 2-4B**). The primary functional outcome of eosinophil activation is their degranulation. Interestingly, we noticed that a small population of $CD38^{+}$ eosinophils has significantly lower side scatter than the rest of the eosinophils suggesting CD38 might be a marker of highly activated eosinophils (**Fig. 2-4C**). This hypothesis was further supported by the observation that $CD38^{+}$ eosinophils express significantly higher levels of CD69 and CD123 than $CD38^{-}$ eosinophils (**Fig. 2-4C**).

Basophils are also significantly more abundant in the esophagus of patients with active EoE than in healthy subjects. Because of low counts in healthy donors and in subjects with GERD and EoE in remission, we could detect and analyze basophils only in the esophagus of patients with active EoE. We clustered basophils based on the expression of activation markers CD25 and CD69 as well as inhibitory molecule KLRG1 and Sialic acid-binding proteins Siglec-3 and Siglec-8 (**Fig. 2-4D**). The analysis showed that, similarly to eosinophils, most clusters expressed at least one of the analyzed activation markers (**Fig. 2-4D**). No preferential association of activation markers was observed. Analysis of individual marker expression showed that Siglec-3 (median = 87.4%) and CCR3 (median = 92.1%) were the most commonly expressed, while the expression of KLRG1 (median = 43.7%) and Siglec-8 (median = 34.6%) was

lower (**Fig. 2-4E**). Interestingly, the median expression of activation markers CD25 (median = 20.3%) and CD69 (median = 32.7%) were relatively low (**Fig. 2-4E**). The presence of CD25 on almost half of the clusters (**Fig.2-D**), including the biggest on,e together with the low median expression of CD25, suggested there might be a relationship between basophil infiltration in the esophagus and their activation. Indeed, we found a significant correlation between the proportion of basophils in the tissue and their expression of CD25⁺ (**Fig. 2-4F**).

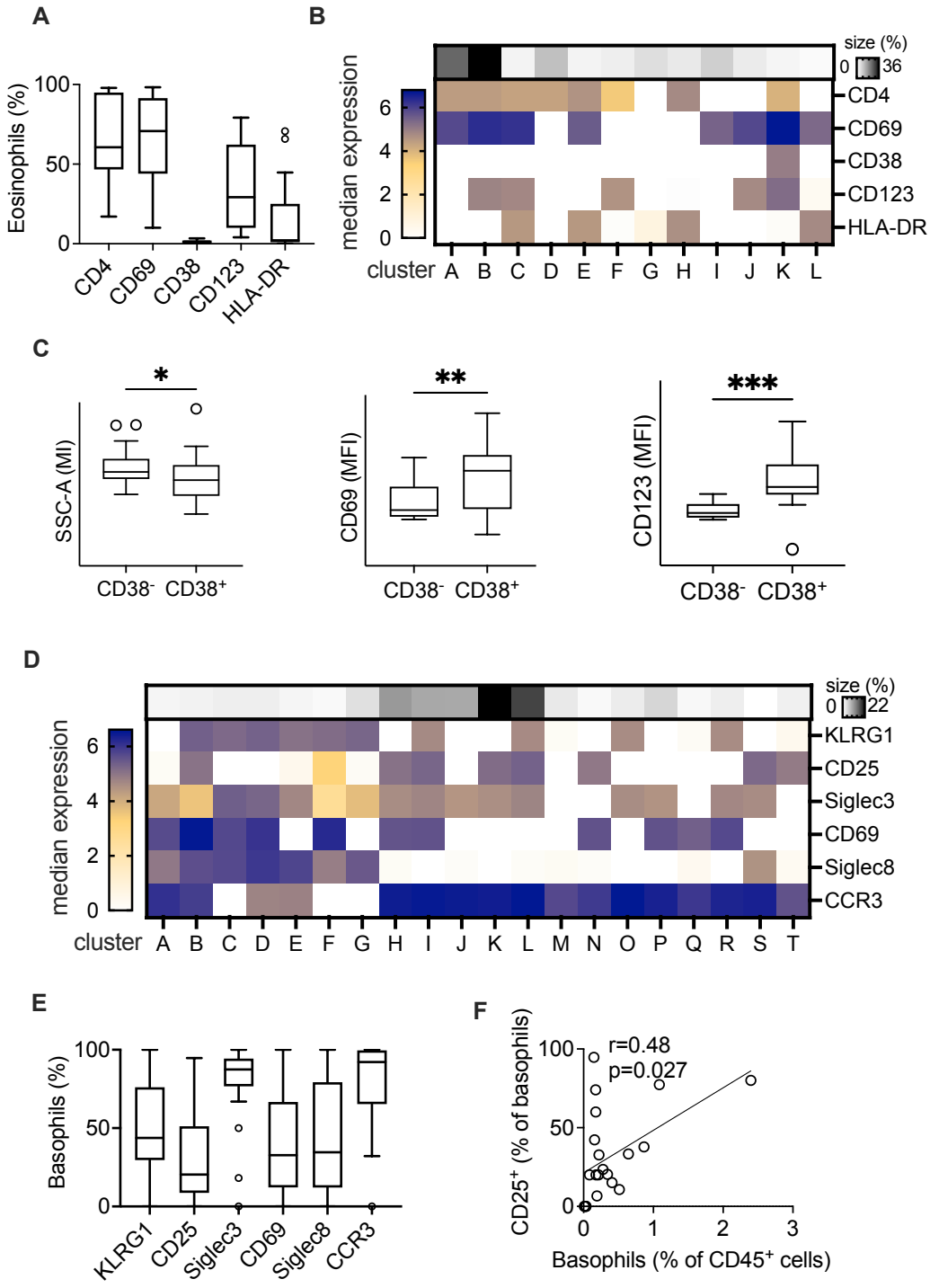

Figure 2-4 Activated eosinophils and basophils are present in the esophagus of EoE patients A) Boxplots representing the distribution of proportions of $CD4^+$, $CD69^+$, $CD38^+$, $CD123^+$, and $HLA\text{-}DR^+$ eosinophils in the esophagus of patients with active EoE **B**) Heat map shows hyperbolic arcsinh transformed median expression of eosinophil activation markers CD4, CD69, CD38, CD123 and HLA-DR on eosinophils isolated from the esophagus of patients with active EoE. The horizontal bar on top represents the size of the cluster. **C**) Boxplot showing a comparison of median intensity (MI) of side scatter (left), median fluorescence intensity (MFI) of CD69 (middle), and MFI of CD123 (right) between populations of $CD38^+$ and $CD38^-$ eosinophils. Y axis is linear. **D**) Heat map shows hyperbolic arcsinh transformed median expression of basophil activation markers CD25 and CD69, inhibitory receptor KLRG1, chemokine receptor CCR3 and Sialic acid-binding proteins Siglec-3 and Siglec-8. The horizontal bar on top represents the size of the cluster. **E**) Boxplots representing the distribution of proportions of $KLRG1^+$, $CD25^+$, $Siglec\text{-}3^+$, $CD69^+$, $Siglec\text{-}8^+$, and $CCR3^+$ basophils in the esophagus of patients with active EoE. *=qval<0.05, **=qval <0.01, ***=qval<0.001 **F**) Correlation between CD25 expression on basophils and proportion of $CD45^+$ cells represented by basophils in the esophageal biopsies of patients with active EoE.

Esophageal mast cell population is markedly changed in active EoE

Mast cells were significantly more frequent in active EoE than in healthy donors (**Fig.2-3B**). Still, the frequency of mast cells in active EoE was the same in patients with remission (**Fig.2-3B**). These findings differ from what we found in eosinophils and indicate that mast cells are not a cell population driving inflammation in EoE. We next investigated the phenotypical changes of mast cells among healthy subjects, patients with active EoE, those in remission, and those with GERD **Fig.2-5**). Mast cell clustering was based on the expression of KLRG1, CD25, Siglec-3, CD69, Siglec-8, CCR3, and CD123. The mast cell subset expressing low KLRG1 levels and Siglec-8, but no CD25, Siglec-3, CD69, CCR3, and CD123 was significantly more frequent in healthy tissue compared to tissue of patients with active EoE, EoE in remission as well as GERD (**Fig.2-5A, B**). $KLRG1^{bright}$ mast cells expressing Siglec-3, CD69, CD123, low levels of CCR3, and no CD25 were significantly more frequent in patients with active EoE than healthy subjects and EoE patients in remission (**Fig.2-5A, B**). A comparison of single markers used for clustering revealed the following differences:
i) Siglec-3-expressing mast cells were more frequent in patients with active EoE compared to healthy donors; ii) CD69-expressing mast cells were more frequent in active EoE than in healthy donors and GERD patients; iii) CCR3-expressing mast cells were more frequent in patients with active EoE patients compared to all other

conditions, and iv) CD123 expressing mast cells were more frequent in active EoE compared to healthy donors and EoE patients in remission (**Fig.2-5C**).

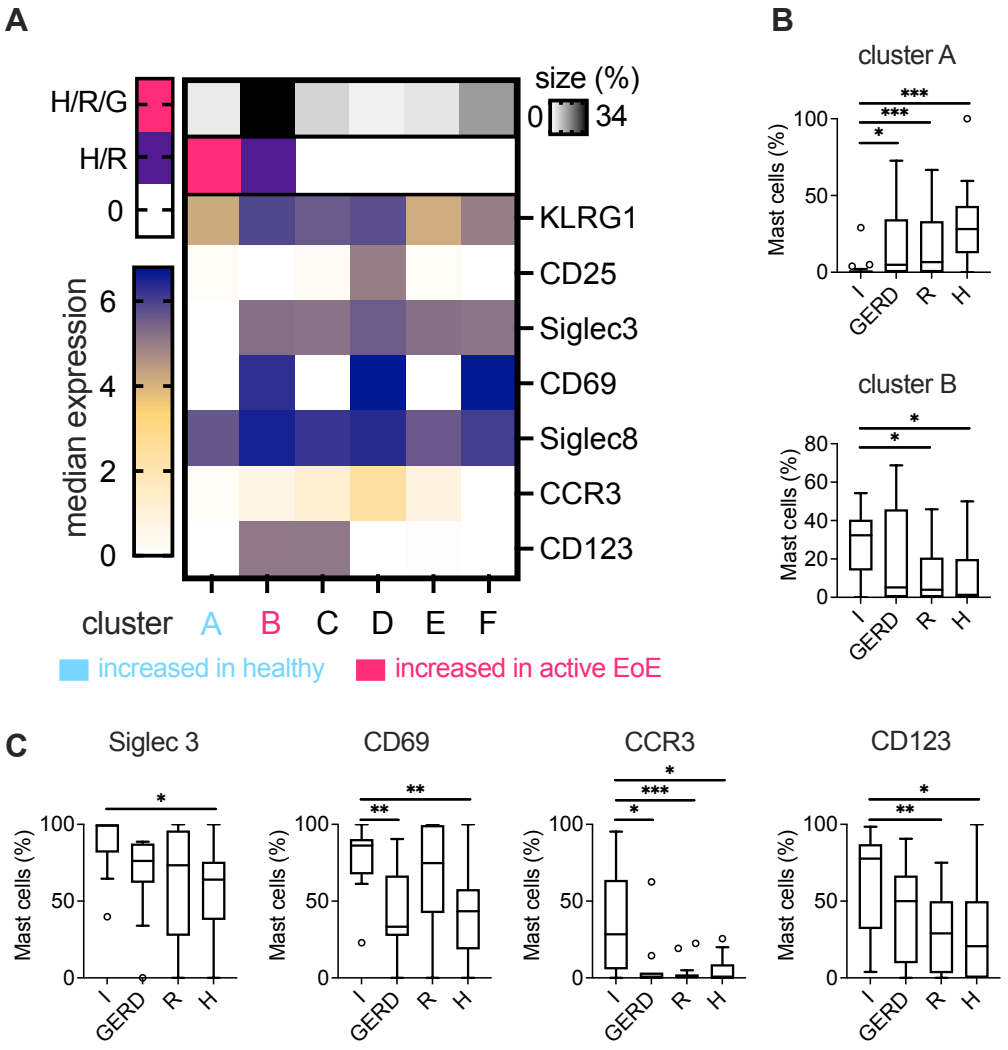

Figure 2-5. The mast cell population of the esophagus is markedly changed in active EoE A) Heat map shows arcsinh transformed median expression of KLRG1, CD25, Siglec-3, CD69, Siglec-8, CCR3, and CD123. The horizontal bar on top represents the size of the cluster; the second from the top shows whether the difference in the frequency of cells in the cluster is significant between H and I; the colour of the cluster name represents whether the cluster is more frequent in donors with active EoE or in healthy donors. **B**) Changes in the proportions of mast cells belonging to clusters A and B in patients with active EoE (I), gastroesophageal reflux disease (GERD), EoE in remission (R), and healthy donors (H). **C**) Changes in the proportion of mast cells positive for Siglec-3, CD69, CCR3, and CD123 between I, R, GERD, and H. *=qval<0.05, **=qval<0.01, ***=qval<0.001

Phenotype and presence of antigen-presenting cell populations are changed in active EoE

Canonical antigen-presenting cells, macrophages (and monocytes), dendritic cells (DCs), and B cells participate in activating Th2 CD4⁺ T cells. Therefore, they might have a significant role in EoE pathogenesis. We investigated the changes in these cell populations by clustering based on the expression of markers related to activation, tissue residence, functional maturation, and markers associated with functionally distinct subsets.

First, DCs were clustered based on the expression of CD123, CD11c, α4 integrin, and Siglec-3. Subsets of plasmacytoid DCs (CD123⁺) expressing α4 integrin and Siglec-3 is significantly more frequent in the inflamed tissue (**Fig.2-6A-B**). In addition, significantly more DCs were positive for Siglec-3 in patients with active EoE.

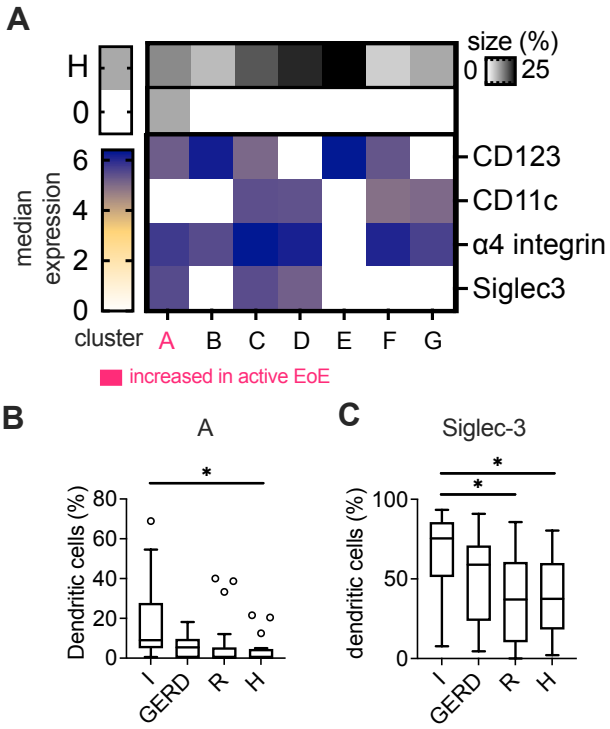

Figure 2-6. Siglec-3⁺ α4 integrin⁺ plasmacytoid dendritic cells accumulate in patients with active EoE. A) Heat map shows arcsinh transformed median expression of CD123, CD11c, α4 integrin, and Siglec-3. The horizontal bar on top represents the size of the cluster; the second from the top shows whether the difference in the frequency of cells in the cluster is significant between H and I; the color of the cluster name represents whether the cluster is more frequent in active EoE or healthy tissue. **B)** Changes in the proportions of cells from clusters A out of dendritic cells in patients with active EoE (I), gastroesophageal reflux disease (GERD), EoE in remission (R), and healthy donors (H). **C)** Changes in the relative abundance of Siglec-3 expressing DCs between I, GERD, R, and H. *=qval<0.05

Monocyte clustering was based on the expression of CD14, CD16, CD11c, CD123, and CD38. No significant difference in the relative abundance of cells from healthy donors and patients with active EoE was observed in any cluster (**Fig.2-7A**). As expected, most of the cells were conventional monocytes ($CD14^{+}CD16^{-}$), while intermediate ($CD14^{+}CD16^{+}$) and nonclassical ($CD14^{-}CD16^{+}$) monocyte cells represented minor fractions (**Fig.2-7A**). CD123-expressing monocytes can develop into $CD123^{+}$ myeloid dendritic cells(277). Since we saw an increase in the subset of plasmacytoid dendritic cells in inflamed tissue (**Fig. 2-6A, B**) we were interested in whether the abundance of $CD123^{+}$ monocytes is higher in active EoE. No significant difference, however, was found in the proportion of $CD123^{+}$ monocytes in different tissues (**Fig.2-7B**). Changes in the activation of monocytes in patients with active EoE were investigated through a comparison of the CD38 expression (278), and no significant differences were revealed (**Fig.2-7B**).

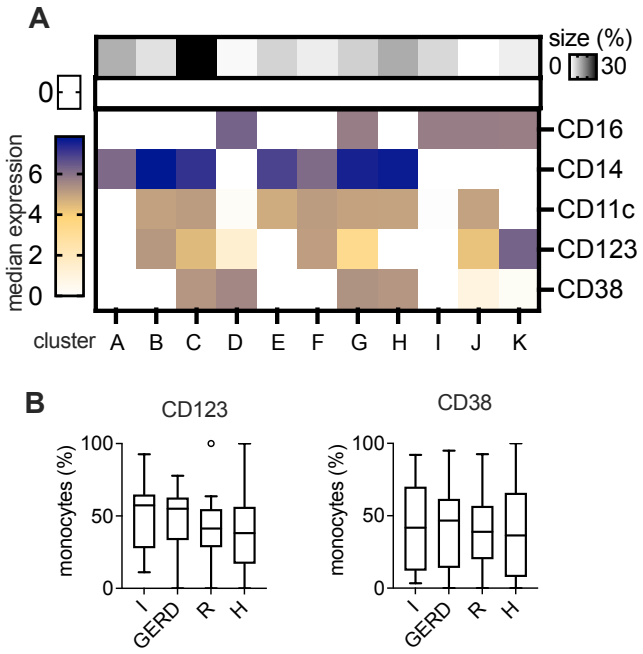

Figure 2-7. Classical monocytes are the prevalent monocyte population in the esophagus. A) Arcsinh transformed median expression of CD16, CD14, CD11c, CD123, and CD38. The horizontal bar on top represents the size of the cluster; the second from the top shows whether the difference in the frequency of cells in the cluster is significant between H and I; the third bar from the top show whether the cluster is more frequent in H or I. **B)** Changes in the proportions of monocytes expressing CD123 and CD38 in patients with active EoE (I), gastroesophageal reflux disease (GERD), EoE in remission (R), and healthy donors (H).

The proportion of B cells was significantly increased in the esophagus of patients with active EoE compared to patients with GERD, EoE patients in remission, and healthy subjects (**Fig.2-8A**). Except for active EoE, B cells are almost non-existent in the esophagus (**Fig.2-8A**). Comparison of B cell subsets inside the B cell population is thus impossible because of low numbers of B cells in GERD, remission, and healthy. We only describe B cells in active EoE based on the IgD and IgA expression in combination with the B cell maturation markers HLA-DR, CD27, CD45RA, and CD38 (**Fig.2-8B**). Analysis of individual markers showed slight variations in the proportions of IgD^+ (median = 36.3%), IgA^+ (median = 20.2%), and IgD^-IgA^- (median = 34.5%) B cells. Most of the B cells expressed markers of early B cell maturation stages CD45RA (median = 87.6%) and HLA-DR (median = 73.9%). In contrast, the markers associated with B cell maturation, such as CD27 (median = 14.1%) and CD38 (median = 24.0%) were less frequent (**Fig.2-8B**). There was a strong correlation between the expression of the plasma cell marker C38 and IgA expression (**Fig.2-8C**). Biopsies with high proportions of CD38 and IgA-expressing B cells also contained low proportions of $HLA\text{-}DR^+$ B cells, and the B cell population in these biopsies represented a significant part of total immune cells (**Fig.2-8C**). Clustering analysis showed that, as expected, IgD and IgA expression was mutually exclusive, with IgD being associated with high HLA-DR expression, suggesting the ability of these cells to stimulate $CD4^+$ T cells, and it confirmed the association of IgA with CD38 (**Fig.2-8D**).

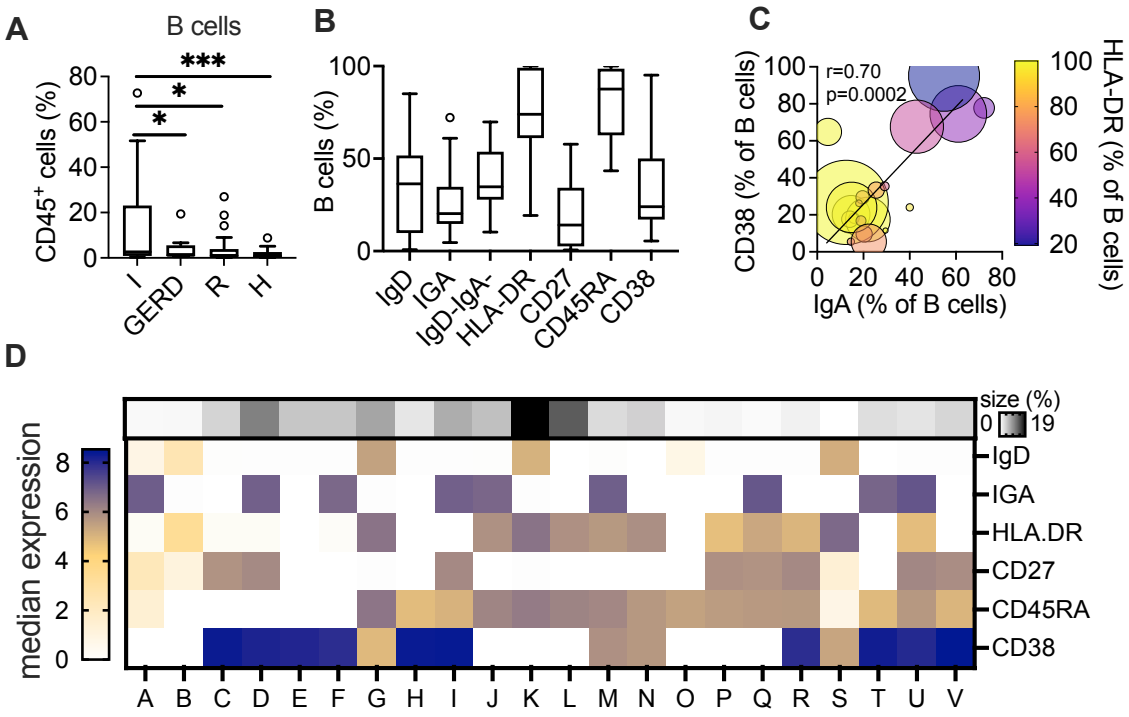

Figure 2-8. B cells accumulate in the esophagus during EoE A) Changes in the proportions of B cells within all $CD45^+$ cells in patients with active EoE (I), gastroesophageal reflux disease (GERD), EoE in remission (R), and healthy donors (H). **B)** Boxplots representing the distribution of proportions of IgD^+, IgA^+, IgD^-IgA^-, $HLA\text{-}DR^+$, $CD27^+$, $CD45RA^+$, and $CD38^+$ B cells in the esophagus of patients with active EoE. **C**) Correlation between the proportion of $CD38^+$ and IgA^+ B cells in the biopsies. Colour represents the expression of HLA-DR, and size of the circle represents the proportion of B cells out of all immune cells in the biopsy **D**) Heat map shows arcsinh transformed median expression of IgD, IgA, HLA-DR, CD27, CD45RA, and CD38. The horizontal bar on top represents the size of the cluster. *=qval<0.05, ***=qval<0.001

T_{EM} $CD4^+$ T cells are activated in active EoE

Next, we asked whether unique populations of activated $CD4^+$ T accumulate in patients with active EOE. As stated above, no differences in the relative abundance of $CD4^+$ T cells between patients with active EoE and healthy subjects were found (**Fig.2-3A**). Clustering analysis was then performed based on the expression of activation markers (CD25, CD38, CD69, HLA-DR, TIGIT, and TIM3). This analysis revealed 11 clusters significantly enriched in active EoE or healthy tissue (**Fig.2-9A-C**). Two clusters (A, B) were significantly more abundant in healthy donors (**Fig.2-9A**). Cells in both clusters expressed HLA-DR, were negative for all other activation markers, and differed in α4 integrin expression (**Fig.2-9A**). Nine clusters (C-K) proportionally increased in patients with active EoE. They contained cells that expressed two or more activation markers while not expressing significant levels of CD45RA, CCR7, or CD57, suggesting they were mostly T_{EM} cells (**Fig.2-9A**). Five clusters (G-K) were more abundant in patients with active EoE compared to both healthy donors and EoE patients in remission (**Fig.2-9B**). All cells in these clusters expressed CD69 (**Fig.2-9A, C**). Cluster K was significantly more frequent in patients with active EoE than in all other conditions (**Fig.2-9A-C**). Comparison of $CD4^+$ T cells positive for individual activation markers between conditions revealed that expression of CD25, CD38, TIGIT, and TIM3 was significantly more frequent on $CD4^+$ T cells from active EoE compared to all other conditions **(Fig.2-9D)**. Expression of CD25 and TIGIT on concatenated $CD4^+$ cells from healthy donors and patients with active EoE showed that there is not only a difference in the proportion of positive cells but also the intensity of expression was significantly higher **(Fig.2-9E)**. These data provide evidence that active EoE is associated with the accumulation of activated T_{EM} $CD4^+$ cells.

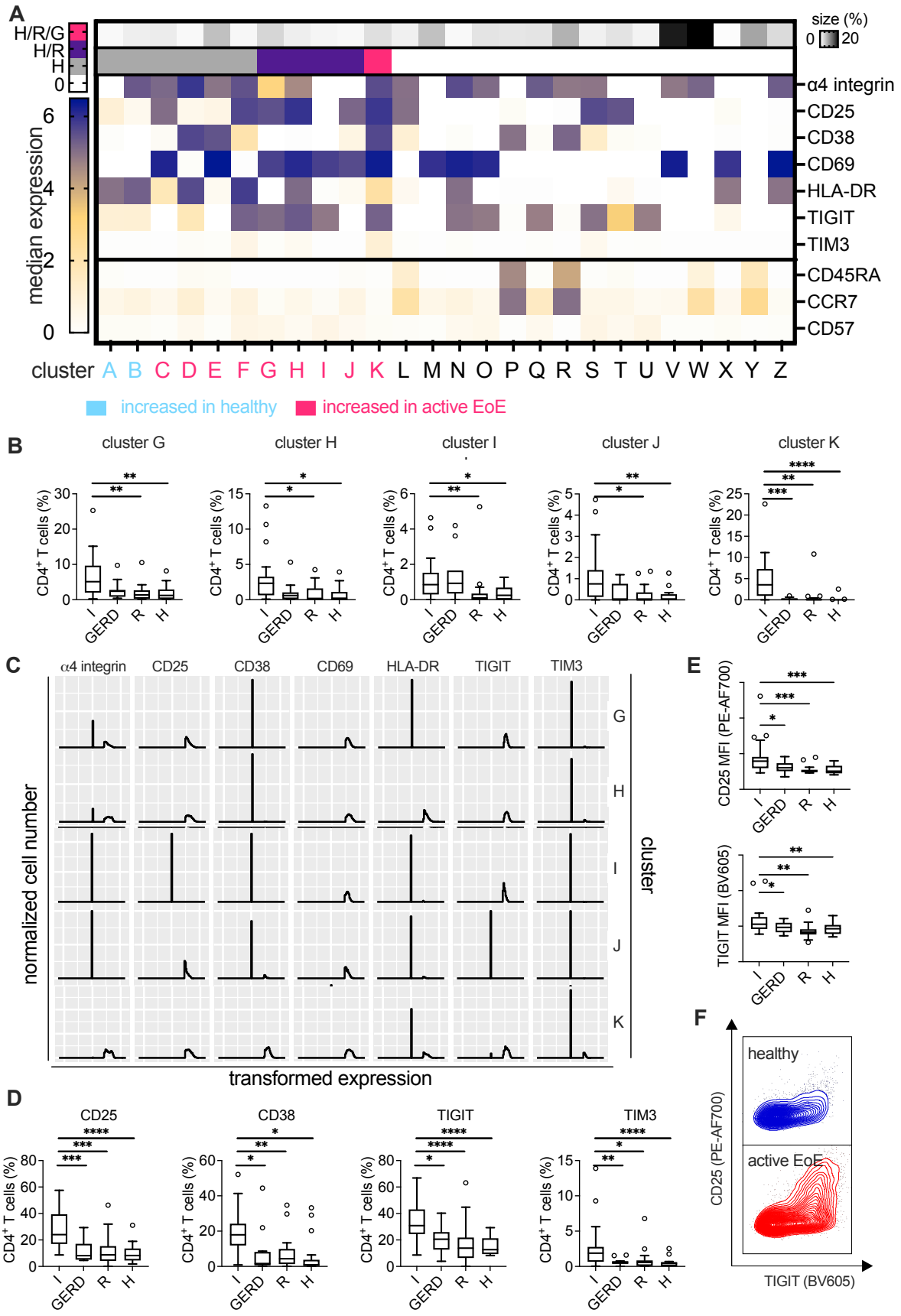
A
H/R/G
H/R
H
0
size (%)
0 20
median expression
6
4
2
0
α4 integrin
CD25
CD38
CD69
HLA-DR
TIGIT
TIM3
CD45RA
CCR7
CD57
cluster A B C D E F G H I J K L M N O P Q R S T U V W X Y Z
increased in healthy
increased in active EoE
B
cluster G
cluster H
cluster I
cluster J
cluster K
CD4+ T cells (%)
I
GERD
R
H
C
α4 integrin
CD25
CD38
CD69
HLA-DR
TIGIT
TIM3
normalized cell number
G
H
I
J
K
cluster
transformed expression
D
CD25
CD38
TIGIT
TIM3
E
CD25 MFI (PE-AF700)
TIGIT MFI (BV605)
F
healthy
active EoE
CD25 (PE-AF700)
TIGIT (BV605)

Figure 2-9 $CD4^+$ T cells in active EoE are activated. **A)** Heat map shows arcsinh transformed median expression of α4 integrin, CD25, CD38, CD69, HLA-DR, TIGIT, TIM3, CD45RA, CCR7, and CD57. Proteins used for clustering are above the black horizontal line, and for analysis of the functional maturation status below the horizontal line. The horizontal bar on top represents the size of the cluster (fraction of cell count in the cluster out of total $CD4^+$ T cells count); the second from the top shows whether the difference in the frequency of cells in the cluster is significant between H and I and the color code represent whether the difference remains significant also for R resp. GERD; the color of the cluster name represents whether the cluster is more frequent in active EoE or healthy tissue. **B)** Changes in the proportions of cells from clusters G-K out of $CD4^+$ T cells between patients with active EoE (I), gastroesophageal reflux disease (GERD), EoE in remission (R), and healthy donors (H). **C)** Histograms of proteins used for clustering on clusters G-K. **D)** Changes in the proportion of $CD4^+$ T cells positive for CD25, CD38, TIGIT, and TIM3 between I, R, GERD, and H. **E**) Changes in the level of expression of CD25 on CD25-expressing cells and the level of expression of TIGIT on TIGIT-expressing cells between I, R, GERD, and H. Median fluorescence intensities are compared. Y axis is linear. **F)** Co-expression of CD25 and TIGIT on concatenated $CD4^+$ T cells from healthy donors (Blue) and patients with active EoE (red). *=qval<0.05, **=qval<0.01, ***=qval<0.001, ****=qval<0.0001

Activated T_{EM} $CD8^+$ T cells accumulate in active EoE

Clustering analysis of $CD8^+$ T cells was performed with the following activation markers: CD25, CD38, CD69, HLA-DR, TIGIT, and TIM3. This analysis revealed one cluster (A), which is significantly more frequent in H than in I biopsies, while two clusters (B-C) were more frequent in I compared to H (**Fig.2-10A, B)**. HLA-DR was similar to $CD4^+$ T cells associated with cluster enriched in healthy tissue (A) (**Fig.2-10A)**. Clusters B and C, enriched in active EoE, represented 2 % and 6 % of $CD8^+$ T cells in active EoE (**Fig.2-10B)**. These two clusters both expressed CD69. Cells in cluster B also expressed CD38, and those in cluster C expressed TIGIT (**Fig.2-10A, C)**. Expression of functional maturation markers CD45RA, CCR7, and CD57 suggested that cells in clusters enriched in active EoE are T_{EM} cells (**Fig.2-10A)**.
Comparison of $CD8^+$ T cells positive for individual activation markers between conditions revealed that expression of CD38 and TIGIT was significantly more frequent in active EoE **(Fig.2-10D)**. These data indicated that active EoE is associated with the accumulation of activated T_{EM} $CD8^+$ T cells, which expressed activation markers different from those found on $CD4^+$ T cells.

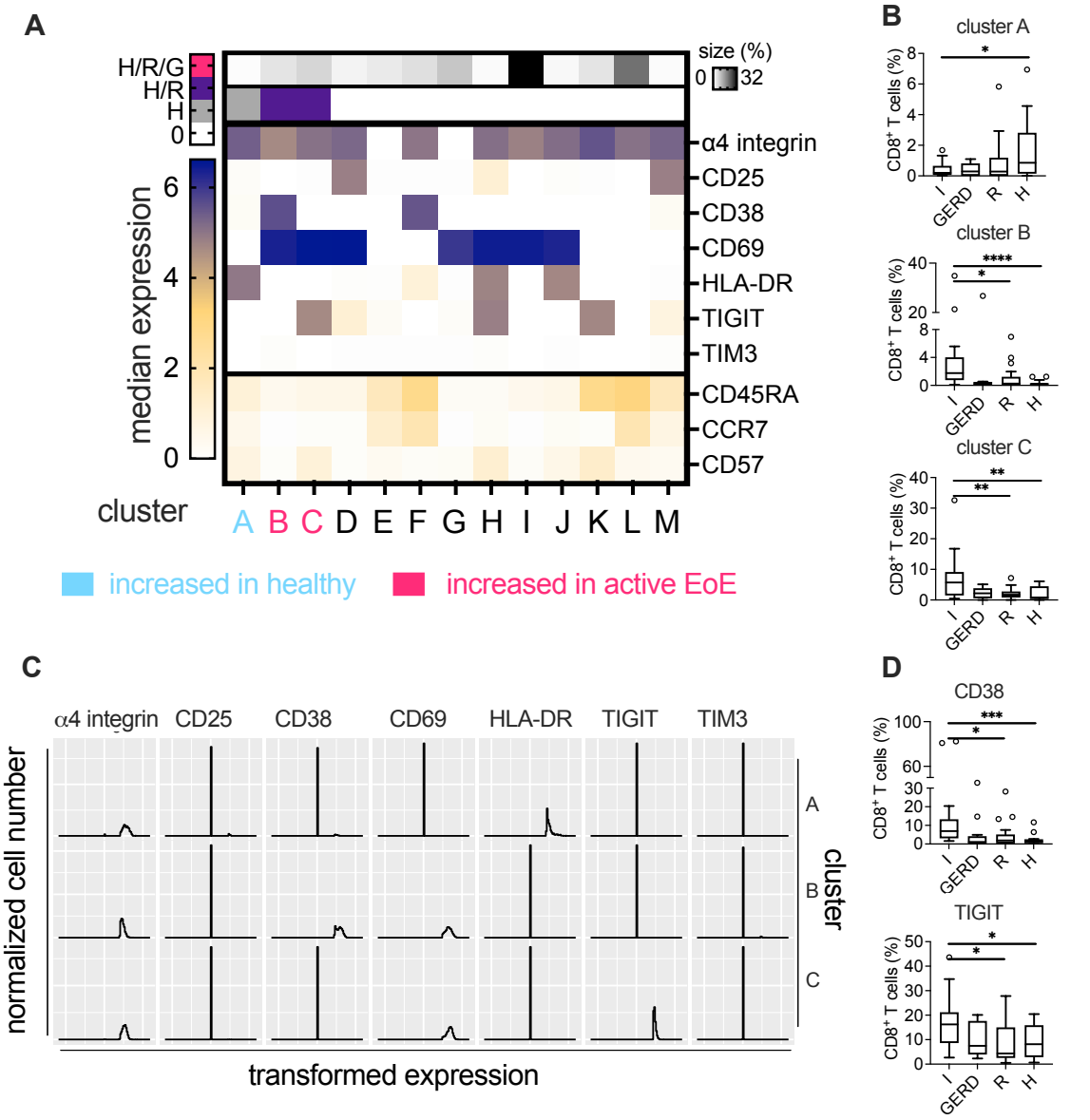

Figure 2-10. CD8⁺ T cells in patients with active EoE are activated. **A)** Heat map shows arcsinh transformed median expression of α4 integrin, CD25, CD38, CD69, HLA-DR, TIGIT, TIM3, CD45RA, CCR7, and CD57. Proteins used for clustering are above the black horizontal line, for analysis of the maturation status below the horizontal line, and for analysis of the functional maturation status below the horizontal line. The horizontal bar on top represents the size of the cluster; the second from the top shows whether the difference in the frequency of cells in the cluster is significant between H and I, and the color code represents whether the difference remains significant for R resp. GERD; the color of the cluster name represents whether the cluster is more frequent in active EoE or healthy tissue. **B)** Changes in the proportions of cells from clusters A, B, and C out of CD8⁺ T cells between patients with active EoE (I), gastroesophageal reflux disease (GERD), EoE in remission (R), and healthy donors (H). **C)** Histograms of proteins used for clustering on cells in clusters A, B, and C. **D)** Changes in the proportion of CD8⁺ T cells positive for CD38 and TIGIT between I, R, GERD, and H. *=qval<0.05, **=qval<0.01, ***=qval<0.001, ****=qval<0.0001

TCR Vδ1$^+$, MAIT cells, and ILCs cells are more activated in patients with active EoE

TCR γδ$^+$ cells represent an essential evolutionary conserved arm of unconventional T cells. We investigated the activation status of TCR Vδ1$^+$, TCR Vδ2$^+$ T cells, and TCR TCR Vδx$^+$ T cells (TCR γδ$^+$TCR Vδ1$^-$ TCR Vδ2$^-$). Because low counts of TCR γδ$^+$ isolated from healthy tissue do not allow clustering analysis, we decided to test the differences in TCR γδ$^+$ cells activation based on the activation marker CD38. CD38 was chosen because it is strongly associated with the activation of T cells, as also previously observed in the IBD studies described above. This analysis revealed that all subsets of TCR γδ$^+$ cells showed a trend towards increased CD38 expression in patients with active EoE compared to healthy donors. TCR Vδ1$^+$ cells and no other TCR γδ$^+$ cells showed a statistically significant increase in CD38 expression (**Fig.2-11**).

Similarly, the proportion of activated MAIT cells expressing CD38 was significantly increased in active EOE compared to healthy donors (**Fig.2-12**).

The TCR-negative counterparts of T cells belonging to the innate system are ILCs and NK cells. ILCs are still relatively unknown cell type, and despite CD38 not being found on their surface in previous studies (279), we observed high CD38 expression on ILCs isolated from patients with active EoE. CD38 expression was significantly higher compared to healthy donors and patients in remission, possibly pointing to increased activation of ILCs in active EoE (**Fig.2-11**).

CD38 is also a marker associated with NK cell activation (149). We observed that NK cells in the esophagus had the highest levels of CD38 compared to all tested lymphoid cell lineages, but the proportion of CD38-expressing NK cells was not significantly increased in patients with active EoE (**Fig.2-11**).

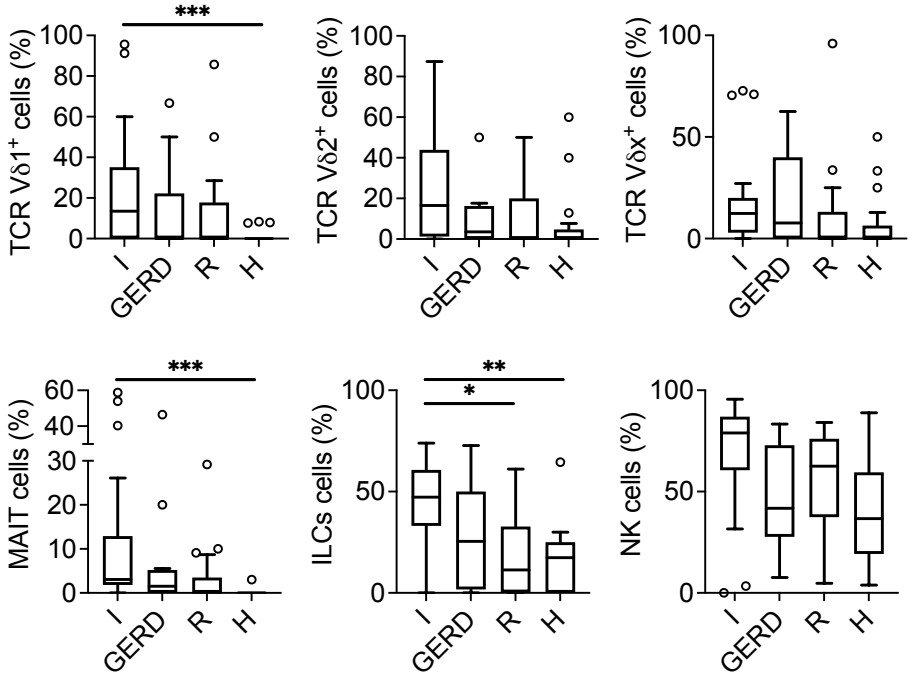

Figure 2-11 TCR Vδ1⁺ cells, MAIT cells, and ILCs are more activated in patients with active EoE. Changes in the proportion of CD38⁺ TCR Vδ1⁺ T cells, TCR Vδ2⁺ T cells, TCR Vδx⁺ T cells, ILCs, and NK cells between patients with active EoE (I), patients with gastroesophageal reflux disease (GERD), patients with EoE in remission (R) and healthy donors (H). *=qval<0.05, **=qval<0.01, ***=qval<0.001

The proportions of CD38⁺ eosinophils and MAIT cells positively correlate

CD38 is the marker of highly activated eosinophils in the esophagus (**Fig. 2-3C**). Since we saw that CD38 expression is increased on several T cell subsets in active EoE (**Fig. 2-9, Fig. 2-10, Fig. 2-11**), we investigated whether the expression of CD38 on eosinophils correlates with the expression of CD38 on some T cell subsets. We discovered a significant positive correlation between CD38 expression on eosinophils and CD38 expression on the MAIT cells (**Tab.2-1, Fig.2-12A**) but not on other T cell subsets (**Tab.2-1**). Thus, we tested the correlation of MAIT cell activation with the infiltration of eosinophils to the esophageal tissue. Interestingly, this analysis revealed a positive correlation between the activation of MAIT cells (expression of CD38) and the number of eosinophils per high-power field (**Fig. 2-12B**).

Table 2-1. Correlation between CD38 expression on eosinophils and T cell subsets, NK cells, and ILCs.
Analysis was performed on the samples taken from patients with active EoE (n=21). Spearman r > 0.5 and P < 0.05 are highlighted in bold.

CD38 on eosinophils vs CD38 on:	CD8 T cells	CD4 T cells	TCR Vδ1 cells	TCR Vδ2 cells	TCR Vδx cells	MAIT cells	NK cells	ILCs
Spearman r	0.1793	0.2494	0.3057	0.2325	-0.08866	**0.6129**	0.001949	-0.2663
95% confidence interval	-0.2862 to 0.5763	-0.2173 to 0.6233	-0.1585 to 0.6592	-0.2343 to 0.6122	-0.5113 to 0.3685	0.2335 to 0.8303	-0.4412 to 0.4443	-0.6343 to 0.2000
P (two-tailed)	0.4368	0.2755	0.1778	0.3105	0.7023	**0.0031**	0.9933	0.2432

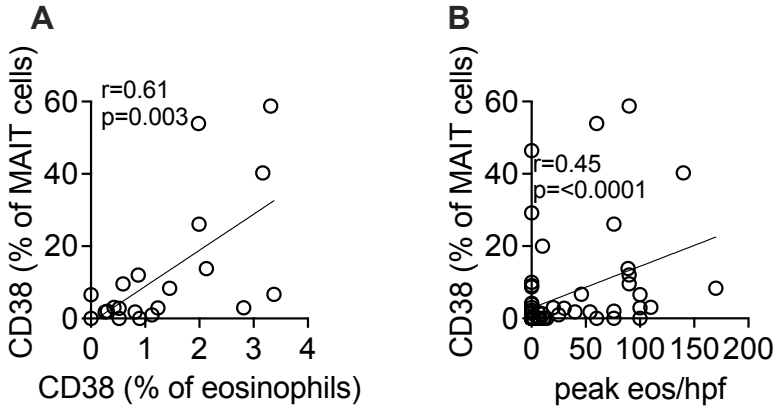

Figure 2-12 CD38 expression on eosinophils is associated with CD38 expression on MAIT cells. A) Correlation between CD38 expression on eosinophils and CD38 expression on MAIT cells (data from biopsies of patients with active EoE; n=21). **B**) Correlation between CD38 expression on MAIT cells and number of eosinophils per high-power field (hpf); (data from all patients involved in the study; n=70).

Eosinophils express MR1, and 5-OP-RU can upregulate its surface levels

The fact that only MAIT cell activation correlated with the activation of eosinophils prompted us to investigate whether these two cell populations may interact with each other and participate in local inflammation.

We hypothesized that eosinophils might present microbial antigens through MR1 to MAIT cells in the EOE mucosa. This possibility is supported by the described increased bacterial load in active EoE biopsies (209) and by the fact that eosinophils may act as APCs presenting short peptides to MHC-II-restricted T cells (280).

MR1 is a ubiquitously expressed molecule. However, different cell types differ in their MR1 surface expression levels and capacity to increase MR1 expression upon exposure to MR1 ligands. We found out that the blood-derived eosinophils express detectable surface levels of MR1, which significantly increased after incubation of eosinophils with 5-OP-RU (**Fig.2-13**). These studies suggested that eosinophils have the potential to present bacterial antigens to MAIT cells.

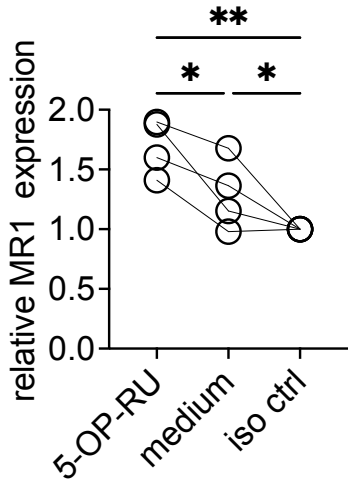

Figure 2-13. Eosinophils express MR1 and have the capacity to increase MR1 expression in response to the MR1 ligand. MR1 expression was determined by flow cytometry and normalized to staining by an isotype control antibody. Medians of four biological replicates are shown. *=qval<0.05, **=qval<0.01

Eosinophils pulsed with 5-OP-RU activate MAIT cells

To directly study the antigen-presentation capability of eosinophils to present MR1 antigens, we isolated these cells from the blood and incubated them with 5-OP-RU - a microbial antigen inducing strong MAIT cell response. These activation studies were performed using eosinophils and with MAIT cells freshly isolated from the same donor. We detected strong MAIT cell activation as indicated by upregulation of the activation marker CD137 on MAIT cells (**Fig.2-14**). Anti-MR1 antibodies significantly blocked MAIT cell activation, thus confirming the MR1 presentation of the microbial antigen to MAIT cells by eosinophils (**Fig.2-14**).

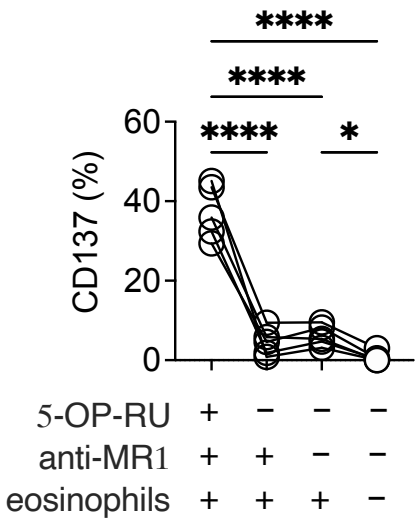

Figure 2-14. Eosinophils induce MR1-restricted activation of MAIT cells. CD137 expression on the MAIT clone was determined by flow cytometry. Medians of five biological replicates are shown. *=qval<0.05, ****=qval<0.0001

Eosinophils-induced MAIT cell activation is TCR-dependent.

We next performed a series of experiments to confirm that eosinophils activate MAIT through engagement of the TCR.

Upon engagement, TCR-CD3 complexes are internalized and degraded, resulting in a reduction of their surface expression (281). Therefore, TCR internalization is direct evidence of its engagement. MAIT cells were incubated overnight with eosinophils in the absence or the presence of 5-OP-RU, and then the surface expression of the TCR heterodimer was investigated by staining T cells with a Va7.2-specific mAb. Unexpectedly, a significant decrease of TCR was observed after overnight incubation with eosinophils alone, without Ag (**Fig.2-15A**), probably as a result of the capacity of eosinophils to engage MAIT cells very efficiently. However, the TCR levels dropped significantly lower if eosinophils were pre-incubated with 5-OP-RU (**Fig.2-15A**) and increased when an anti-MR1 antibody was added to the co-culture (**Fig.2-15A**). These results strongly suggested that MAIT TCR is involved in activating MAIT cells by 5-OP-RU-treated eosinophils.

Next, we used another assay to confirm that MAIT cells were activated upon interaction with eosinophils and Ag. We examined in MAIT cells the phosphorylation of ERK, which is also direct and fast evidence of TCR engagement. A significant

increase in ERK phosphorylation was observed after 1.5 min of co-incubation (**Fig.2-15B**).

To further confirm the engagement of the TCR, 5-OP-RU pre-incubated eosinophils were used to stimulate β2M-deficient Jurkat T cells which had been transduced with the MAIT TCR genes and which were selected for expression of the TCR protein. As a control, we used Jurkat cells not expressing the MAIT TCR. These model cells do not express MR1, thus, their use excludes the possibility of self-presentation. The experiment resulted in luciferase production in a 5-OP-RU dose-dependent manner, confirming that 5-OP-RU pre-treated eosinophils can trigger activation of MAIT TCR (**Fig.2-15C**). This response was blocked by an anti-MR1 antibody, thus further confirming the relevance of MR1-Ag presentation (**Fig.2-15C**).

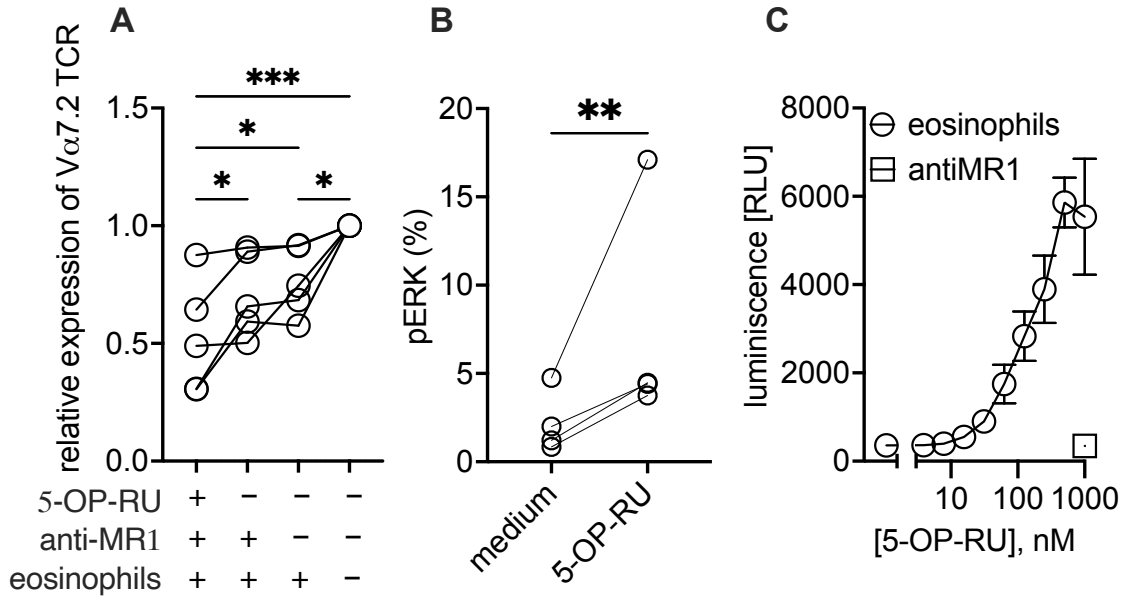

Figure 2-15. Eosinophils-induced activation of MAIT cells is TCR mediated. **A**) Eosinophils pulsed with 5-OP-RU (100nM) induce MR1-dependent downregulation of Vα7.2 TCR on MAIT cells. MFI of Vα7.2 TCR in all investigated conditions were normalized to MFI of untreated T cells. Medians of five biological replicates are shown. *=qval<0.05, ***=qval<0.001 **B**) Phosphorylation of ERK in MAIT cells after incubation with 5-OP-RU (100nM) pulsed eosinophils. Medians of four biological replicates are shown. **=qval<0.01 **C**) The luciferase expression by β2M-KO NFAT-Luc Jurkat cells transduced with MAIT TCR triggered by 5-OP-RU pulsed eosinophils. Luminescence is expressed as the median ± SD of technical triplicates. The data shown are representative of three independent experiments, and one representative experiment is shown.

MAIT cells stimulated by eosinophils produce cytokines that can activate eosinophils

Activated MAIT cells can produce large amounts of many different soluble factors (75, 282). We found that co-culture of eosinophils pulsed with 5-OP-RU and MAIT cells led to a significant increase of both GM-CSF and IFN-γ in the supernatant, which was blocked by anti-MR1 mAbs (**Fig.2-16A, B**). As both cytokines can also be produced by eosinophils (283, 284), we performed intracellular staining to identify the cells producing the soluble factors. These experiments revealed that GM-CSF and IFN-γ are produced by MAIT cells in these experimental conditions (**Fig.2-16C**).

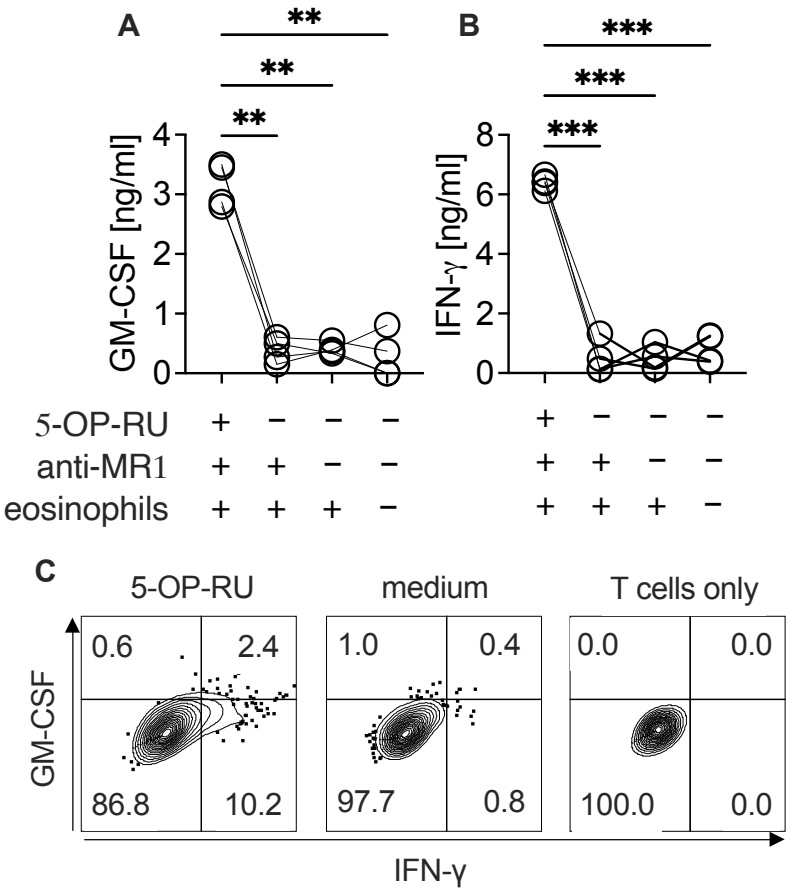

Figure 2-16. Eosinophils induce the production of cytokines by MAIT cells. **A-B**) Eosinophils pulsed with 5-OP-RU (80nM) induce MR1-dependent expression of GM-CSF and IFN-γ. Medians of five biological replicates are shown. **=qval<0.01, ***=qval<0.001 **C**) Examples of intracellular staining of GM-CSF and IFN-γ in MAIT cell clone after co-culture with eosinophils pulsed with 5-OP-RU. The data shown are representative of three independent experiments, and one representative experiment is shown.

Eosinophils are less potent and less efficient in MAIT cell stimulation than monocytes

The capacity of eosinophils to induce cytokine production by MAIT cells was compared to that of monocytes, which represent professional antigen-presenting cells. This comparison revealed that eosinophils are less efficient than monocytes. (**Fig.2-17**). The response of MAIT cells to different Ag doses showed that the Ag potency was decreased; thus, more Ag was needed to induce 50% of maximal response. These findings might indicate eosinophils' less efficient capacity to generate stimulatory MR1-Ag complexes. We also observed that the total amounts of produced cytokines were lower when eosinophils were the APC. These findings, instead may suggest that eosinophils do not express sufficient co-stimulatory molecules or do not produce soluble factors that enhance cytokine release by T cells. Similar results were obtained using two types of MAIT cells, namely a MAIT cell clone (**Fig.2-17A, B**) and a bulk MAIT cell population derived from blood (**Fig.2-17C, D**). Similar differences in Ag potency and efficacy were observed by measuring IFN-γ (**Fig.2-17A, C**) and TNF-α (**Fig.2-17B, D**).

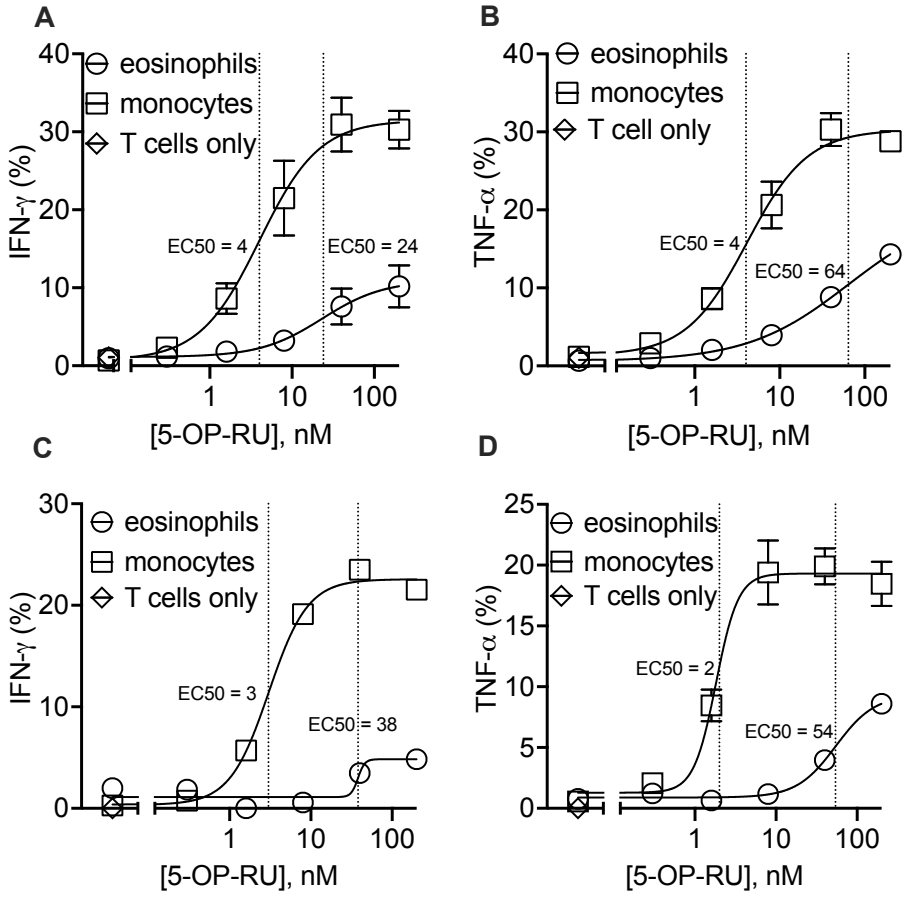

Figure 2-17. Eosinophils are less potent and less efficient in MAIT cell activation than monocytes. **A, B**) Eosinophils and monocytes pulsed with 5-OP-RU induce GM-CSF and IFN-γ production by MAIT cell clone. EC50 of 5-OP-RU is lower in monocytes for both cytokines. **C, D**) Eosinophils and monocytes pulsed with 5-OP-RU induce GM-CSF and IFN-γ production by MAIT cells from the same donor. EC50 of 5-OP-RU is lower in monocytes for both cytokines. Cytokine production was determined by intracellular staining and flow cytometry. The data shown are representative of three independent experiments, and one representative experiment is shown.

Eosinophils upregulate activation markers after coculture with MAIT cells

Eosinophils-induced activation of MAIT cells resulted in the production of cytokines that may have an activating function on eosinophils. Analysis of eosinophils expressing the activation marker CD69 revealed a significantly increased expression on 5-OP-RU pulsed eosinophils co-cultured with MAIT cells (**Fig.2-18A**). Simultaneously, we also observed an increase in CD66b levels in the same eosinophils (**Fig.2-18B**). This marker is associated with the activation and adhesion of eosinophils (285).

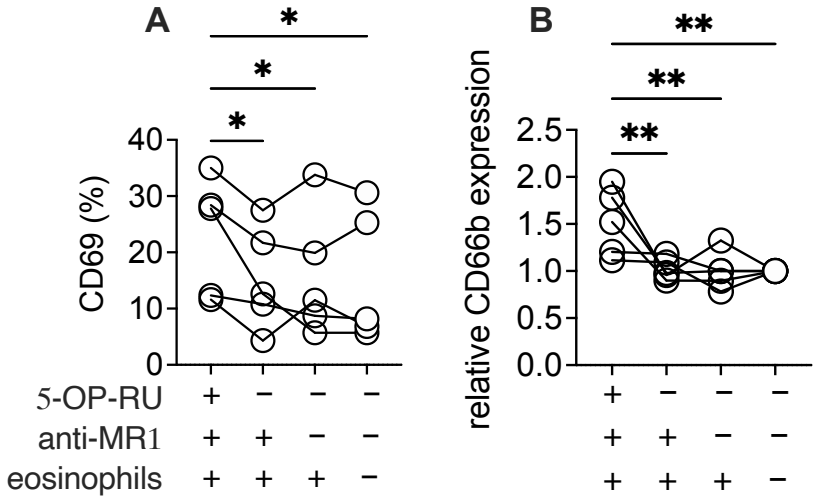

Figure 2-18. MAIT cells induce the activation of eosinophils. **A**) Eosinophils pulsed with 5-OP-RU (100nM) upregulate activation marker CD69 after co-culture with MAIT cells. *=qval<0.05, **B**) Eosinophils pulsed with 5-OP-RU (100nM) upregulate activation marker CD66b after co-culture with MAIT cells. MFI of CD66b in all investigated conditions were normalized to MFI of CD66b on untreated eosinophils. **=qval<0.01; Medians of five biological replicates are shown.

Discussion

Our studies provide a description of changes in immune cell subsets composition, activation, and functional maturation in the esophageal tissue of patients with Eosinophilic esophagitis (EoE).

We discovered an accumulation of $CD45^+$ cells in the esophagus of patients with active EoE. When comparing the relative abundance of individual immune cell subsets, we confirmed that active EoE is associated with eosinophil infiltration to the esophagus. Most eosinophils in the esophagus of patients with active EoE expressed activation markers, which fits with the known presence of eosinophil granule proteins in the esophageal tissue of EoE patients (286). Also, the esophageal tissue of patients with active EoE contains a higher relative abundance of mast cells, basophils, and B cell subsets (IgD^-IgA^-, IgA^+, IgD^+) compared to healthy tissue.

Mast cell accumulation is associated with EoE, and mastocytosis often persists after the resolution of eosinophilia (287, 288). Our findings indicate that the relative abundance of mast cells remains unchanged after the onset of remission in patients with EoE. Mast cells in active EoE and EoE in remission are phenotypically different with a less mature phenotype (they are more CD123-positive) (289) associated with inflamed tissue. Mast cells in inflamed tissue also express more CCR3 than in remission, suggesting they might be attracted to the esophagus by CCR3-binding chemokines (eotaxins, MCP2-4, RANTES) similarly to eosinophils (290). The expression of the activation marker CD69 is higher in active EoE than in healthy donors but not higher than in patients with EoE in remission, as previously reported (287, 288, 291). Perhaps, mast cells migrate to the esophagus alongside eosinophils, become activated in active EoE, and stay activated during remission.

The adaptive immune system is thought to play a key role in EoE pathogenesis. A healthy esophagus is largely deficient in B lymphocytes (292). We found that the presence of B cells in the esophagus significantly increases in active EoE. It was previously described that IgE-producing B cells are present in the inflamed mucosa and that they could have a role in mast cell activation (293). We observed that also IgA and IgD-expressing B cells are more abundant in active EoE. Simultaneously, most of the B cells in the esophagus of patients with active EoE are in early maturation stages, and only a quarter of them expressed plasma cell markers. However, a significant part of these plasma cells expresses IgA. IgA is absent in the healthy

esophagus (201) and it might contribute to EoE by the induction of eosinophil degranulation (294).

T cells, and mostly the Th2 subset, are important mediators of EoE (203). Their activation requires the presence of efficient antigen-presenting cells in addition to the presence of antigen. As DCs represent the most efficient antigen-presenting cells, changes in the DCs population likely impact T cell activation. We observed the accumulation of Siglec-3^{+} plasmacytoid DCs in patients with active EoE. Interestingly, we also noticed that CD123^{+}CD11c^{+} DCs occur in the esophagus at a much higher frequency than was reported for the blood (277). This suggests that the local environment in the esophagus may trigger the development of CD123^{+}CD11c^{+} cells or that, in a non-mutually exclusive manner, these cells preferentially migrate from the peripheral blood to the esophagus. The functional properties of these cells compared to conventional CD123^{-}CD11c^{+} and CD123^{+}CD11c^{-} DCs remains to be investigated.

Investigation of T cells was focused on the changes in their activation and functional maturation stages. We found that CD4^{+} T cells are significantly more activated in patients with active EoE. The activation is mainly connected with the expression of the activation markers CD25 and CD38, and most of the activated CD4^{+} T cells are CD45RA^{-}CCR7^{-}CD57^{-} suggestive of an effector memory phenotype (41). Furthermore, a significant increase in the expression inhibitory receptors TIM3 and TIGIT suggests intense and persistent activation of CD4^{+} T cells (295, 296). We also showed that both CD25 and TIGIT are largely co-expressed, and the MFI of positive cells for both is higher in patients with active EoE. CD127^{-}CD25^{+}TIGIT^{+} CD4^{+} T cells represent a population enriched in Treg cells with the ability to inhibit Th1 and Th17 cell responses(297).

Similarly to CD4^{+} T cells, also CD8^{+} T cells expressed more activation markers in patients with active EoE. CD38 and TIGIT were predominantly expressed in this T cell subset. CD38 was also upregulated in patients with active EoE on TCR Vδ1^{+} cells, ILCs, and MAIT cells pointing to activation of these cells (298). However, when we compared the presence of activated T cells with that of activated eosinophils, we found a significant correlation only with the activation of MAIT cells. These findings indicated that MAIT cells might have a role in local inflammation.

Furthermore, the published observation that bacterial load is increased in samples from the esophagus of EOE patients compared to healthy controls (209) further supports a potential local activation of microbial-responsive MAIT cells. MAIT cells

recognize bacterial antigens bound to the MR1 molecule. It was recently shown that MAIT cells have an important role in the pathogenesis of atopic dermatitis, and blocking MAIT cell activation led to the improvement of atopic dermatitis in mice model (299). Importantly, antagonists of MAIT cells led to diminished recruitment of IL-4 and IL-13 producing cells, including basophils and ILCs, and also promoted a decreased activation of skin-infiltrating eosinophils (299). Eosinophils can serve as APCs for MHC-II restricted T cells (280), but their capacity to present antigens to MR1 restricted T cells were never investigated. As eosinophils can represent up to 50 % of immune cells isolated from EOE biopsies, we investigated the possible crosstalk between MAIT cells and eosinophils exposed to stimulatory MR1 ligand of bacterial origin.

We demonstrated that eosinophils could upregulate surface MR1 levels upon incubation with the bacterial ligand 5-OP-RU. More importantly, 5-OP-RU-pulsed eosinophils activated MAIT cells in an MR1-restricted and TCR-mediated manner. In response, MAIT cells produced cytokines, including GM-CSF, TNF-α, and IFN-γ. GM-CSF is chemotactic for eosinophils, induces their activation, and increases their survival (300-302). TNF-α induces the production of H_2O_2 by eosinophils (303) and increases their survival (304). Lastly, IFN-γ was shown to enhance eosinophil effector function induced by GM-CSF (305). Therefore, we can hypothesize that MAIT cells, when activated by microbial antigens locally presented by eosinophils, may contribute to the perpetuation of migration of eosinophils to the esophageal tissue in patients with EoE. In addition, eosinophils co-cultured with MAIT cells upregulated the activation markers CD69 and CD66b on their surface (285, 306), supporting the hypothesis that they become activated by soluble factors produced by MAIT cells. Although eosinophils are less potent in MAIT cell stimulation than canonical antigen-presenting cells such as monocytes, their vast majority in inflamed EOE tissue suggests they can play a prominent role in activating MAIT cells in this inflammatory condition.

These studies revealed a possible crosstalk between eosinophils and MAIT cells in EoE, in which eosinophils exposed to increased concentration of bacterial products activate MAIT cells. In turn, activated MAIT cells release soluble factors, which attract and activate eosinophils.

References

1. Murphy K, Travers, P., Walport, M., & Janeway, C. Janeway's immunobiology. 6th. ed. science G, editor. New York2008.
2. Mowat AM, Agace WW. Regional specialization within the intestinal immune system. Nat Rev Immunol. 2014;14(10):667-85.
3. Schneeberger EE, Lynch RD. Structure, function, and regulation of cellular tight junctions. Am J Physiol. 1992;262(6 Pt 1):L647-61.
4. Nochi T, Kiyono H. Innate immunity in the mucosal immune system. Curr Pharm Des. 2006;12(32):4203-13.
5. Zanin M, Baviskar P, Webster R, Webby R. The Interaction between Respiratory Pathogens and Mucus. Cell Host Microbe. 2016;19(2):159-68.
6. Johansson ME, Sjovall H, Hansson GC. The gastrointestinal mucus system in health and disease. Nat Rev Gastroenterol Hepatol. 2013;10(6):352-61.
7. Allen A, Hutton DA, Pearson JP. The MUC2 gene product: a human intestinal mucin. Int J Biochem Cell Biol. 1998;30(7):797-801.
8. Mahida YR, Rose F, Chan WC. Antimicrobial peptides in the gastrointestinal tract. Gut. 1997;40(2):161-3.
9. Lubbers R, van Essen MF, van Kooten C, Trouw LA. Production of complement components by cells of the immune system. Clin Exp Immunol. 2017;188(2):183-94.
10. Dunkelberger JR, Song WC. Complement and its role in innate and adaptive immune responses. Cell Res. 2010;20(1):34-50.
11. Akira S, Uematsu S, Takeuchi O. Pathogen recognition and innate immunity. Cell. 2006;124(4):783-801.
12. Janeway CA, Jr., Medzhitov R. Innate immune recognition. Annu Rev Immunol. 2002;20:197-216.
13. Matzinger P. The danger model: a renewed sense of self. Science. 2002;296(5566):301-5.
14. Mesin L, Ersching J, Victora GD. Germinal Center B Cell Dynamics. Immunity. 2016;45(3):471-82.
15. Klein U, Tu Y, Stolovitzky GA, Keller JL, Haddad J, Jr., Miljkovic V, et al. Transcriptional analysis of the B cell germinal center reaction. Proc Natl Acad Sci U S A. 2003;100(5):2639-44.
16. Lamm ME. The IgA mucosal immune system. Am J Kidney Dis. 1988;12(5):384-7.
17. Brandtzaeg P. Role of secretory antibodies in the defence against infections. Int J Med Microbiol. 2003;293(1):3-15.
18. Schwartz RH. T cell anergy. Annu Rev Immunol. 2003;21:305-34.
19. Ruddle NH, Akirav EM. Secondary lymphoid organs: responding to genetic and environmental cues in ontogeny and the immune response. J Immunol. 2009;183(4):2205-12.
20. Neyt K, Perros F, GeurtsvanKessel CH, Hammad H, Lambrecht BN. Tertiary lymphoid organs in infection and autoimmunity. Trends Immunol. 2012;33(6):297-305.
21. Bousso P. T-cell activation by dendritic cells in the lymph node: lessons from the movies. Nat Rev Immunol. 2008;8(9):675-84.
22. Obst R. The Timing of T Cell Priming and Cycling. Front Immunol. 2015;6:563.
23. Lange J, Rivera-Ballesteros O, Buggert M. Human mucosal tissue-resident memory T cells in health and disease. Mucosal Immunol. 2022;15(3):389-97.

24. Masopust D, Choo D, Vezys V, Wherry EJ, Duraiswamy J, Akondy R, et al. Dynamic T cell migration program provides resident memory within intestinal epithelium. J Exp Med. 2010;207(3):553-64.
25. Hammarlund E, Lewis MW, Hansen SG, Strelow LI, Nelson JA, Sexton GJ, et al. Duration of antiviral immunity after smallpox vaccination. Nat Med. 2003;9(9):1131-7.
26. Crotty S, Felgner P, Davies H, Glidewell J, Villarreal L, Ahmed R. Cutting edge: long-term B cell memory in humans after smallpox vaccination. J Immunol. 2003;171(10):4969-73.
27. Seder RA, Ahmed R. Similarities and differences in CD4+ and CD8+ effector and memory T cell generation. Nat Immunol. 2003;4(9):835-42.
28. Foulds KE, Zenewicz LA, Shedlock DJ, Jiang J, Troy AE, Shen H. Cutting edge: CD4 and CD8 T cells are intrinsically different in their proliferative responses. J Immunol. 2002;168(4):1528-32.
29. Banerjee A, Gordon SM, Intlekofer AM, Paley MA, Mooney EC, Lindsten T, et al. Cutting edge: The transcription factor eomesodermin enables CD8+ T cells to compete for the memory cell niche. J Immunol. 2010;185(9):4988-92.
30. Zhu J, Yamane H, Paul WE. Differentiation of effector CD4 T cell populations (*). Annu Rev Immunol. 2010;28:445-89.
31. Raphael I, Nalawade S, Eagar TN, Forsthuber TG. T cell subsets and their signature cytokines in autoimmune and inflammatory diseases. Cytokine. 2015;74(1):5-17.
32. Nelms K, Keegan AD, Zamorano J, Ryan JJ, Paul WE. The IL-4 receptor: signaling mechanisms and biologic functions. Annu Rev Immunol. 1999;17:701-38.
33. Licona-Limon P, Kim LK, Palm NW, Flavell RA. TH2, allergy and group 2 innate lymphoid cells. Nat Immunol. 2013;14(6):536-42.
34. Zhao P, Xiao X, Ghobrial RM, Li XC. IL-9 and Th9 cells: progress and challenges. Int Immunol. 2013;25(10):547-51.
35. Hoppenot D, Malakauskas K, Lavinskiene S, Bajoriuniene I, Kalinauskaite V, Sakalauskas R. Peripheral blood Th9 cells and eosinophil apoptosis in asthma patients. Medicina (Kaunas). 2015;51(1):10-7.
36. Duhen T, Geiger R, Jarrossay D, Lanzavecchia A, Sallusto F. Production of interleukin 22 but not interleukin 17 by a subset of human skin-homing memory T cells. Nat Immunol. 2009;10(8):857-63.
37. Tian T, Yu S, Ma D. Th22 and related cytokines in inflammatory and autoimmune diseases. Expert Opin Ther Targets. 2013;17(2):113-25.
38. Lee W, Lee GR. Transcriptional regulation and development of regulatory T cells. Exp Mol Med. 2018;50(3):e456.
39. Jiang S, Dong C. A complex issue on CD4(+) T-cell subsets. Immunol Rev. 2013;252(1):5-11.
40. Sallusto F, Geginat J, Lanzavecchia A. Central memory and effector memory T cell subsets: function, generation, and maintenance. Annu Rev Immunol. 2004;22:745-63.
41. Larbi A, Fulop T. From "truly naive" to "exhausted senescent" T cells: when markers predict functionality. Cytometry A. 2014;85(1):25-35.
42. Pasman L, Kasper DL. Building conventions for unconventional lymphocytes. Immunol Rev. 2017;279(1):52-62.
43. Calabi F, Jarvis JM, Martin L, Milstein C. Two classes of CD1 genes. Eur J Immunol. 1989;19(2):285-92.

44. de la Salle H, Mariotti S, Angenieux C, Gilleron M, Garcia-Alles LF, Malm D, et al. Assistance of microbial glycolipid antigen processing by CD1e. Science. 2005;310(5752):1321-4.
45. Facciotti F, Ramanjaneyulu GS, Lepore M, Sansano S, Cavallari M, Kistowska M, et al. Peroxisome-derived lipids are self antigens that stimulate invariant natural killer T cells in the thymus. Nat Immunol. 2012;13(5):474-80.
46. Dougan SK, Kaser A, Blumberg RS. CD1 expression on antigen-presenting cells. Curr Top Microbiol Immunol. 2007;314:113-41.
47. Van Rhijn I, Godfrey DI, Rossjohn J, Moody DB. Lipid and small-molecule display by CD1 and MR1. Nat Rev Immunol. 2015;15(10):643-54.
48. Mori L, Lepore M, De Libero G. The Immunology of CD1- and MR1-Restricted T Cells. Annu Rev Immunol. 2016;34:479-510.
49. Van Rhijn I, Kasmar A, de Jong A, Gras S, Bhati M, Doorenspleet ME, et al. A conserved human T cell population targets mycobacterial antigens presented by CD1b. Nat Immunol. 2013;14(7):706-13.
50. de Jong A, Cheng TY, Huang S, Gras S, Birkinshaw RW, Kasmar AG, et al. CD1a-autoreactive T cells recognize natural skin oils that function as headless antigens. Nat Immunol. 2014;15(2):177-85.
51. Lepore M, de Lalla C, Gundimeda SR, Gsellinger H, Consonni M, Garavaglia C, et al. A novel self-lipid antigen targets human T cells against CD1c(+) leukemias. J Exp Med. 2014;211(7):1363-77.
52. Rossjohn J, Gras S, Miles JJ, Turner SJ, Godfrey DI, McCluskey J. T cell antigen receptor recognition of antigen-presenting molecules. Annu Rev Immunol. 2015;33:169-200.
53. de Jong A. Activation of human T cells by CD1 and self-lipids. Immunol Rev. 2015;267(1):16-29.
54. Godfrey DI, MacDonald HR, Kronenberg M, Smyth MJ, Van Kaer L. NKT cells: what's in a name? Nat Rev Immunol. 2004;4(3):231-7.
55. Bendelac A, Savage PB, Teyton L. The biology of NKT cells. Annu Rev Immunol. 2007;25:297-336.
56. Kawano T, Cui J, Koezuka Y, Toura I, Kaneko Y, Motoki K, et al. CD1d-restricted and TCR-mediated activation of valpha14 NKT cells by glycosylceramides. Science. 1997;278(5343):1626-9.
57. Pei B, Vela JL, Zajonc D, Kronenberg M. Interplay between carbohydrate and lipid in recognition of glycolipid antigens by natural killer T cells. Ann N Y Acad Sci. 2012;1253:68-79.
58. Kain L, Webb B, Anderson BL, Deng S, Holt M, Costanzo A, et al. The identification of the endogenous ligands of natural killer T cells reveals the presence of mammalian alpha-linked glycosylceramides. Immunity. 2014;41(4):543-54.
59. Godfrey DI, Kronenberg M. Going both ways: immune regulation via CD1d-dependent NKT cells. J Clin Invest. 2004;114(10):1379-88.
60. Terabe M, Swann J, Ambrosino E, Sinha P, Takaku S, Hayakawa Y, et al. A nonclassical non-Valpha14Jalpha18 CD1d-restricted (type II) NKT cell is sufficient for down-regulation of tumor immunosurveillance. J Exp Med. 2005;202(12):1627-33.
61. Chang DH, Deng H, Matthews P, Krasovsky J, Ragupathi G, Spisek R, et al. Inflammation-associated lysophospholipids as ligands for CD1d-restricted T cells in human cancer. Blood. 2008;112(4):1308-16.

62. Hayday AC. [gamma][delta] cells: a right time and a right place for a conserved third way of protection. Annu Rev Immunol. 2000;18:975-1026.
63. Hayday AC. Gammadelta T cells and the lymphoid stress-surveillance response. Immunity. 2009;31(2):184-96.
64. Arden B, Clark SP, Kabelitz D, Mak TW. Human T-cell receptor variable gene segment families. Immunogenetics. 1995;42(6):455-500.
65. Vantourout P, Hayday A. Six-of-the-best: unique contributions of gammadelta T cells to immunology. Nat Rev Immunol. 2013;13(2):88-100.
66. De Libero G, Lau SY, Mori L. Phosphoantigen Presentation to TCR gammadelta Cells, a Conundrum Getting Less Gray Zones. Front Immunol. 2014;5:679.
67. Burk MR, Mori L, De Libero G. Human V gamma 9-V delta 2 cells are stimulated in a cross-reactive fashion by a variety of phosphorylated metabolites. Eur J Immunol. 1995;25(7):2052-8.
68. Sandstrom A, Peigne CM, Leger A, Crooks JE, Konczak F, Gesnel MC, et al. The intracellular B30.2 domain of butyrophilin 3A1 binds phosphoantigens to mediate activation of human Vgamma9Vdelta2 T cells. Immunity. 2014;40(4):490-500.
69. Willcox CR, Vantourout P, Salim M, Zlatareva I, Melandri D, Zanardo L, et al. Butyrophilin-like 3 Directly Binds a Human Vgamma4(+) T Cell Receptor Using a Modality Distinct from Clonally-Restricted Antigen. Immunity. 2019;51(5):813-25 e4.
70. McCarthy NE, Eberl M. Human gammadelta T-Cell Control of Mucosal Immunity and Inflammation. Front Immunol. 2018;9:985.
71. Porcelli S, Yockey CE, Brenner MB, Balk SP. Analysis of T cell antigen receptor (TCR) expression by human peripheral blood CD4-8- alpha/beta T cells demonstrates preferential use of several V beta genes and an invariant TCR alpha chain. J Exp Med. 1993;178(1):1-16.
72. Treiner E, Duban L, Bahram S, Radosavljevic M, Wanner V, Tilloy F, et al. Selection of evolutionarily conserved mucosal-associated invariant T cells by MR1. Nature. 2003;422(6928):164-9.
73. Tilloy F, Treiner E, Park SH, Garcia C, Lemonnier F, de la Salle H, et al. An invariant T cell receptor alpha chain defines a novel TAP-independent major histocompatibility complex class Ib-restricted alpha/beta T cell subpopulation in mammals. J Exp Med. 1999;189(12):1907-21.
74. Lepore M, Kalinichenko A, Colone A, Paleja B, Singhal A, Tschumi A, et al. Parallel T-cell cloning and deep sequencing of human MAIT cells reveal stable oligoclonal TCRbeta repertoire. Nat Commun. 2014;5:3866.
75. Dusseaux M, Martin E, Serriari N, Peguillet I, Premel V, Louis D, et al. Human MAIT cells are xenobiotic-resistant, tissue-targeted, CD161hi IL-17-secreting T cells. Blood. 2011;117(4):1250-9.
76. Ussher JE, Bilton M, Attwod E, Shadwell J, Richardson R, de Lara C, et al. CD161++ CD8+ T cells, including the MAIT cell subset, are specifically activated by IL-12+IL-18 in a TCR-independent manner. Eur J Immunol. 2014;44(1):195-203.
77. Sharma PK, Wong EB, Napier RJ, Bishai WR, Ndung'u T, Kasprowicz VO, et al. High expression of CD26 accurately identifies human bacteria-reactive MR1-restricted MAIT cells. Immunology. 2015;145(3):443-53.
78. Gherardin NA, Souter MN, Koay HF, Mangas KM, Seemann T, Stinear TP, et al. Human blood MAIT cell subsets defined using MR1 tetramers. Immunol Cell Biol. 2018;96(5):507-25.

79. Walker LJ, Kang YH, Smith MO, Tharmalingham H, Ramamurthy N, Fleming VM, et al. Human MAIT and CD8alphaalpha cells develop from a pool of type-17 precommitted CD8+ T cells. Blood. 2012;119(2):422-33.
80. Treiner E, Lantz O. CD1d- and MR1-restricted invariant T cells: of mice and men. Curr Opin Immunol. 2006;18(5):519-26.
81. Reantragoon R, Kjer-Nielsen L, Patel O, Chen Z, Illing PT, Bhati M, et al. Structural insight into MR1-mediated recognition of the mucosal associated invariant T cell receptor. J Exp Med. 2012;209(4):761-74.
82. Kjer-Nielsen L, Patel O, Corbett AJ, Le Nours J, Meehan B, Liu L, et al. MR1 presents microbial vitamin B metabolites to MAIT cells. Nature. 2012;491(7426):717-23.
83. Riegert P, Wanner V, Bahram S. Genomics, isoforms, expression, and phylogeny of the MHC class I-related MR1 gene. J Immunol. 1998;161(8):4066-77.
84. Harriff MJ, Karamooz E, Burr A, Grant WF, Canfield ET, Sorensen ML, et al. Endosomal MR1 Trafficking Plays a Key Role in Presentation of Mycobacterium tuberculosis Ligands to MAIT Cells. PLoS Pathog. 2016;12(3):e1005524.
85. McWilliam HE, Eckle SB, Theodossis A, Liu L, Chen Z, Wubben JM, et al. The intracellular pathway for the presentation of vitamin B-related antigens by the antigen-presenting molecule MR1. Nat Immunol. 2016;17(5):531-7.
86. Le Bourhis L, Martin E, Peguillet I, Guihot A, Froux N, Core M, et al. Antimicrobial activity of mucosal-associated invariant T cells. Nat Immunol. 2010;11(8):701-8.
87. Gold MC, Cerri S, Smyk-Pearson S, Cansler ME, Vogt TM, Delepine J, et al. Human mucosal associated invariant T cells detect bacterially infected cells. PLoS Biol. 2010;8(6):e1000407.
88. Georgel P, Radosavljevic M, Macquin C, Bahram S. The non-conventional MHC class I MR1 molecule controls infection by Klebsiella pneumoniae in mice. Mol Immunol. 2011;48(5):769-75.
89. Le Bourhis L, Dusseaux M, Bohineust A, Bessoles S, Martin E, Premel V, et al. MAIT cells detect and efficiently lyse bacterially-infected epithelial cells. PLoS Pathog. 2013;9(10):e1003681.
90. Kurioka A, Ussher JE, Cosgrove C, Clough C, Fergusson JR, Smith K, et al. MAIT cells are licensed through granzyme exchange to kill bacterially sensitized targets. Mucosal Immunol. 2015;8(2):429-40.
91. Eckle SB, Birkinshaw RW, Kostenko L, Corbett AJ, McWilliam HE, Reantragoon R, et al. A molecular basis underpinning the T cell receptor heterogeneity of mucosal-associated invariant T cells. J Exp Med. 2014;211(8):1585-600.
92. Soudais C, Samassa F, Sarkis M, Le Bourhis L, Bessoles S, Blanot D, et al. In Vitro and In Vivo Analysis of the Gram-Negative Bacteria-Derived Riboflavin Precursor Derivatives Activating Mouse MAIT Cells. J Immunol. 2015;194(10):4641-9.
93. Corbett AJ, Eckle SB, Birkinshaw RW, Liu L, Patel O, Mahony J, et al. T-cell activation by transitory neo-antigens derived from distinct microbial pathways. Nature. 2014;509(7500):361-5.
94. Harriff MJ, McMurtrey C, Froyd CA, Jin H, Cansler M, Null M, et al. MR1 displays the microbial metabolome driving selective MR1-restricted T cell receptor usage. Sci Immunol. 2018;3(25).
95. Patel O, Kjer-Nielsen L, Le Nours J, Eckle SB, Birkinshaw R, Beddoe T, et al. Recognition of vitamin B metabolites by mucosal-associated invariant T cells. Nat Commun. 2013;4:2142.

96. Koay HF, Godfrey DI, Pellicci DG. Development of mucosal-associated invariant T cells. Immunol Cell Biol. 2018;96(6):598-606.
97. Liu CH, Liu H, Ge B. Innate immunity in tuberculosis: host defense vs pathogen evasion. Cell Mol Immunol. 2017;14(12):963-75.
98. Dias J, Leeansyah E, Sandberg JK. Multiple layers of heterogeneity and subset diversity in human MAIT cell responses to distinct microorganisms and to innate cytokines. Proc Natl Acad Sci U S A. 2017;114(27):E5434-E43.
99. Turtle CJ, Delrow J, Joslyn RC, Swanson HM, Basom R, Tabellini L, et al. Innate signals overcome acquired TCR signaling pathway regulation and govern the fate of human CD161(hi) CD8alpha(+) semi-invariant T cells. Blood. 2011;118(10):2752-62.
100. Gherardin NA, Keller AN, Woolley RE, Le Nours J, Ritchie DS, Neeson PJ, et al. Diversity of T Cells Restricted by the MHC Class I-Related Molecule MR1 Facilitates Differential Antigen Recognition. Immunity. 2016;44(1):32-45.
101. Meermeier EW, Laugel BF, Sewell AK, Corbett AJ, Rossjohn J, McCluskey J, et al. Human TRAV1-2-negative MR1-restricted T cells detect S. pyogenes and alternatives to MAIT riboflavin-based antigens. Nat Commun. 2016;7:12506.
102. Lepore M, Kalinichenko A, Calogero S, Kumar P, Paleja B, Schmaler M, et al. Functionally diverse human T cells recognize non-microbial antigens presented by MR1. Elife. 2017;6.
103. Mori L, De Libero G. 'Bohemian Rhapsody' of MR1T cells. Nat Immunol. 2020;21(2):108-10.
104. Vacchini A, Chancellor A, Spagnuolo J, Mori L, De Libero G. MR1-Restricted T Cells Are Unprecedented Cancer Fighters. Front Immunol. 2020;11:751.
105. Crowther MD, Dolton G, Legut M, Caillaud ME, Lloyd A, Attaf M, et al. Genome-wide CRISPR-Cas9 screening reveals ubiquitous T cell cancer targeting via the monomorphic MHC class I-related protein MR1. Nat Immunol. 2020;21(2):178-85.
106. Morowitz MJ, Carlisle EM, Alverdy JC. Contributions of intestinal bacteria to nutrition and metabolism in the critically ill. Surg Clin North Am. 2011;91(4):771-85, viii.
107. Pabst R, Russell MW, Brandtzaeg P. Tissue distribution of lymphocytes and plasma cells and the role of the gut. Trends Immunol. 2008;29(5):206-8; author reply 9-10.
108. Wershil BK, Furuta GT. 4. Gastrointestinal mucosal immunity. J Allergy Clin Immunol. 2008;121(2 Suppl):S380-3; quiz S415.
109. McGhee JR, Fujihashi K. Inside the mucosal immune system. PLoS Biol. 2012;10(9):e1001397.
110. Xavier RJ, Podolsky DK. Unravelling the pathogenesis of inflammatory bowel disease. Nature. 2007;448(7152):427-34.
111. Graham DB, Xavier RJ. Pathway paradigms revealed from the genetics of inflammatory bowel disease. Nature. 2020;578(7796):527-39.
112. Orholm M, Munkholm P, Langholz E, Nielsen OH, Sorensen TI, Binder V. Familial occurrence of inflammatory bowel disease. N Engl J Med. 1991;324(2):84-8.
113. Tysk C, Lindberg E, Jarnerot G, Floderus-Myrhed B. Ulcerative colitis and Crohn's disease in an unselected population of monozygotic and dizygotic twins. A study of heritability and the influence of smoking. Gut. 1988;29(7):990-6.
114. Kaplan GG, Ng SC. Understanding and Preventing the Global Increase of Inflammatory Bowel Disease. Gastroenterology. 2017;152(2):313-21 e2.
115. Kostic AD, Xavier RJ, Gevers D. The microbiome in inflammatory bowel disease: current status and the future ahead. Gastroenterology. 2014;146(6):1489-99.

116. Roda G, Chien Ng S, Kotze PG, Argollo M, Panaccione R, Spinelli A, et al. Crohn's disease. Nat Rev Dis Primers. 2020;6(1):22.
117. Hugot JP, Chamaillard M, Zouali H, Lesage S, Cezard JP, Belaiche J, et al. Association of NOD2 leucine-rich repeat variants with susceptibility to Crohn's disease. Nature. 2001;411(6837):599-603.
118. Huang H, Fang M, Jostins L, Umicevic Mirkov M, Boucher G, Anderson CA, et al. Fine-mapping inflammatory bowel disease loci to single-variant resolution. Nature. 2017;547(7662):173-8.
119. Yamazaki K, McGovern D, Ragoussis J, Paolucci M, Butler H, Jewell D, et al. Single nucleotide polymorphisms in TNFSF15 confer susceptibility to Crohn's disease. Hum Mol Genet. 2005;14(22):3499-506.
120. Ellinghaus D, Jostins L, Spain SL, Cortes A, Bethune J, Han B, et al. Analysis of five chronic inflammatory diseases identifies 27 new associations and highlights disease-specific patterns at shared loci. Nat Genet. 2016;48(5):510-8.
121. Jostins L, Ripke S, Weersma RK, Duerr RH, McGovern DP, Hui KY, et al. Host-microbe interactions have shaped the genetic architecture of inflammatory bowel disease. Nature. 2012;491(7422):119-24.
122. Duerr RH, Taylor KD, Brant SR, Rioux JD, Silverberg MS, Daly MJ, et al. A genome-wide association study identifies IL23R as an inflammatory bowel disease gene. Science. 2006;314(5804):1461-3.
123. Salem M, Ammitzboell M, Nys K, Seidelin JB, Nielsen OH. ATG16L1: A multifunctional susceptibility factor in Crohn disease. Autophagy. 2015;11(4):585-94.
124. Cooney R, Baker J, Brain O, Danis B, Pichulik T, Allan P, et al. NOD2 stimulation induces autophagy in dendritic cells influencing bacterial handling and antigen presentation. Nat Med. 2010;16(1):90-7.
125. Sewell GW, Kaser A. Interleukin-23 in the Pathogenesis of Inflammatory Bowel Disease and Implications for Therapeutic Intervention. J Crohns Colitis. 2022;16(Supplement_2):ii3-ii19.
126. Uniken Venema WT, Voskuil MD, Dijkstra G, Weersma RK, Festen EA. The genetic background of inflammatory bowel disease: from correlation to causality. J Pathol. 2017;241(2):146-58.
127. Torres J, Mehandru S, Colombel JF, Peyrin-Biroulet L. Crohn's disease. Lancet. 2017;389(10080):1741-55.
128. Levine A, Sigall Boneh R, Wine E. Evolving role of diet in the pathogenesis and treatment of inflammatory bowel diseases. Gut. 2018;67(9):1726-38.
129. Ananthakrishnan AN, Higuchi LM, Huang ES, Khalili H, Richter JM, Fuchs CS, et al. Aspirin, nonsteroidal anti-inflammatory drug use, and risk for Crohn disease and ulcerative colitis: a cohort study. Ann Intern Med. 2012;156(5):350-9.
130. Ungaro R, Bernstein CN, Gearry R, Hviid A, Kolho KL, Kronman MP, et al. Antibiotics associated with increased risk of new-onset Crohn's disease but not ulcerative colitis: a meta-analysis. Am J Gastroenterol. 2014;109(11):1728-38.
131. Ananthakrishnan AN, Khalili H, Konijeti GG, Higuchi LM, de Silva P, Korzenik JR, et al. A prospective study of long-term intake of dietary fiber and risk of Crohn's disease and ulcerative colitis. Gastroenterology. 2013;145(5):970-7.
132. Gevers D, Kugathasan S, Denson LA, Vazquez-Baeza Y, Van Treuren W, Ren B, et al. The treatment-naive microbiome in new-onset Crohn's disease. Cell Host Microbe. 2014;15(3):382-92.

133. Clooney AG, Sutton TDS, Shkoporov AN, Holohan RK, Daly KM, O'Regan O, et al. Whole-Virome Analysis Sheds Light on Viral Dark Matter in Inflammatory Bowel Disease. Cell Host Microbe. 2019;26(6):764-78 e5.
134. Manichanh C, Rigottier-Gois L, Bonnaud E, Gloux K, Pelletier E, Frangeul L, et al. Reduced diversity of faecal microbiota in Crohn's disease revealed by a metagenomic approach. Gut. 2006;55(2):205-11.
135. Dicksved J, Halfvarson J, Rosenquist M, Jarnerot G, Tysk C, Apajalahti J, et al. Molecular analysis of the gut microbiota of identical twins with Crohn's disease. ISME J. 2008;2(7):716-27.
136. Sepehri S, Kotlowski R, Bernstein CN, Krause DO. Microbial diversity of inflamed and noninflamed gut biopsy tissues in inflammatory bowel disease. Inflamm Bowel Dis. 2007;13(6):675-83.
137. Matsuoka K, Kanai T. The gut microbiota and inflammatory bowel disease. Semin Immunopathol. 2015;37(1):47-55.
138. Eckburg PB, Bik EM, Bernstein CN, Purdom E, Dethlefsen L, Sargent M, et al. Diversity of the human intestinal microbial flora. Science. 2005;308(5728):1635-8.
139. Louis P, Flint HJ. Formation of propionate and butyrate by the human colonic microbiota. Environ Microbiol. 2017;19(1):29-41.
140. Takahashi K, Nishida A, Fujimoto T, Fujii M, Shioya M, Imaeda H, et al. Reduced Abundance of Butyrate-Producing Bacteria Species in the Fecal Microbial Community in Crohn's Disease. Digestion. 2016;93(1):59-65.
141. Kumari R, Ahuja V, Paul J. Fluctuations in butyrate-producing bacteria in ulcerative colitis patients of North India. World J Gastroenterol. 2013;19(22):3404-14.
142. Wang W, Chen L, Zhou R, Wang X, Song L, Huang S, et al. Increased proportions of Bifidobacterium and the Lactobacillus group and loss of butyrate-producing bacteria in inflammatory bowel disease. J Clin Microbiol. 2014;52(2):398-406.
143. Joossens M, Huys G, Cnockaert M, De Preter V, Verbeke K, Rutgeerts P, et al. Dysbiosis of the faecal microbiota in patients with Crohn's disease and their unaffected relatives. Gut. 2011;60(5):631-7.
144. Park JH, Kotani T, Konno T, Setiawan J, Kitamura Y, Imada S, et al. Promotion of Intestinal Epithelial Cell Turnover by Commensal Bacteria: Role of Short-Chain Fatty Acids. PLoS One. 2016;11(5):e0156334.
145. Riviere A, Selak M, Lantin D, Leroy F, De Vuyst L. Bifidobacteria and Butyrate-Producing Colon Bacteria: Importance and Strategies for Their Stimulation in the Human Gut. Front Microbiol. 2016;7:979.
146. Parada Venegas D, De la Fuente MK, Landskron G, Gonzalez MJ, Quera R, Dijkstra G, et al. Short Chain Fatty Acids (SCFAs)-Mediated Gut Epithelial and Immune Regulation and Its Relevance for Inflammatory Bowel Diseases. Front Immunol. 2019;10:277.
147. Lupp C, Robertson ML, Wickham ME, Sekirov I, Champion OL, Gaynor EC, et al. Host-mediated inflammation disrupts the intestinal microbiota and promotes the overgrowth of Enterobacteriaceae. Cell Host Microbe. 2007;2(2):119-29.
148. Darfeuille-Michaud A, Boudeau J, Bulois P, Neut C, Glasser AL, Barnich N, et al. High prevalence of adherent-invasive Escherichia coli associated with ileal mucosa in Crohn's disease. Gastroenterology. 2004;127(2):412-21.
149. Mallone R, Funaro A, Zubiaur M, Baj G, Ausiello CM, Tacchetti C, et al. Signaling through CD38 induces NK cell activation. Int Immunol. 2001;13(4):397-409.

150. Moayyedi P, Surette MG, Kim PT, Libertucci J, Wolfe M, Onischi C, et al. Fecal Microbiota Transplantation Induces Remission in Patients With Active Ulcerative Colitis in a Randomized Controlled Trial. Gastroenterology. 2015;149(1):102-9 e6.
151. Pullan RD, Thomas GA, Rhodes M, Newcombe RG, Williams GT, Allen A, et al. Thickness of adherent mucus gel on colonic mucosa in humans and its relevance to colitis. Gut. 1994;35(3):353-9.
152. Rhodes JM. Mucins and inflammatory bowel disease. QJM. 1997;90(2):79-82.
153. Shirazi T, Longman RJ, Corfield AP, Probert CS. Mucins and inflammatory bowel disease. Postgrad Med J. 2000;76(898):473-8.
154. Buisine MP, Desreumaux P, Debailleul V, Gambiez L, Geboes K, Ectors N, et al. Abnormalities in mucin gene expression in Crohn's disease. Inflamm Bowel Dis. 1999;5(1):24-32.
155. Dorofeyev AE, Vasilenko IV, Rassokhina OA, Kondratiuk RB. Mucosal barrier in ulcerative colitis and Crohn's disease. Gastroenterol Res Pract. 2013;2013:431231.
156. Chassaing B, Koren O, Goodrich JK, Poole AC, Srinivasan S, Ley RE, et al. Dietary emulsifiers impact the mouse gut microbiota promoting colitis and metabolic syndrome. Nature. 2015;519(7541):92-6.
157. Boltin D, Perets TT, Vilkin A, Niv Y. Mucin function in inflammatory bowel disease: an update. J Clin Gastroenterol. 2013;47(2):106-11.
158. Zeissig S, Burgel N, Gunzel D, Richter J, Mankertz J, Wahnschaffe U, et al. Changes in expression and distribution of claudin 2, 5 and 8 lead to discontinuous tight junctions and barrier dysfunction in active Crohn's disease. Gut. 2007;56(1):61-72.
159. de Souza HS, Fiocchi C. Immunopathogenesis of IBD: current state of the art. Nat Rev Gastroenterol Hepatol. 2016;13(1):13-27.
160. Levine B, Mizushima N, Virgin HW. Autophagy in immunity and inflammation. Nature. 2011;469(7330):323-35.
161. Yang L, Li P, Fu S, Calay ES, Hotamisligil GS. Defective hepatic autophagy in obesity promotes ER stress and causes insulin resistance. Cell Metab. 2010;11(6):467-78.
162. Ouellette AJ. Paneth cells and innate mucosal immunity. Curr Opin Gastroenterol. 2010;26(6):547-53.
163. Noguchi E, Homma Y, Kang X, Netea MG, Ma X. A Crohn's disease-associated NOD2 mutation suppresses transcription of human IL10 by inhibiting activity of the nuclear ribonucleoprotein hnRNP-A1. Nat Immunol. 2009;10(5):471-9.
164. Kamada N, Hisamatsu T, Okamoto S, Chinen H, Kobayashi T, Sato T, et al. Unique CD14 intestinal macrophages contribute to the pathogenesis of Crohn disease via IL-23/IFN-gamma axis. J Clin Invest. 2008;118(6):2269-80.
165. Hart AL, Al-Hassi HO, Rigby RJ, Bell SJ, Emmanuel AV, Knight SC, et al. Characteristics of intestinal dendritic cells in inflammatory bowel diseases. Gastroenterology. 2005;129(1):50-65.
166. Middel P, Raddatz D, Gunawan B, Haller F, Radzun HJ. Increased number of mature dendritic cells in Crohn's disease: evidence for a chemokine mediated retention mechanism. Gut. 2006;55(2):220-7.
167. Mora JR, Bono MR, Manjunath N, Weninger W, Cavanagh LL, Rosemblatt M, et al. Selective imprinting of gut-homing T cells by Peyer's patch dendritic cells. Nature. 2003;424(6944):88-93.

168. Berlin C, Bargatze RF, Campbell JJ, von Andrian UH, Szabo MC, Hasslen SR, et al. alpha 4 integrins mediate lymphocyte attachment and rolling under physiologic flow. Cell. 1995;80(3):413-22.
169. Wagner N, Lohler J, Kunkel EJ, Ley K, Leung E, Krissansen G, et al. Critical role for beta7 integrins in formation of the gut-associated lymphoid tissue. Nature. 1996;382(6589):366-70.
170. Boyapati R, Satsangi J, Ho GT. Pathogenesis of Crohn's disease. F1000Prime Rep. 2015;7:44.
171. Zenewicz LA, Antov A, Flavell RA. CD4 T-cell differentiation and inflammatory bowel disease. Trends Mol Med. 2009;15(5):199-207.
172. Brand S. Crohn's disease: Th1, Th17 or both? The change of a paradigm: new immunological and genetic insights implicate Th17 cells in the pathogenesis of Crohn's disease. Gut. 2009;58(8):1152-67.
173. Teng MW, Bowman EP, McElwee JJ, Smyth MJ, Casanova JL, Cooper AM, et al. IL-12 and IL-23 cytokines: from discovery to targeted therapies for immune-mediated inflammatory diseases. Nat Med. 2015;21(7):719-29.
174. Uhlig HH, Powrie F. Translating Immunology into Therapeutic Concepts for Inflammatory Bowel Disease. Annu Rev Immunol. 2018;36:755-81.
175. O'Connor W, Jr., Zenewicz LA, Flavell RA. The dual nature of T(H)17 cells: shifting the focus to function. Nat Immunol. 2010;11(6):471-6.
176. Weaver CT, Hatton RD. Interplay between the TH17 and TReg cell lineages: a (co-)evolutionary perspective. Nat Rev Immunol. 2009;9(12):883-9.
177. Makita S, Kanai T, Oshima S, Uraushihara K, Totsuka T, Sawada T, et al. CD4+CD25bright T cells in human intestinal lamina propria as regulatory cells. J Immunol. 2004;173(5):3119-30.
178. Zhu L, Shi T, Zhong C, Wang Y, Chang M, Liu X. IL-10 and IL-10 Receptor Mutations in Very Early Onset Inflammatory Bowel Disease. Gastroenterology Res. 2017;10(2):65-9.
179. Jaeger N, Gamini R, Cella M, Schettini JL, Bugatti M, Zhao S, et al. Single-cell analyses of Crohn's disease tissues reveal intestinal intraepithelial T cells heterogeneity and altered subset distributions. Nat Commun. 2021;12(1):1921.
180. Bottois H, Ngollo M, Hammoudi N, Courau T, Bonnereau J, Chardiny V, et al. KLRG1 and CD103 Expressions Define Distinct Intestinal Tissue-Resident Memory CD8 T Cell Subsets Modulated in Crohn's Disease. Front Immunol. 2020;11:896.
181. Boschetti G, Nancey S, Moussata D, Cotte E, Francois Y, Flourie B, et al. Enrichment of Circulating and Mucosal Cytotoxic CD8+ T Cells Is Associated with Postoperative Endoscopic Recurrence in Patients with Crohn's Disease. J Crohns Colitis. 2016;10(3):338-45.
182. Lee JC, Lyons PA, McKinney EF, Sowerby JM, Carr EJ, Bredin F, et al. Gene expression profiling of CD8+ T cells predicts prognosis in patients with Crohn disease and ulcerative colitis. J Clin Invest. 2011;121(10):4170-9.
183. Giacomelli R, Parzanese I, Frieri G, Passacantando A, Pizzuto F, Pimpo T, et al. Increase of circulating gamma/delta T lymphocytes in the peripheral blood of patients affected by active inflammatory bowel disease. Clin Exp Immunol. 1994;98(1):83-8.
184. Bucht A, Soderstrom K, Esin S, Grunewald J, Hagelberg S, Magnusson I, et al. Analysis of gamma delta V region usage in normal and diseased human intestinal biopsies and peripheral blood by polymerase chain reaction (PCR) and flow cytometry. Clin Exp Immunol. 1995;99(1):57-64.

185. Andreu-Ballester JC, Amigo-Garcia V, Catalan-Serra I, Gil-Borras R, Ballester F, Almela-Quilis A, et al. Deficit of gammadelta T lymphocytes in the peripheral blood of patients with Crohn's disease. Dig Dis Sci. 2011;56(9):2613-22.
186. Mann ER, McCarthy NE, Peake ST, Milestone AN, Al-Hassi HO, Bernardo D, et al. Skin- and gut-homing molecules on human circulating gammadelta T cells and their dysregulation in inflammatory bowel disease. Clin Exp Immunol. 2012;170(2):122-30.
187. Cuvelier CA, De Wever N, Mielants H, De Vos M, Veys EM, Roels H. Expression of T cell receptors alpha beta and gamma delta in the ileal mucosa of patients with Crohn's disease and with spondylarthropathy. Clin Exp Immunol. 1992;90(2):275-9.
188. McVay LD, Li B, Biancaniello R, Creighton MA, Bachwich D, Lichtenstein G, et al. Changes in human mucosal gamma delta T cell repertoire and function associated with the disease process in inflammatory bowel disease. Mol Med. 1997;3(3):183-203.
189. Libera J, Wittner M, Kantowski M, Woost R, Eberhard JM, de Heer J, et al. Decreased Frequency of Intestinal CD39(+) gammadelta(+) T Cells With Tissue-Resident Memory Phenotype in Inflammatory Bowel Disease. Front Immunol. 2020;11:567472.
190. Cai Z, Wang S, Li J. Treatment of Inflammatory Bowel Disease: A Comprehensive Review. Front Med (Lausanne). 2021;8:765474.
191. Kumar A, Cole A, Segal J, Smith P, Limdi JK. A review of the therapeutic management of Crohn's disease. Therap Adv Gastroenterol. 2022;15:17562848221078456.
192. van Dullemen HM, van Deventer SJ, Hommes DW, Bijl HA, Jansen J, Tytgat GN, et al. Treatment of Crohn's disease with anti-tumor necrosis factor chimeric monoclonal antibody (cA2). Gastroenterology. 1995;109(1):129-35.
193. Hanauer SB, Feagan BG, Lichtenstein GR, Mayer LF, Schreiber S, Colombel JF, et al. Maintenance infliximab for Crohn's disease: the ACCENT I randomised trial. Lancet. 2002;359(9317):1541-9.
194. Colombel JF, Sandborn WJ, Reinisch W, Mantzaris GJ, Kornbluth A, Rachmilewitz D, et al. Infliximab, azathioprine, or combination therapy for Crohn's disease. N Engl J Med. 2010;362(15):1383-95.
195. Sandborn WJ, Feagan BG, Stoinov S, Honiball PJ, Rutgeerts P, Mason D, et al. Certolizumab pegol for the treatment of Crohn's disease. N Engl J Med. 2007;357(3):228-38.
196. Sands BE, Feagan BG, Rutgeerts P, Colombel JF, Sandborn WJ, Sy R, et al. Effects of vedolizumab induction therapy for patients with Crohn's disease in whom tumor necrosis factor antagonist treatment failed. Gastroenterology. 2014;147(3):618-27 e3.
197. Feagan BG, Sandborn WJ, Gasink C, Jacobstein D, Lang Y, Friedman JR, et al. Ustekinumab as Induction and Maintenance Therapy for Crohn's Disease. N Engl J Med. 2016;375(20):1946-60.
198. Liacouras CA, Furuta GT, Hirano I, Atkins D, Attwood SE, Bonis PA, et al. Eosinophilic esophagitis: updated consensus recommendations for children and adults. J Allergy Clin Immunol. 2011;128(1):3-20.e6; quiz 1-2.
199. Landres RT, Kuster GG, Strum WB. Eosinophilic esophagitis in a patient with vigorous achalasia. Gastroenterology. 1978;74(6):1298-301.
200. Lucendo AJ. Cellular and molecular immunological mechanisms in eosinophilic esophagitis: an updated overview of their clinical implications. Expert Rev Gastroenterol Hepatol. 2014;8(6):669-85.
201. Kaymak T, Hruz P, Niess JH. Immune system and microbiome in the esophagus: implications for understanding inflammatory diseases. FEBS J. 2022;289(16):4758-72.

202. Straumann A, Katzka DA. Diagnosis and Treatment of Eosinophilic Esophagitis. Gastroenterology. 2018;154(2):346-59.
203. Straumann A, Bauer M, Fischer B, Blaser K, Simon HU. Idiopathic eosinophilic esophagitis is associated with a T(H)2-type allergic inflammatory response. J Allergy Clin Immunol. 2001;108(6):954-61.
204. Clayton F, Peterson K. Eosinophilic Esophagitis: Pathophysiology and Definition. Gastrointest Endosc Clin N Am. 2018;28(1):1-14.
205. Lim AH, Wong S, Nguyen NQ. Eosinophilic Esophagitis and IgG4: Is There a Relationship? Dig Dis Sci. 2021;66(12):4099-108.
206. Blanchard C, Stucke EM, Burwinkel K, Caldwell JM, Collins MH, Ahrens A, et al. Coordinate interaction between IL-13 and epithelial differentiation cluster genes in eosinophilic esophagitis. J Immunol. 2010;184(7):4033-41.
207. Sleiman PM, Wang ML, Cianferoni A, Aceves S, Gonsalves N, Nadeau K, et al. GWAS identifies four novel eosinophilic esophagitis loci. Nat Commun. 2014;5:5593.
208. Kaymak T, Kaya B, Wuggenig P, Nuciforo S, Goldi A, Swiss Eo ECSG, et al. IL-20 subfamily cytokines impair the oesophageal epithelial barrier by diminishing filaggrin in eosinophilic oesophagitis. Gut. 2022.
209. Harris JK, Fang R, Wagner BD, Choe HN, Kelly CJ, Schroeder S, et al. Esophageal microbiome in eosinophilic esophagitis. PLoS One. 2015;10(5):e0128346.
210. Kleuskens MTA, Haasnoot ML, Herpers BM, Ampting M, Bredenoord AJ, Garssen J, et al. Butyrate and propionate restore interleukin 13-compromised esophageal epithelial barrier function. Allergy. 2022;77(5):1510-21.
211. Rothenberg ME, Spergel JM, Sherrill JD, Annaiah K, Martin LJ, Cianferoni A, et al. Common variants at 5q22 associate with pediatric eosinophilic esophagitis. Nat Genet. 2010;42(4):289-91.
212. Noti M, Wojno ED, Kim BS, Siracusa MC, Giacomin PR, Nair MG, et al. Thymic stromal lymphopoietin-elicited basophil responses promote eosinophilic esophagitis. Nat Med. 2013;19(8):1005-13.
213. Iwakura N, Fujiwara Y, Tanaka F, Tanigawa T, Yamagami H, Shiba M, et al. Basophil infiltration in eosinophilic oesophagitis and proton pump inhibitor-responsive oesophageal eosinophilia. Aliment Pharmacol Ther. 2015;41(8):776-84.
214. Poulsen LK, Hummelshoj L. Triggers of IgE class switching and allergy development. Ann Med. 2007;39(6):440-56.
215. Clayton F, Fang JC, Gleich GJ, Lucendo AJ, Olalla JM, Vinson LA, et al. Eosinophilic esophagitis in adults is associated with IgG4 and not mediated by IgE. Gastroenterology. 2014;147(3):602-9.
216. Weidlich S, Nennstiel S, Jesinghaus M, Brockow K, Slotta-Huspenina J, Bajbouj M, et al. IgG4 is Elevated in Eosinophilic Esophagitis but Not in Gastroesophageal Reflux Disease Patients. J Clin Gastroenterol. 2020;54(1):43-9.
217. Kouro T, Takatsu K. IL-5- and eosinophil-mediated inflammation: from discovery to therapy. Int Immunol. 2009;21(12):1303-9.
218. Blanchard C, Mingler MK, Vicario M, Abonia JP, Wu YY, Lu TX, et al. IL-13 involvement in eosinophilic esophagitis: transcriptome analysis and reversibility with glucocorticoids. J Allergy Clin Immunol. 2007;120(6):1292-300.
219. Le-Carlson M, Seki S, Abarbanel D, Quiros A, Cox K, Nadeau KC. Markers of antigen presentation and activation on eosinophils and T cells in the esophageal tissue of patients with eosinophilic esophagitis. J Pediatr Gastroenterol Nutr. 2013;56(3):257-62.

220. Peterson KA, Cobell WJ, Clayton FC, Krishnamurthy C, Ying J, Pease LF, 3rd, et al. Extracellular Eosinophil Granule Protein Deposition in Ringed Esophagus with Sparse Eosinophils. Dig Dis Sci. 2015;60(9):2646-53.
221. Saffari H, Hoffman LH, Peterson KA, Fang JC, Leiferman KM, Pease LF, 3rd, et al. Electron microscopy elucidates eosinophil degranulation patterns in patients with eosinophilic esophagitis. J Allergy Clin Immunol. 2014;133(6):1728-34 e1.
222. Davoine F, Lacy P. Eosinophil cytokines, chemokines, and growth factors: emerging roles in immunity. Front Immunol. 2014;5:570.
223. Wang YH, Hogan SP, Fulkerson PC, Abonia JP, Rothenberg ME. Expanding the paradigm of eosinophilic esophagitis: mast cells and IL-9. J Allergy Clin Immunol. 2013;131(6):1583-5.
224. Abonia JP, Franciosi JP, Rothenberg ME. TGF-beta1: Mediator of a feedback loop in eosinophilic esophagitis--or should we really say mastocytic esophagitis? J Allergy Clin Immunol. 2010;126(6):1205-7.
225. Niranjan R, Mavi P, Rayapudi M, Dynda S, Mishra A. Pathogenic role of mast cells in experimental eosinophilic esophagitis. Am J Physiol Gastrointest Liver Physiol. 2013;304(12):G1087-94.
226. Padigel UM, Lee JJ, Nolan TJ, Schad GA, Abraham D. Eosinophils can function as antigen-presenting cells to induce primary and secondary immune responses to Strongyloides stercoralis. Infect Immun. 2006;74(6):3232-8.
227. Liacouras CA, Wenner WJ, Brown K, Ruchelli E. Primary eosinophilic esophagitis in children: successful treatment with oral corticosteroids. J Pediatr Gastroenterol Nutr. 1998;26(4):380-5.
228. Dirksen U, Brennan B, Le Deley MC, Cozic N, van den Berg H, Bhadri V, et al. High-Dose Chemotherapy Compared With Standard Chemotherapy and Lung Radiation in Ewing Sarcoma With Pulmonary Metastases: Results of the European Ewing Tumour Working Initiative of National Groups, 99 Trial and EWING 2008. J Clin Oncol. 2019;37(34):3192-202.
229. Furuta GT, Liacouras CA, Collins MH, Gupta SK, Justinich C, Putnam PE, et al. Eosinophilic esophagitis in children and adults: a systematic review and consensus recommendations for diagnosis and treatment. Gastroenterology. 2007;133(4):1342-63.
230. Molina-Infante J, Ferrando-Lamana L, Ripoll C, Hernandez-Alonso M, Mateos JM, Fernandez-Bermejo M, et al. Esophageal eosinophilic infiltration responds to proton pump inhibition in most adults. Clin Gastroenterol Hepatol. 2011;9(2):110-7.
231. Netzer P, Gschossmann JM, Straumann A, Sendensky A, Weimann R, Schoepfer AM. Corticosteroid-dependent eosinophilic oesophagitis: azathioprine and 6-mercaptopurine can induce and maintain long-term remission. Eur J Gastroenterol Hepatol. 2007;19(10):865-9.
232. Arias A, Gonzalez-Cervera J, Tenias JM, Lucendo AJ. Efficacy of dietary interventions for inducing histologic remission in patients with eosinophilic esophagitis: a systematic review and meta-analysis. Gastroenterology. 2014;146(7):1639-48.
233. Dellon ES, Spergel JM. Biologics in eosinophilic gastrointestinal diseases. Ann Allergy Asthma Immunol. 2022.
234. Bates D, Machler M, Bolker BM, Walker SC. Fitting Linear Mixed-Effects Models Using lme4. Journal of Statistical Software. 2015;67(1):1-48.
235. Alexa A RJ. topGO: Enrichment Analysis for Gene Ontology. R package. 2022.
236. Benjamini Y, Krieger AM, Yekutieli D. Adaptive linear step-up procedures that control the false discovery rate. Biometrika. 2006;93(3):491-507.

237. Levine JH, Simonds EF, Bendall SC, Davis KL, Amir EAD, Tadmor MD, et al. Data-Driven Phenotypic Dissection of AML Reveals Progenitor-like Cells that Correlate with Prognosis. Cell. 2015;162(1):184-97.
238. Benjamini Y, Hochberg Y. Controlling the False Discovery Rate - a Practical and Powerful Approach to Multiple Testing. J R Stat Soc B. 1995;57(1):289-300.
239. Benaglia T, Chauveau D, Hunter DR, Young DS. mixtools: An R Package for Analyzing Finite Mixture Models. J Stat Softw. 2009;32(6):1-29.
240. Weber LM, Nowicka M, Soneson C, Robinson MD. diffcyt: Differential discovery in high-dimensional cytometry via high-resolution clustering. Commun Biol. 2019;2:183.
241. Nowicka M, Krieg C, Crowell HL, Weber LM, Hartmann FJ, Silvia Guglietta, et al. CyTOF workflow: differential discovery in high-throughput high-dimensional cytometry datasets [version 4; peer review: 2 approved]
. F1000Res. 2019(6):748.
242. Van Gassen S, Callebaut B, Van Helden MJ, Lambrecht BN, Demeester P, Dhaene T, et al. FlowSOM: Using self-organizing maps for visualization and interpretation of cytometry data. Cytometry A. 2015;87(7):636-45.
243. Robinson MD, McCarthy DJ, Smyth GK. edgeR: a Bioconductor package for differential expression analysis of digital gene expression data. Bioinformatics. 2010;26(1):139-40.
244. Friedrich M, Pohin M, Powrie F. Cytokine Networks in the Pathophysiology of Inflammatory Bowel Disease. Immunity. 2019;50(4):992-1006.
245. Catalan-Serra I, Sandvik AK, Bruland T, Andreu-Ballester JC. Gammadelta T Cells in Crohn's Disease: A New Player in the Disease Pathogenesis? J Crohns Colitis. 2017;11(9):1135-45.
246. Lo Presti E, Di Mitri R, Mocciaro F, Di Stefano AB, Scibetta N, Unti E, et al. Characterization of gammadelta T Cells in Intestinal Mucosa From Patients With Early-Onset or Long-Standing Inflammatory Bowel Disease and Their Correlation With Clinical Status. J Crohns Colitis. 2019;13(7):873-83.
247. Casalegno Garduno R, Dabritz J. New Insights on CD8(+) T Cells in Inflammatory Bowel Disease and Therapeutic Approaches. Front Immunol. 2021;12:738762.
248. Motamedi M, Xu L, Elahi S. Correlation of transferrin receptor (CD71) with Ki67 expression on stimulated human and mouse T cells: The kinetics of expression of T cell activation markers. J Immunol Methods. 2016;437:43-52.
249. Li S, Simoni Y, Becht E, Loh CY, Li N, Lachance D, et al. Human Tumor-Infiltrating MAIT Cells Display Hallmarks of Bacterial Antigen Recognition in Colorectal Cancer. Cell Rep Med. 2020;1(3):100039.
250. Kleinschek MA, Boniface K, Sadekova S, Grein J, Murphy EE, Turner SP, et al. Circulating and gut-resident human Th17 cells express CD161 and promote intestinal inflammation. J Exp Med. 2009;206(3):525-34.
251. Sallusto F, Kremmer E, Palermo B, Hoy A, Ponath P, Qin S, et al. Switch in chemokine receptor expression upon TCR stimulation reveals novel homing potential for recently activated T cells. Eur J Immunol. 1999;29(6):2037-45.
252. Longphre M, Li D, Gallup M, Drori E, Ordonez CL, Redman T, et al. Allergen-induced IL-9 directly stimulates mucin transcription in respiratory epithelial cells. J Clin Invest. 1999;104(10):1375-82.
253. Gerlach K, McKenzie AN, Neurath MF, Weigmann B. IL-9 regulates intestinal barrier function in experimental T cell-mediated colitis. Tissue Barriers. 2015;3(1-2):e983777.

254. Martin JC, Chang C, Boschetti G, Ungaro R, Giri M, Grout JA, et al. Single-Cell Analysis of Crohn's Disease Lesions Identifies a Pathogenic Cellular Module Associated with Resistance to Anti-TNF Therapy. Cell. 2019;178(6):1493-508 e20.
255. Rubin SJS, Bai L, Haileselassie Y, Garay G, Yun C, Becker L, et al. Mass cytometry reveals systemic and local immune signatures that distinguish inflammatory bowel diseases. Nat Commun. 2019;10(1):2686.
256. Cepek KL, Shaw SK, Parker CM, Russell GJ, Morrow JS, Rimm DL, et al. Adhesion between epithelial cells and T lymphocytes mediated by E-cadherin and the alpha E beta 7 integrin. Nature. 1994;372(6502):190-3.
257. Littman DR, Rudensky AY. Th17 and regulatory T cells in mediating and restraining inflammation. Cell. 2010;140(6):845-58.
258. Honda K, Littman DR. The microbiome in infectious disease and inflammation. Annu Rev Immunol. 2012;30:759-95.
259. Fung TC, Bessman NJ, Hepworth MR, Kumar N, Shibata N, Kobuley D, et al. Lymphoid-Tissue-Resident Commensal Bacteria Promote Members of the IL-10 Cytokine Family to Establish Mutualism. Immunity. 2016;44(3):634-46.
260. Ihara S, Hirata Y, Koike K. TGF-beta in inflammatory bowel disease: a key regulator of immune cells, epithelium, and the intestinal microbiota. J Gastroenterol. 2017;52(7):777-87.
261. Rojo JM, Kerner JD, Janeway CA, Jr. Selective induction of growth factor production and growth factor receptor expression by different signals to a single T cell. Eur J Immunol. 1989;19(11):2061-7.
262. Monteleone G, Monteleone I, Fina D, Vavassori P, Del Vecchio Blanco G, Caruso R, et al. Interleukin-21 enhances T-helper cell type I signaling and interferon-gamma production in Crohn's disease. Gastroenterology. 2005;128(3):687-94.
263. Caruso R, Fina D, Peluso I, Stolfi C, Fantini MC, Gioia V, et al. A functional role for interleukin-21 in promoting the synthesis of the T-cell chemoattractant, MIP-3alpha, by gut epithelial cells. Gastroenterology. 2007;132(1):166-75.
264. Geginat J, Lanzavecchia A, Sallusto F. Proliferation and differentiation potential of human CD8+ memory T-cell subsets in response to antigen or homeostatic cytokines. Blood. 2003;101(11):4260-6.
265. Klicznik MM, Morawski PA, Hollbacher B, Varkhande SR, Motley SJ, Kuri-Cervantes L, et al. Human CD4(+)CD103(+) cutaneous resident memory T cells are found in the circulation of healthy individuals. Sci Immunol. 2019;4(37).
266. Beura LK, Wijeyesinghe S, Thompson EA, Macchietto MG, Rosato PC, Pierson MJ, et al. T Cells in Nonlymphoid Tissues Give Rise to Lymph-Node-Resident Memory T Cells. Immunity. 2018;48(2):327-38 e5.
267. Deusch K, Luling F, Reich K, Classen M, Wagner H, Pfeffer K. A major fraction of human intraepithelial lymphocytes simultaneously expresses the gamma/delta T cell receptor, the CD8 accessory molecule and preferentially uses the V delta 1 gene segment. Eur J Immunol. 1991;21(4):1053-9.
268. Carena I, Shamshiev A, Donda A, Colonna M, Libero GD. Major histocompatibility complex class I molecules modulate activation threshold and early signaling of T cell antigen receptor-gamma/delta stimulated by nonpeptidic ligands. J Exp Med. 1997;186(10):1769-74.
269. Landau SB, Probert CS, Stevens CA, Balk SP, Blumberg RS. Over-utilization of the J delta 3 gene-segment in Crohn's disease. J Clin Lab Immunol. 1996;48(1):33-44.

270. Di Marco Barros R, Roberts NA, Dart RJ, Vantourout P, Jandke A, Nussbaumer O, et al. Epithelia Use Butyrophilin-like Molecules to Shape Organ-Specific gammadelta T Cell Compartments. Cell. 2016;167(1):203-18 e17.
271. Taman H, Fenton CG, Hensel IV, Anderssen E, Florholmen J, Paulssen RH. Genome-wide DNA Methylation in Treatment-naive Ulcerative Colitis. J Crohns Colitis. 2018;12(11):1338-47.
272. Mayassi T, Ladell K, Gudjonson H, McLaren JE, Shaw DG, Tran MT, et al. Chronic Inflammation Permanently Reshapes Tissue-Resident Immunity in Celiac Disease. Cell. 2019;176(5):967-81 e19.
273. Melo AM, Mylod E, Fitzgerald V, Donlon NE, Murphy DM, Foley EK, et al. Tissue distribution of gammadelta T cell subsets in oesophageal adenocarcinoma. Clin Immunol. 2021;229:108797.
274. Chodaczek G, Papanna V, Zal MA, Zal T. Body-barrier surveillance by epidermal gammadelta TCRs. Nat Immunol. 2012;13(3):272-82.
275. Harry W. Schroeder AR, Claudia Berek,. Clinical Immunology (Fifth Edition). 2019.
276. Jensen GS, Mant MJ, Belch AJ, Berenson JR, Ruether BA, Pilarski LM. Selective expression of CD45 isoforms defines CALLA+ monoclonal B-lineage cells in peripheral blood from myeloma patients as late stage B cells. Blood. 1991;78(3):711-9.
277. Shi J, Ikeda K, Maeda Y, Shinagawa K, Ohtsuka A, Yamamura H, et al. Identification of CD123+ myeloid dendritic cells as an early-stage immature subset with strong tumoristatic potential. Cancer Lett. 2008;270(1):19-29.
278. Amici SA, Young NA, Narvaez-Miranda J, Jablonski KA, Arcos J, Rosas L, et al. CD38 Is Robustly Induced in Human Macrophages and Monocytes in Inflammatory Conditions. Front Immunol. 2018;9:1593.
279. Simoni Y, Fehlings M, Kloverpris HN, McGovern N, Koo SL, Loh CY, et al. Human Innate Lymphoid Cell Subsets Possess Tissue-Type Based Heterogeneity in Phenotype and Frequency. Immunity. 2017;46(1):148-61.
280. Akuthota P, Wang H, Weller PF. Eosinophils as antigen-presenting cells in allergic upper airway disease. Curr Opin Allergy Clin Immunol. 2010;10(1):14-9.
281. Valitutti S, Muller S, Salio M, Lanzavecchia A. Degradation of T cell receptor (TCR)-CD3-zeta complexes after antigenic stimulation. J Exp Med. 1997;185(10):1859-64.
282. Toubal A, Nel I, Lotersztajn S, Lehuen A. Mucosal-associated invariant T cells and disease. Nat Rev Immunol. 2019;19(10):643-57.
283. Moqbel R, Levi-Schaffer F, Kay AB. Cytokine generation by eosinophils. J Allergy Clin Immunol. 1994;94(6 Pt 2):1183-8.
284. Spencer LA, Szela CT, Perez SA, Kirchhoffer CL, Neves JS, Radke AL, et al. Human eosinophils constitutively express multiple Th1, Th2, and immunoregulatory cytokines that are secreted rapidly and differentially. J Leukoc Biol. 2009;85(1):117-23.
285. Yoon J, Terada A, Kita H. CD66b regulates adhesion and activation of human eosinophils. J Immunol. 2007;179(12):8454-62.
286. Peterson KA, Gleich GJ, Limaye NS, Crispin H, Robson J, Fang J, et al. Eosinophil granule major basic protein 1 deposition in eosinophilic esophagitis correlates with symptoms independent of eosinophil counts. Dis Esophagus. 2019;32(11).
287. Janarthanam R, Bolton SM, Wechsler JB. Role of mast cells in eosinophilic esophagitis. Curr Opin Gastroenterol. 2022.

288. Strasser DS, Seger S, Bussmann C, Pierlot GM, Groenen PMA, Stalder AK, et al. Eosinophilic oesophagitis: relevance of mast cell infiltration. Histopathology. 2018;73(3):454-63.
289. Schernthaner GH, Hauswirth AW, Baghestanian M, Agis H, Ghannadan M, Worda C, et al. Detection of differentiation- and activation-linked cell surface antigens on cultured mast cell progenitors. Allergy. 2005;60(10):1248-55.
290. de Paulis A, Annunziato F, Di Gioia L, Romagnani S, Carfora M, Beltrame C, et al. Expression of the chemokine receptor CCR3 on human mast cells. Int Arch Allergy Immunol. 2001;124(1-3):146-50.
291. Diaz-Agustin B, Escribano L, Bravo P, Herrero S, Nunez R, Navalon R, et al. The CD69 early activation molecule is overexpressed in human bone marrow mast cells from adults with indolent systemic mast cell disease. Br J Haematol. 1999;106(2):400-5.
292. Lucendo AJ, Navarro M, Comas C, Pascual JM, Burgos E, Santamaria L, et al. Immunophenotypic characterization and quantification of the epithelial inflammatory infiltrate in eosinophilic esophagitis through stereology: an analysis of the cellular mechanisms of the disease and the immunologic capacity of the esophagus. Am J Surg Pathol. 2007;31(4):598-606.
293. Vicario M, Blanchard C, Stringer KF, Collins MH, Mingler MK, Ahrens A, et al. Local B cells and IgE production in the oesophageal mucosa in eosinophilic oesophagitis. Gut. 2010;59(1):12-20.
294. Abu-Ghazaleh RI, Fujisawa T, Mestecky J, Kyle RA, Gleich GJ. IgA-induced eosinophil degranulation. J Immunol. 1989;142(7):2393-400.
295. Banerjee H, Kane LP. Immune regulation by Tim-3. F1000Res. 2018;7:316.
296. Chauvin JM, Zarour HM. TIGIT in cancer immunotherapy. J Immunother Cancer. 2020;8(2).
297. Joller N, Lozano E, Burkett PR, Patel B, Xiao S, Zhu C, et al. Treg cells expressing the coinhibitory molecule TIGIT selectively inhibit proinflammatory Th1 and Th17 cell responses. Immunity. 2014;40(4):569-81.
298. Morra M, Zubiaur M, Terhorst C, Sancho J, Malavasi F. CD38 is functionally dependent on the TCR/CD3 complex in human T cells. FASEB J. 1998;12(7):581-92.
299. Naidoo K, Woods K, Pellefigues C, Cait A, O'Sullivan D, Gell K, et al. MR1-dependent immune surveillance of the skin contributes to pathogenesis and is a photobiological target of UV light therapy in a mouse model of atopic dermatitis. Allergy. 2021;76(10):3155-70.
300. Warringa RA, Mengelers HJ, Kuijper PH, Raaijmakers JA, Bruijnzeel PL, Koenderman L. In vivo priming of platelet-activating factor-induced eosinophil chemotaxis in allergic asthmatic individuals. Blood. 1992;79(7):1836-41.
301. Lopez AF, Williamson DJ, Gamble JR, Begley CG, Harlan JM, Klebanoff SJ, et al. Recombinant human granulocyte-macrophage colony-stimulating factor stimulates in vitro mature human neutrophil and eosinophil function, surface receptor expression, and survival. J Clin Invest. 1986;78(5):1220-8.
302. Owen WF, Jr., Rothenberg ME, Silberstein DS, Gasson JC, Stevens RL, Austen KF, et al. Regulation of human eosinophil viability, density, and function by granulocyte/macrophage colony-stimulating factor in the presence of 3T3 fibroblasts. J Exp Med. 1987;166(1):129-41.
303. Zeck-Kapp G, Czech W, Kapp A. TNF alpha-induced activation of eosinophil oxidative metabolism and morphology--comparison with IL-5. Exp Dermatol. 1994;3(4):176-88.

304. Kankaanranta H, Ilmarinen P, Zhang X, Adcock IM, Lahti A, Barnes PJ, et al. Tumour necrosis factor-alpha regulates human eosinophil apoptosis via ligation of TNF-receptor 1 and balance between NF-kappaB and AP-1. PLoS One. 2014;9(2):e90298.
305. Yamaguchi T, Kimura H, Kurabayashi M, Kozawa K, Kato M. Interferon-gamma enhances human eosinophil effector functions induced by granulocyte-macrophage colony-stimulating factor or interleukin-5. Immunol Lett. 2008;118(1):88-95.
306. Hartnell A, Robinson DS, Kay AB, Wardlaw AJ. CD69 is expressed by human eosinophils activated in vivo in asthma and in vitro by cytokines. Immunology. 1993;80(2):281-6.

Curriculum Vitae

Ján Deván

Personal data

Born	25.11.1993
Nationality	Slovak
email	janodevan@gmail.com

Education and qualifications

2018 – 2022	PhD study at **University of Basel, Faculty of Science, Cell biology** (*Switzerland*)
2018	Masters degree at **Masaryk University Brno, Faculty of Science, Molecular biologyand genetics**. Graduated with Honors
2016 – 2018	Master´s study at **Masaryk University Brno, Faculty of Science, Molecular biologyand genetics** (*Czech Republic*)
2016	National certificate for handling laboratory animals
2016	Bachelor degree at **Masaryk University Brno, Faculty of Science, Molecular biologyand genetics**. State exam: A
2013 – 2016	Bachelor´s study at **Masaryk University Brno, Faculty of Science, Molecular biologyand genetics** (*Czech Republic*)

Work experience

2018 – 2022	Department of Biomedicine, University of Basel, Switzerland
2014 – 2018	CEITEC Masaryk university Brno, Czech Republic